

NUMERICAL ANALYSIS OF VELOCITY AND BOUNDARY SHEAR STRESS DISTRIBUTION IN A MEANDERING CHANNEL

*A Thesis Submitted in Partial Fulfillment of the Requirements for the
Degree of*

**Master of Technology
In
Civil Engineering**



DEEPIKA PRIYADARSHINI PALAI

**DEPARTMENT OF CIVIL ENGINEERING
NATIONAL INSTITUTE OF TECHNOLOGY, ROURKELA
2015**

NUMERICAL ANALYSIS OF VELOCITY AND BOUNDARY SHEAR STRESS DISTRIBUTION IN A MEANDERING CHANNEL

*A Thesis Submitted in Partial Fulfillment of the Requirements for the
Degree of*

Master of Technology

In

Civil Engineering

**WITH SPECIALIZATION IN
WATER RESOURCES ENGINEERING**

Under the guidance and supervision of

Dr. K .C. Patra

Submitted By:

DEEPIKA PRIYADARSHINI PALAI

(ROLL NO. 213CE4107)



**DEPARTMENT OF CIVIL ENGINEERING
NATIONAL INSTITUTE OF TECHNOLOGY, ROURKELA
2015**



**National Institute Technology
Rourkela**

CERTIFICATE

This is to certify that the thesis entitled “**NUMERICAL ANALYSIS OF VELOCITY AND BOUNDARY SHEAR STRESS DISTRIBUTION IN A MEANDERING CHANNEL**” being submitted by **DEEPIKA PRIYADARSHINI PALAI** in partial fulfillment of the requirements for the award of *Master of Technology* Degree in *Civil Engineering with specialization in Water Resources Engineering* at National Institute of Technology Rourkela, is an authentic work carried out by his under my guidance and supervision.

To the best of my knowledge, the matter embodied in this report has not been submitted to any other university/institute for the award of any degree or diploma.

Place: Rourkela

Date:

Dr. Kanhu Charan Patra

Professor

Department of Civil Engineering

ACKNOWLEDGEMENT

A complete research work can never be the work of any one alone. The contributions of many different people, in their different ways, have made this possible. One page can never be sufficient to convey the sense of gratitude to those whose guidance and assistance was essential for the completion of this project.

I am deeply grateful to National Institute of Technology, Rourkela for providing me the opportunity to pursue my Master's degree with all necessary facilities.

I would like to express my hearty and sincere gratitude to my project supervisor Prof. K.C. Patra whom sincere and affectionate supervision has helped me to carry out my project work. I would also like to thank my committee members, Professor, Shishir Sahoo; Head of the Civil Department. And also I am sincerely thankful to Prof. Ramakar Jha, Prof. K.Khatua and Prof. A. Kumar for their kind cooperation and necessary advice.

A special expressions of thanks to Mr. Abhinash Mohanta and Mr. Arpan Pradhan Ph.D. Scholar of Civil Engineering Department, for his suggestions, comments and entire support throughout the project work. I express to my particular thanks to my dear friends Arunima, Anta, Saudmini, Sumit Banarjii, Rajendra, Jyoti, Sanjay and Sovan for their continuous support and suggestions.

Last but not least I would like to thanks to my father Mr. Sarat Chandra Palai and mother Mrs. Sushama Behera, who taught me the value of hard work by their own example. Thanks a lot for your understanding and constant support and to my brother Sashanka Sekhar Palai for his encouragement. They rendered me enormous support during the whole tenure of my study at NIT Rourkela. Words cannot express how grateful I am in my Father, Mother, and Brother for all of the sacrifices that you have made on my behalf. Your prayer for me was that sustained me thus far.

DEEPIKA PRIYADARSHINI PALAI

ABSTRACT

Rivers are one of the most important sources of water, which are constantly changing. It is vital to recognize and perceive components which influence the conduct and the morphology of the waterway or channel, for example, the type of the Meander River, conduit geometry, the state of the channel bed and the profile of the channel. In particular, these factors are valuable for meandering channel which has unsteady flow patterns. The geometry selected for this study is that of a meandering channel. In this research work the parameters, water depth and incoming discharge of the main channel were gradually varied. This aggregate subject speaks to the variety of speed profile along the width and profundity of the channel has been systematically broken down at curve peak along a wander way of a crooked channel of 60° crossover edge. Riverway considered is starting with one curve pinnacle then onto the next twist zenith, which changes its course at the crossover. Bend apex is the position of maximum curvature and crossover represents the section at which the sinuous channel changes its sign. Flow structure in meandering channel is more complex than straight channels due to the 3-Dimensional nature of the flow. The constant variation of channel geometry along the water course associated with secondary currents makes the depth averaged velocity computation difficult. The present experimental meandering channel is wide (aspect ratio = $b/h > 5$) and with a sinuosity of 2.04. Then the numerical method is applied to calculate water surface elevation in a meandering channel configuration, the output of calculations show good agreement with the experimental data. As statistical hydraulic models can significantly reduce costs associated with the experimental models, an effort has been made through the present investigation to establish the different flow characteristics of a meandering channel such as longitudinal velocity distribution, depth averaged velocity distribution. As a complementary study of the experimental research undertaken in this work,

three numerical hydrodynamic tools viz. three-dimensional CFD model (ANSYS – FLUENT), two dimensional numerical model National Center of Computational Hydrodynamic and Engineering of 2D (CCHE2D) developed by NCCHE, University of Mississippi, US and a quasi1D model Conveyance Estimation System (CES) developed by HR Wallingford, UK are applied to simulate the flow in meandering channels. This study aims to validate CFD simulations of free surface flow by using Volume of Fluid (VOF) method by comparing the data observed in the hydraulics laboratory of the National Institute of Technology, Rourkela. The volume of fluid (VOF) method was used to allow the free-surface to bend freely with the underlying turbulence. In this study Smagorinsky model is used to carry out for both three dimensional and two dimensional flow simulation. The LES results are shown to accurately predict the flow features, specifically the distribution of secondary circulations for in-bank channels at varying depth and width ratios in meandering sections.

Keyword- Aspect Ratio, Depth average velocity, Bend apex, Crossover, CFD simulation, LES turbulence model, Longitudinal Velocity profile, VOF method, Smagorinsky model, CCHE2D, CES.

CONTENTS

CONTENTS	PAGE NO.
Certificate	i
Acknowledgement	ii
Abstract	iv
Table of Content	vi
List of Figures	ix
List of tables	xi
List of abbreviations	xii
List of symbols	xiii
1 INTRODUCTION	1-11
1.1. Overview	1
1.2. Meander Path	3
1.3. Velocity Distribution	4
1.4. Boundary Shear Stress	5
1.5. Numerical Modelling	6
1.5.1. ANSYS	6
1.5.2. CES	7
1.5.3. CCHE2D	8
1.6. Advantages of numerical modelling	8
1.7. Objectives of present study	9
1.8. Organization of thesis	10
2 LITERATURE RIVEW	12-27
2.1. Overview	
2.2. Previous research on longitudinal velocity distribution	13
2.3. Previous research on boundary shear	18
2.4. Previous research on numerical modelling on open channel flow	23
2.4.1. ANSYS	23
2.4.2. CES	26
2.4.3. CCHE2D	26
3 EXPERIMENTAL SET UP AND PROCEDURE	28-37
3.1. Overview	28
3.2. Design and construction of channel	28
3.3. Apparatus and requirement's used	30
3.4.1. Experimental channel	31

3.4.2. Location of measurement	33
3.4.3. Measurement of bed slope	34
3.4.4. Measurement of longitudinal velocity	34
3.4.5. Measurement of boundary shear stress	35
4 NUMERICAL MODELLING	38-47
4.1. Description of numerical model parameters	38
4.2. Turbulence modelling	39
4.2.1. Turbulence models	42
4.3. Governing Equations	42
4.3.1. Volume of fluid (VOF) model	43
4.3.1.1. Volumetric Fraction Equation	44
4.3.1.2. Material Properties	45
4.3.1.3. Momentum Equation	45
4.3.2. Mixture Model	46
4.3.2.1. Continuity Equation	46
4.3.2.2. Momentum Equation	46
4.3.2.3. Volume Fraction Equation for Secondary flow	47
4.3.2.4. Smagorinsky model	47
5 NUMERICAL SIMULATION	48-68
5.1. Methodology of ANSYS	48
5.1.1. Processing	49
5.1.1.1. Creation of geometry	49
5.1.2. Mesh Generation	51
5.1.2.1. Courant number	53
5.1.2.2. Set up physics	54
5.1.2.3. Inlet and Outlet Boundary condition	56
5.1.2.4. Wall	56
5.1.2.5. Free Surface	57
5.1.3. Near Wall modelling	57
5.2. Methodology of CES	60
5.2.1. Development of model for CES	61
5.2.1.1. Outline of steps for modelling through CES	62
5.3. CCHE 2D	64
5.3.1. General Procedure	65
5.3.1.1. Mesh Generation	65
5.3.1.2. Specification of boundary condition	66
5.3.1.3. Parameter setting	67
5.3.1.4. Simulation	67

5.3.1.5. Result Visualization and Interpretation	68
6 VALIDATION AND VERIFICATION OF RESULTS	69-86
6.1. Numerical Analysis Results	69
6.1.1. Longitudinal velocity distribution in channel depth	71
6.2. Depth Average Velocity distribution for different water depths	71
6.2.1. Experimental Results	72
6.3. Stage Discharge Relationship	72
6.4. Distribution of Boundary Shear Stress results	73
6.5. Numerical Validation	
6.5.1. Validation of Depth Average Velocity results with a 1-D CES tool	73
6.5.2 Validation of Numerical Results for 0.11m	75
6.6. Contours of Longitudinal Velocity	76
6.6.1 Comparison of Velocity Contours having Depth of flow for $\alpha=2.54$	76
6.6.2 Comparison of Velocity Contours having Depth of flow for $\alpha=9.33$	77
6.7. Streamlines Along The Bend	78
6.8. Numerical 2d Simulation by CCHE 2D	80
6.8.1. Visualization of Results By CCHE 2D	82
6.8.1.1. Water Surface Level	83
6.8.1.2. Longitudinal Velocity	83
6.8.1.3 Velocity magnitude	83
6.8.1.4. Boundary Shear Stress distribution	84
6.8.1.5. Flow field, along the channel	84
6.8.1.6. Flow field at bend apex	85
6.8.1.7. Specific discharge throughout the channel	85
6.8.1.8. Flow depth analysis throughout the channel	86
7 CONCLUSIONS AND FUTURE WORK	87-89
7.1 Conclusions	87
7.2. Scope for future work	89
8 REFERENCES	90-94
Appendix-1	
(List of publications papers)	94

LIST OF FIGURES

SL. NO.	DESCRIPTION OF THE FIGURES	PAGE NO.
1.1	Straight Channel	2
1.2	Braided Channel	2
1.3	Meandering Channel	2
1.4	Properties of River Meander (Leopold and Langbein, 1966)	3
1.5	Contours of constant velocity in various open channel sections (Chow, 1959)	4
3.1	Plan view of the experimental set up of channel	30
3.2	Pitot tube Arrangement	31
3.3	Inclined Manometer	31
3.4	Front view of RCC OverHead Tank	32
3.5	Flow straighteners	32
3.6	Flooded Meandering Channel	32
3.7	Flow at Bend Apex of the channel	32
3.8	Tail Gate of Volumetric Tank	33
3.9	Photo of Volumetric tank	33
3.10	The grid diagram used for the experiments	34
5.1	Geometry Setup of a meandering Channel	49
5.2	Cross sectional geometry of the meandering channel	50
5.3	Different Geometrical entities used in a meandering channel	51
5.4	Meshing of inlet, outlet & free surface of meandering channel	54
5.5	A schematic diagram of meandering channel with boundary condition	55
5.6	The subdivisions of near wall region	59
5.7	Wall function used to resolve boundary layer	59
5.8	Meshing of meandering channel	66
6.1	Velocity contour of different experimental sections	69
6.2	Longitudinal Velocity Profile of a bend apex section for $\alpha=2.54$	70
6.3	Longitudinal Velocity Profile of a crossover section for $\alpha=2.54$	71
6.4	Longitudinal Velocity Profile of a bend apex section for $\alpha=9.33$	71
6.5	Longitudinal Velocity Profile of a crossover section for $\alpha=9.33$	71
6.6	Comparison of Depth Average Velocity Profile with various depths	72
6.7	A graph of Stage- Discharge Relationship	73
6.8	Boundary shear stress at bend apex	73
6.9	Boundary shear stress at crossover	74

6.10	Comparison of Depth Average Velocity Profile at bend apex	74
6.11	Comparison of Depth Average Velocity Profile at crossover	75
6.12	Comparison of Depth Average Velocity Profile for 0.11m	76
6.13	Comparison of Depth Average Velocity Profile for 0.03m	76
6.14	Comparison of Velocity contour for $\alpha=2.54$ at bend apex	77
6.15	Comparison of Velocity contour for $\alpha=2.54$ at crossover	78
6.16	Comparison of Velocity contour for $\alpha=9.33$ at bend apex	78
6.17	Comparison of Velocity contour for $\alpha=9.33$ at crossover	78
6.18	Simulation Result for streamline vector	79
6.19	Contour of Water surface level	83
6.20	Contour of Longitudinal Velocity(m/sec)	83
6.21	Contour of Velocity Magnitude(m/sec)	83
6.22	Contour of Boundary Shear stress distribution	84
6.23	Contour of flow field along the channel	84
6.24	Contour of flow field at bend apex	85
6.25	Contour of Specific discharge throughout the channel	85
6.26	Contour of flow depth analysis throughout the channel	86

LIST OF TABLES

SL NO	DESCRIPTION OF TABLE	PAGE
1.1	Degree of meander	1
3.1	Details of experimental parameters for meandering channel	26
5.1	Mesh information for FLU	44
5.2	Mesh statistics for FLU	44
5.3	Boundary information for FLU	47

LIST OF ABBREVIATIONS

CFD	Computational Fluid Dynamics
N-S	Navier-Stokes
FVM	Finite Volume Method
FEM	Finite Element Method
FDM	Finite Difference Method
ADV	Acoustic Doppler velocity meter
IDCM	Interactive Divide Channel Method
MDCM	Modified Divide Channel Method
SKM	Shiono Knight Method
ASM	Algebraic Reynolds Stress model
RSM	Reynolds Stress Model
LES	Large Eddy Simulation
LDA	Laser Doppler Anemometer
FVM	Finite Volume Method
VOF	Volume of Fluid
HOL	Height of liquid
DES	Detached eddy simulation
SAS	Scale adaptive simulation
SST	Scale adaptive Simulation Turbulence
RANS	Reynolds Averaged Navier-Stokes
DNS	Direct Numerical Simulation
SGS	Sub Grid Scale

LIST OF SYMBOLS

A	Cross Sectional Area;
B	Top width of compound channel;
C_r	Courant number;
C_s	Smagorinsky constant;
D	Hydraulic Depth;
D_r	Relative Depth;
\vec{F}	Body force;
G	Gaussian filters;
H	Total depth of flow;
P	wetted perimeter;
Q	discharge;
R	hydraulic radius;
S	bed slope of the channel;
S	Slope of the energy gradient line;
S_m	Mass exchange between two phase (water and air);
$\overline{S_{ij}}$	Resolved strain rate tensor;
U_t	Velocity tangent to the wall;
U_b	Bulk Velocity along Stream-line of flow;
\bar{U}	Average velocity;
V	Flow Velocity;
b	Main channel width;
c	log-layer constant dependent on wall roughness;

LIST OF SYMBOLS

g	acceleration due to gravity;
h	main channel bank full depth;
k	Von Karman constant;
m_{qp}	Mass transfer from phase q to phase p;
m_{pq}	Mass transfer from phase p to phase q;
n	Number of phase;
p	Reynolds averaged pressure;
t	Time;
u	Instantaneous Velocity;
\bar{u}	Mean velocity;
u'	Fluctuating Velocity;
u^+	Near wall velocity;
u_*	Friction velocity;
\vec{v}_m	Mass average velocity;
\vec{v}_{dr}	Drift Velocity;
y	lateral distance along the channel bed;
y^+	Dimensionless distance from the wall;
z	vertical distance from the channel bed;
u, v, w	Velocity components in x, y, z direction;
α	Width Ratio;
α_k	Volume fraction of phase k;

LIST OF SYMBOLS

\emptyset	Converging angle;
δ	Aspect Ratio;
θ	Angle between channel bed and horizontal;
μ_t	Turbulent viscosity;
μ	Dynamic Viscosity;
μ_m	Viscosity of the mixture;
ϑ	Kinematic viscosity;
ν_R	Eddy viscosity of the residual motion;
ρ	Fluid Density;
ρ_m	Mixture density;
τ_w	Wall shear stress;
τ	Boundary shear stress;
γ	Unit weight of water;
ε	Rate of turbulent kinetic energy dissipation;
ω	specific rate of dissipation;
η	Kolmogorov scale;
Ω	Vorticity;
Δt	Time Step size;
Δl	Grid cell size;

LIST OF SYMBOLS

<i>Avg.</i>	Average;
<i>a/act.</i>	Actual;
<i>fp</i>	Flood Plain;
<i>Fr</i>	Froude Number;
<i>h</i>	Hydraulic;
<i>in</i>	Inlet;
<i>Max</i>	Maximum;
<i>mc</i>	Main Channel;
<i>mod.</i>	Modelled;
<i>out</i>	Outlet;
<i>Re</i>	Reynolds Number;
<i>R</i>	Relative;
<i>Sec.</i>	Section;
<i>T</i>	Total;
<i>t</i>	Theoretical;
<i>Vel.</i>	Velocity;
<i>W</i>	Wall;
<i>i, j, k</i>	x, y, z directions respectively;
<i>K</i>	Conveyance

INTRODUCTION

1.1 OVERVIEW

Water is one of the prime factors which is responsible for life on the earth. Waterways are dependably wondrous things and the historic livelihood of a habitation. Individuals have been living close to the banks of rivers for quite a long time for the enthusiasm of nourishment, water and transport. However, flooding in rivers has always been danger for mankind as this causes a huge loss of property and lives. Moreover, the frequency of occurrence of floods has increased recently due to result of climate change, excessive human intervention, growing population on the banks of rivers and industrialization. Hence it is essential to take measures to understand flooding situations by analyzing the physics behind it. Generally, river engineer's to use the water powered model to make a flood prediction. The hydraulic model integrates many flow features such as average velocity, accurate discharge, water level profile and forecasting of shear stress. Earlier for producing hydraulic models capable of modeling all these flow features detailed knowledge of open channel hydrodynamics is required. Here first comes the understanding of geometry and hydraulic parameters of the river streams. Even the flow properties in rivers vary with the geometrical shape.

A Channel is a wide watercourse between two landmasses that lie near to one another. A channel can likewise be the most profound piece of a conduit or a limited waterway that join two bigger waterways. For the most part there are 3 sorts of channels. They are

1.1.1 Straight channel:

If on a channel no variation occurs in its passage along its flow path, then it is called a straight channel. The channel is usually controlled by a direct zone of fault in the underlying rock, like a fault or joint system.

1.1.2. Braided channel:

These are the channels consist of a network of small channels. During periods of low discharge , in streams having highly variable discharge and easily eroded banks, sediment gets deposited to form bars and islands that are exposed. In such a stream the water flows in a braided pattern around the islands and bars, dividing and reuniting as it flows downstream. Such a channel is termed a braided channel.

1.1.3. Meandering channel:

If a channel deviates from its axial path and a curvature of reverse order developed with short straight reaches, it is known as meandering channel. Because of the velocity structure of a stream and especially in streams flowing over low gradients which easily eroded banks, straight channels will eventually erode into meandering channel.



Figure1.1 Straight Channel Figure1.2 Braided Channel Figure1.3 Meandering Channel

A river is considered straight, if its length is straight for about 10 to 12 times its channel width, which is not usually possible in natural conditions. Sinuosity is characterized as the proportion of the valley slope to channel slope. Rivers having sinuosity greater than 1.5 are considered to be meandering. Nearly all natural rivers meander. In general, a meander is a curve in a sinuous water course which is formed when flowing water in a stream erodes the

outer bank and widens its valley. Theoretically a sine produced bendwell represents a meander channel. River meandering is an entangled methodology which includes the collaboration of move through channel twists, bank disintegration, and silt transport. In rivers, the meander wind development is an unpredictable wonder that results from erosion on the external bank and deposition on the inner side. So the investigation of meandering channels under different geometric and hydraulic condition is necessary to understand the flow properties, for example, distribution of velocity and boundary shear, which are better indicators of secondary flows, with the variation of different parameters like aspect ratio, sinuosity, ratio of minimum radius of curvature of width and hydraulic parameter such as relative depth and aspect ratio.

1.2 MEANDER PATH

Meander path is a flow path undertaken by a river. The meander path under study is taken starting with one curve summit then onto the next twist peak. The axis of the bend is the section at which the river has the most extreme curvature. A channel while moving from one bend apex to the other passes through the crossover. A crossover is a segment at the purpose of expression where the meander path changes its course as shown in Fig. 1.4. The concave bank or the outer bank becomes the convex bank or the inner bank after the crossover and similarly the convex bank or the inner bank becomes the concave bank or the outer bank. In the Fig. 1.4 W shows the width of the channel, λ represents the wavelength, L shows the length of channel for one wavelength and r_c represents the radius of the channel.

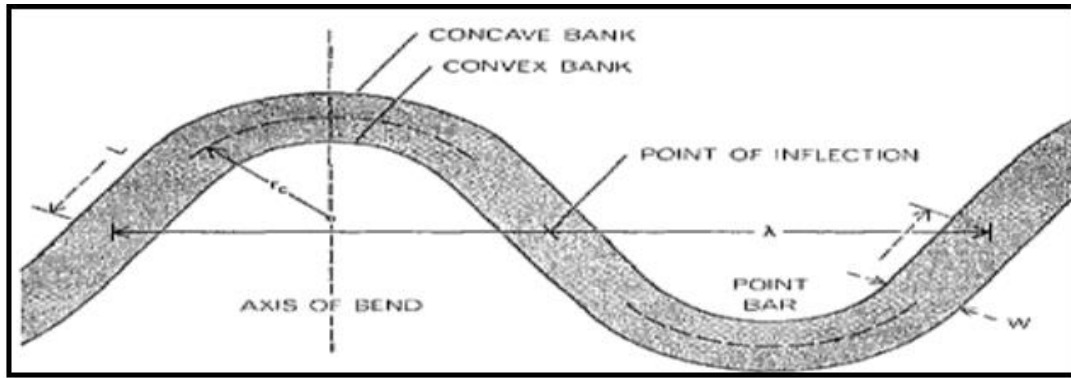


Figure 1.4: Properties of River Meander (Leopold and Langbein, 1966)

1.3 VELOCITY DISTRIBUTION

Velocity distribution benefits to recognize the velocity magnitude at individual point across a flow section. Many researchers have been done on various aspects of velocity distribution in curved meander rivers, but no logical effort has been made to study the variation of velocity along a meander path. In straight channel velocity distribution differs with changed width-depth ratio, while in meandering channel velocity distribution differs with aspect ratio, sinuosity, etc. making the flow more complex to investigate. In laminar stream max flow wise velocity occurs at water level; for turbulent streams, it happens at about 5-25% of the water depth underneath the water surface (Chow, 1959). Typical stream wise velocity contour lines (isovels) for flow in different cross sections are shown in Fig. 1.5.

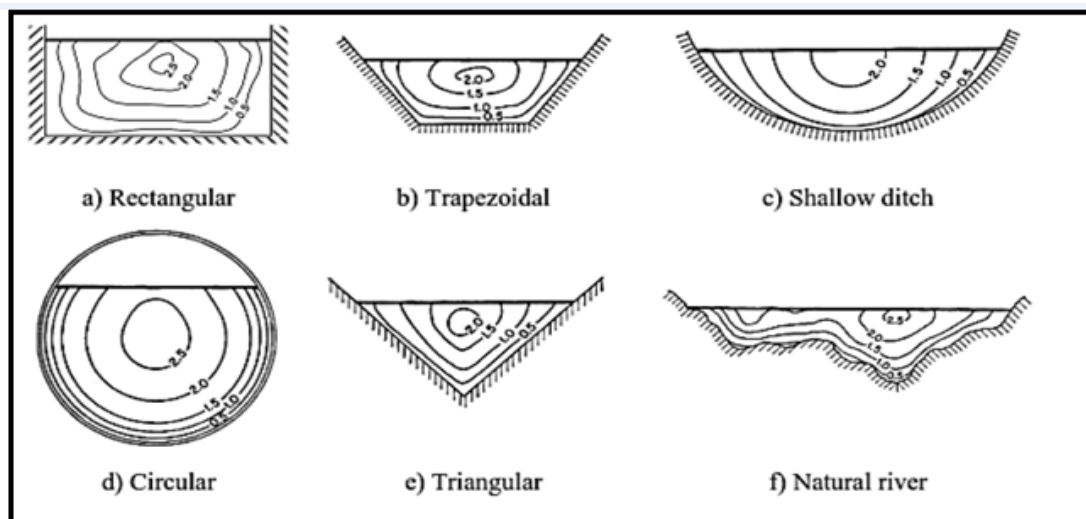


Figure.1.5: Contours of constant velocity in various open channel sections (Chow, 1959)

The above velocity contours satisfy for straight channels as the highest velocity is considered to be present somewhere in the middle of cross-sectional area below the free water surface. This condition is not true in case of meandering river as the local maximum velocity is seen to occur at the convex side of the channel. In this project the experimental channel under study of changes its course and both the clockwise and anticlockwise curves of the meandering channel are analyzed. Hence the movement of velocity can be studied from one bank of the channel to the other bank. The depth average velocity is quite difficult to model flows in meandering rectangular channel as the inward and external banks apply equivalent shear delay the fluid flow that at last controls the depth-averaged velocity. Depth-averaged velocity means the average velocity for a depth 'h' is assumed to occur at a height of 0.4h from the bed level.

1.4 BOUNDARY SHEAR STRESS

When water flows in a channel the force developed in the flow direction is resisted by the reaction from channel bed and side walls. This resistive force is manifested in the form of boundary shear force. The distribution of boundary shear force along the wetted perimeter directly affects the flow structure in an open channel. Understanding of boundary shear stress distribution is necessary to define the velocity profile and fluid field. Also, computation of bed form resistance, sediment transport, side wall correction, cavitations, channel migration, conveyance estimation and dispersion are among the hydraulic problems which can be solved by bearing the idea of boundary shear stress distribution. From hypothetical considerations, in steady, uniform flow in the boundary shear stress is related to channel bed slope, hydraulic radius and unit weight of fluid. Tominaga *et al.*(1989) and Knight and Demetriou (1983) declared that boundary shear stress increases where secondary currents flow towards the wall and shear stress decreases as they flow away from the wall. The presence of the secondary flow cells in the main flow influences the distribution of shear stress along the

channel wetted perimeter which is illustrated in Fig.1.6. In meandering channels the factors increases by many folds due to growth in 3-Dimensional nature of the flow. Sinuosity of meandering channel is considered to be a critical parameter for calculating the percentage of shear force at channel walls and bed.

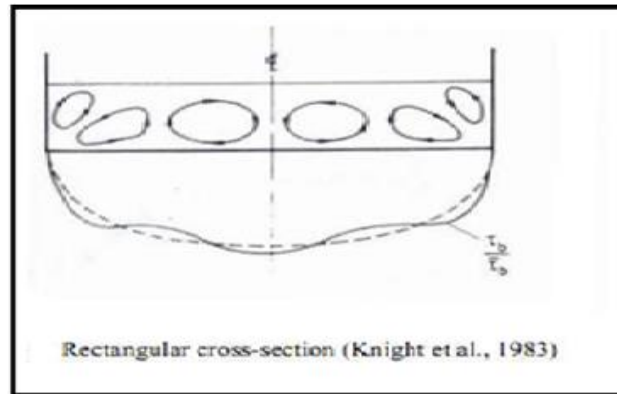


Figure1.6: Schematic influence of secondary flow cells on boundary shear distribution

1.5 NUMERICAL MODELLING

Computational Fluid Dynamics (CFD) is a computer based numerical analysis tool. The basic principle in the application of CFD is to analyze fluid flow in-detail by solving a system of nonlinear governing equations over the region of interest, after applying specified boundary conditions. A step has been taken to do numerical analysis on a meandering channel flow for in bank. The use of computational fluid dynamics was another integral component for the completion of this project since it was the main tool of simulation. In general, a CFD is a means to accurately predict phenomena in applications such as fluid flow, heat transfer, mass transfer, and chemical reactions.

1.5.1 ANSYS

There are a variety of CFD programs available that possess capabilities for modeling multiphase flow. Some common programs include ANSYS and COMSOL, which are both multiphysics modeling software packages and FLUENT, which is a fluid-flow-specific software package. A CFD is a popular tool for solving transport problems because of its

ability to give results for problems where no correlations or experimental data exist and also to produce results not possible in a laboratory situation and also useful for design since it can be directly translated to a physical setup and is cost-effective (Bakker et al., 2001).

In the present work, an effort has been made to investigate the velocity profiles for meandering channel by using a computational fluid dynamics (CFD) modeling tool, named as FLUENT. The CFD model developed for a real open-channel was first validated by comparing the velocity profile obtained by the numerical simulation with the actual measurement carried out by experimentation in the same channel using Preston tube. The simulated flow field in each case is compared with corresponding laboratory measurements of velocity and water surface elevation. Different models are utilized to solve Navier-Stokes equations which are the governing equation for any fluid flow. Finite volume method is connected to discretize the governing equations. The accuracy of computational results mainly depends on the mesh quality and the model used to simulate the flow.

1.5.2 CONVEYANCE ESTIMATION SYSTEM (CES)

CES developed by joint Agency/DEFRA research program on flood defense, reduces uncertainties in the estimation of river flood levels, discharge capacities, velocities and extent of inundation and is now recommended in the UK and other European nations as a major tool for estimating discharge, depth averaged velocities and boundary shear for natural channels of straight and meandering plan form as well as for laboratory flumes. CES considers all the physical flow processes that are present in a flow situation and where necessary, includes empirical or calibration coefficients based on previous research and expert advice. The Conveyance describes mainly three key components of the Conveyance Estimation System (CES): the Roughness Advisor, the Conveyance Generator and the Uncertainty Estimator. It gives an overview of the hydraulic equations and fundamental channel flow processes, with emphasis on their relevance to the successful model application and usage.

1.5.3 CCHE2D

National Center for Computational Hydro-Science and Engineering (NCCHE) University of Mississippi, USA, alternatively referred to as (CCHE2D).The **CCHE2D** model is an integrated package for simulation and analysis of free surface flows, sediment transport and morphological processes. It is a two-dimensional depth-averaged, unsteady, flow and sediment transport model. The flow model is based on depth-averaged Navier-Stokes equations.TheCCHE2D mesh generator allows the rapid creation of complex structured mesh systems for the CCHE2D model with several integrated useful techniques and methods. The CCHE2D Mesh Generator provides meshes for CCHE2D-GUI and CCHE2D numerical model, while the CCHE2D-GUI provides a graphical interface to handle the data input and visualization for CCHE2D numerical model. The CCHE2D-GUI is a graphical user's environment for the CCHE2D model with four main functions: preparation of initial conditions and boundary conditions, preparation of model parameters, run numerical simulations, and visualization of modeling results.

1.6 ADVANTAGES OF NUMERICAL MODELLING

In spite of exact results and clear understanding of stream phenomena; experimental approach has some disadvantages such as difficult data collection and data can be collected for a limited number of points because of instrument operation limitations; the model is usually not at full scale and the three dimensional flow behavior or some complex turbulent structure which is the nature of any open channel flow cannot effectively capture through experiments. So in these circumstances, computational approach can be adopted to overcome some of these issues and thus provide a corresponding tool. In comparison to experimental studies; computational methodology is repeatable, can simulate at full scale; can generate the flow taking all the data points into consideration & moreover can take greatest technical challenge *i.e.*; prediction of turbulence. The complex turbulent structures like secondary flow cells,

vortices, Reynolds stresses can be identified by numerical modeling effectively, which are very vital to the investigation of energy outflow in open channel flows. Numerous researchers in the recent centuries have numerically modeled open channel flows and has successfully validated with the experimental results.

1.7 OBJECTIVE OF PRESENT STUDY

The present work is aimed to study the distribution of velocity profile and boundary shear stress in a meandering channel. The distribution of velocity profile at a bend apex and cross over along the channel depends on aspect ratio, relative depth. Out of these parameters aspect ratio plays a major role in the estimation of velocity distribution in meandering channels. It is concluded from the literature review that very less work is regarded lateral distribution of depth-averaged velocity in a meandering channel. Still lack of qualitative and quantitative experimental data on the depth averaged velocity in meandering channels is silent a matter of concern. The present study aims to collect velocity data from the meandering channel at different depth in bend apex and cross over. Hence, the present study follows an analysis of resistance and discharge in a meandering channel flow.

The present study focuses on the following aspects:

- ❑ Study of change in the water surface profile as the water moves in the meander path, changing its course of travel at the crossover.
- ❑ Determination of horizontal profile of longitudinal velocity along the width of channel. The horizontal profiles are studied at the bed, $0.2H$, $0.4H$, $0.6H$, $0.8H$ and $0.9H$ above the channel bed. H being the average depth of flow of water in the corresponding section. The horizontal profile helps to analyze the movement or position of maximum velocity at every section along the meander path.

- ❑ To study the distribution of stream wise depth-averaged velocity at different section for two different flow depth. Also to study its variation at different flow depths for in bank flow conditions.
- ❑ To quantify the effects of the flow variables such as width ratio, depth ratio, aspect ratio etc. for the prediction of flow.
- ❑ To simulate a 60° simple meandering channel for analysing the flow phenomena such as velocity distribution of a meandering channel by Large Eddy Simulation (LES) model using a CFD tool.
- ❑ To validate the depth averaged velocity data with quasi one dimensional model Conveyance Estimation System (CES) for overbank flow conditions.
- ❑ To simulate the experimental meandering channel for analyzing the flow phenomena at bend apex and cross over by Smagoriski turbulence model using CCHE2D numerical tool.

1.8 ORGANISATION OF THESIS

The thesis consists of six chapters. General *introduction* is given in Chapter 1, *literature survey* is presented in Chapter 2, *experimental set up* is described in Chapter 3, *description of numerical modeling* are explained in Chapter 4, *numerical simulation* is described in Chapter 5, Chapter 6 comprises *verification of numerical models* and *discussion of result* and finally the *conclusions and scope of further work* is presented in Chapter 7. In lastly, referances and publications are present in this thesis.

General view of the river flow system is provided at a glance in the first chapter. Also the chapter introduces types of channel, meander path, concept of velocity distribution and boundary shear is also described. It gives an overview of numerical modelling in open channel flows.

Second chapter contains the detailed of literature study by numerous researcher on velocity distribution and boundary shear of meandering channel for in bank flow. The previous research works arranged according to the year of publication with the latest work in the latter.

The laboratory setup and whole experimental procedure are clearly described in chapter three. The methodology adopted for obtaining velocity distribution, boundary shear stress and boundary shear force is also discussed. Also the detailed information about the instrument used for taking an observation and geometry of experimental flume is described in this chapter.

The description of the numerical model parameter regarding turbulence modeling, governing equation related to turbulence model and finite volume method is briefly described in chapter four. This chapter also discusses the technique adopted for analyzing the flow variables. The 1-D, 2-D and 3-D numerical tools are briefly described in this chapter.

Chapter five presents significant contribution to numerical simulation of the meandering channel. The numerical model and the software used within this research are also discussed in this chapter. The methodology adopted for performing simulation is clearly discussed in this chapter. This chapter also gives the brief idea about the VOF model, Volume of fraction and LES turbulence model, CES and CCHE 2D software.

Chapter six presents the validation of experimental data with three numerical tools and analyzed the result by depth average velocity distribution , longitudinal velocity profile, velocity contour and streamline flow with two different aspect ratio for bend apex and crossover also. It also described the several velocity contours by using CCHE-2D numerical tools.

Lastly, in chapter seven conclusions is pointed out by simulations and observations of numerical and experimental results. After that scope for the further work is listed out in this chapter.

References that have been made in subsequent chapters are provided at the end of the thesis.

LITERATURE REVIEW

2.1 OVERVIEW

In this chapter a detailed literature survey is essential to any expressive and fruitful research in any subject. The present work is no exemption and consequently a focused and intensive review of the literature was completed covering various aspects concerning the meandering channels. In the literature review the researchers considered mostly on hydraulic engineering problem which was identified with the behavior of rivers and channels gathered to obtain the various features and attributes of meandering rivers. Almost river systems, analysis of its velocity distribution, boundary shear distribution along its meander path study is very critical. In a river the flow characteristics are overbearing for different conditions, for example, flood control, channel design, and renewal projects include the transport of pollutants and sediments. Flow in meandering channels is common in natural rivers, and research work was conducted in this category of channel for flood control, discharge estimation and stream restoration.

Flow structure in meandering channels is unpredictable when contrasted with straight channels. This is because of the velocity distributions in meandering paths as exhibited via researchers. The level of meandering was calculated by the term of sinuosity, which is characterized as the proportion of channel length to valley length. **Chow (1959)** said the level of meandering as follows:

Sinuosity ratio	Degree of meandering
1.0-1.2	Minor
1.2-1.5	Appreciable
1.5 and greater	Severe

Table 2.1:-Degree of meandering

In a meander path the flow investigation is not only limited to its velocity distribution, but also the shear force variations for the bed is also considered to get an outline of the shear force sharing in meander path of different section in between them. Therefore this chapter is divided into sections related to the earlier research carried out on velocity distributions and boundary shear force distribution of meandering channels.

The forecast of the flow qualities in meandering channels is a challenging assignment for rivers engineers because of the three-dimensional nature of flow. The prevailing element comprises of the cooperation impact between the quick moving streams in the wandering channel. This results in a high shear layer at the meandering channel, prompting the era of substantial scale vortices with longitudinal axes. However, the centre of the present work is on modelling flow in meandering channels.

2.2 PREVIOUS RESEARCH ON LONGITUDINAL VELOCITY DISTRIBUTION

The longitudinal velocity shows the speed at which the flow is moving in the stream wise direction. If a number of velocity estimations are taken throughout the depth over the channel, it is possible to create a distribution of the isovels that represents contour lines. Each of these lines stands for the same velocity magnitude over the channel. The isovels achieve values as low as zero in the vicinity of the channel perimeter and increment to a maximum value below the water surface in the area surrounding the centre of the channel. These isovels are influenced by the secondary currents that result in a lump in their distribution.

Thomson (1876) studies concerning the flow in meandering channels are mentioned for they give understanding to the nature, flow qualities and related mechanisms happening in a simple meandering channel where the path of river or flume continues changing along its course.

Coles (1956) proposed a semi-empirical equation of velocity distribution, which can be connected to external region, wall region of plate and open channel.

The Soil Conservation Service (1963) proposed an empirically-based model which provides for description for meander losses by adjusting the basic value of Manning's n utilizing sinuosity of the channel only. The balanced estimation of Manning's n was proposed for three distinct scopes of sinuosity.

Toebes and Sooky (1967) conducted analyses in a small laboratory channel with sinuosity 1.09. They proposed a conformity to the roughness f as a element of hydraulic radius below a critical value of the Froude number. From the experimental result they reasoned that energy loss per unit length for meandering channel was up to 2.5 times as huge as those for a uniform channel of same width and for the same hydraulic radius and discharge.

Chang (1983) examined the energy expenditure in meandering channels and determined an analytical model for getting the energy gradient, based on fully developed secondary movement. By making simplifying assumptions he found himself able to simplify the model for wide rectangular areas.

Johannesson and Parker (1989a) introduced an investigative model for ascertaining the lateral distribution of depth averaged primary flow velocity in meandering rivers. By utilizing an approximate "moment method" they accounted for the auxiliary flow in the convective transport of primary flow momentum, yielding satisfactory results of the redistribution of primary flow velocity.

James (1994) explored the variety of approaches for bend loss in meandering channel proposed by different investigators. He tried the consequences of the techniques by using the data of FCF, trapezoidal channel of Willets, at the University of Aberdeen, and the trapezoidal channels measured by the U.S. Army Corps of Engineers at the River Experiment Station, Vicksburg. His customized methods predicted well the stage discharge relationships

for meandering channels. He proposed some new methods representing extra resistance because of twist by suitable changes of past techniques.

Shiono, et al. (1999) investigated the impact of sinuosity and bed slope on the discharge evaluation of a meandering channel. Dimensional analysis was utilized to derive the conveyance capacity of a meandering channel which facilitated in finding the stage-discharge relationship for meandering channels. The study demonstrated that the discharge increased with an increase in bed slope and decreased with increase in sinuosity for the same channel.

Sarma, et al. (2000) attempted to describe the velocity distribution law in open channel flows by taking generalized type of binary version of velocity distribution, which joins the logarithmic law of the inner area and parabolic law of the outer region. The law developed by taking velocity-dip into record.

Patra, Kar and Bhattacharya (2004) established the longitudinal velocity distribution for meandering channels are strongly considered by flow interaction. They proposed exact comparisons which were discovered to be in normal rivers by producing all the interaction effect. Here experimental results are accepting with other smooth and rough sections of symmetrical and unsymmetrical channels.

Wilkerson, et al. (2005) developed two models which is predicting depth-averaged velocity distributions using data from past investigators for straight trapezoidal channels. The 1st model gives velocity information for calibrating the model coefficients and 2nd model used for prescribed coefficients. When depth-averaged velocity data are available that time 1st model is suggested. When predicted depth-averaged velocities are required to be within 20% of actual velocities then 2nd model is utilized.

Patra and Khatua (2006) observed roughness coefficient that Manning's n , Chezy's C , Darcy's f are not only shows the roughness attributes of a channel but also the energy loss in the flow of channels.

Afzal et al. (2007) analyzed the power law velocity profile in completely created turbulent pipe and channel flows regarding of the envelope of the friction factor. This model gives good approximation for low Reynolds number in composed procedure of actual system compared to log law.

Khatua (2008) proposed consequence of energy loss in a meandering channel. It is considered in different depth of flow which gives the resistance factors Manning's n , Chezy's C , and Darcy-Weisbach f for meandering channel. Stage-discharge relationship is given from in-bank to the over-bank flow in the channel.

Pinaki (2010) investigated a progression of laboratory tests for smooth and rigid meandering channels and created mathematical equation utilizing dimension analysis to assess roughness coefficients of smooth meandering channels of less width proportion and sinuosity.

Seo and Park (2010) got the lab and numerical studies to discover the impacts of auxiliary flow on flow structures and scattering of pollutants in bended channels. Essential flow is found to be skewed towards the inward bank at the bend while flow gets to be symmetric at the cross-over.

Absi (2011) scientific arrangement of the Reynolds-Averaged Navier-Stokes equation was completed to get conventional differential equation for velocity distribution in open channel. The proposed equation was useful in foreseeing the maximum velocity underneath the free surface. Two distinct degrees of estimate was finished. A semi-analytical solution of the proposed customary differential equation for the full dip-modified-log-wake law and another simple dip-modified-log-wake law.

Bonakdriet. al. (2011) considered numerical investigation of a flow field of a 90° bend. Expectation of data was carried out by utilizing Artificial Neural Network and Genetic Algorithm. CFD model was utilized to examine the flow patterns and the velocity profiles. ANN was used to foresee data at locations where experimental data was not available.

Khatua and Patra (2012) developed a mathematical model utilizing dimension analysis by taking arrangement of experiments data to assess roughness coefficients for smooth and rigid meandering channels. The vital variables are needed for stage-discharge relationship such as velocity, hydraulic radius, viscosity, gravitational acceleration, bed slope, sinuosity, and aspect ratio.

Khatua et. al. (2013) proposed a discharge predictive method for meandering channels considering the variety of roughness with depth of flow. The execution of the model was assessed by contrasting and a few different models by different researchers.

Dash (2013) analysed the critical parameters affecting the flow activities and flow resistance in term of Manning's n in a meandering channel. The factors influencing roughness coefficient are non-dimensionalized for predict and find their dependency with different parameters. A mathematical model was defined to predict the roughness coefficient which was practical to predict the stage-discharge relationship.

Mohanty(2013) anticipated lateral depth-averaged velocity distribution in a trapezoidal meandering channel. A nonlinear type of equation involving overbank flow depth, main channel flow depth, incoming discharge of the main channel and floodplains etc. was formulated. A quasi1D model Conveyance Estimation System (CES) was significant to the same experimental compound meandering channel to approve with the experimental depth averaged velocity.

Pradhan(2014) analysed the flow along the meander path of a highly sinuous rigid channel. Variations in the water surface profile throughout the meander path and longitudinal velocity

distributions along the width and depth of the channel, i.e. the horizontal and vertical velocity profiles were investigated.

*Mohanta(2014)*proposed the Flow Modelling of a Non Prismatic compound channel By Using CFD. Large eddy simulation model is used to accurately predict the flow features, specifically the distribution of secondary circulations for both in-bank and over-bank flows at different width ratios in symmetrically converging flood plain compound sections.

2.3 PREVIOUS RESEARCH ON BOUNDARY SHEAR

*Wormleaton (1996)*stated that the impacts of this shear layer extend across the width of the floodplain and it decreases to realize zero toward the external edges of the floodplain.

*Cruff (1965)*appraisal the boundary shear stress by the utilization of the Preston tube technique as well as the Karman-Prandtl logarithmic velocity-law from uniform flow in a rectangular channel. Despite the fact that he did not compute boundary shear stresses distribution in a rectangular channel with overbank flow, mainly his work was known for a technique which was help to calculate the apparent shear stress and momentum transfer between a channel and its flood plain.

*Ghosh and Jena (1972)*gives the boundary shear distribution for rough and smooth in a compound channel. Utilizing the Preston tube technique combined with the Patel calibration, they discovered the boundary shear distribution along the wetted perimeter of the total channel for various depths of flow. From the investigation, it is clearly shows that the maximum shear stress on the channel bed and approximately midway between the centre line and corner. From the experimental analysis the shear distribution is probable to estimate τ_c' the average shear stress in the channel. It is analysed that roughening the total periphery of the boundary shear in the meandering channel could be redistributed with the maximum shear at the channel bed.

Myers (1978) found that the effects of the shear layer were greater at lower overbank flow depths and decrease as the flow increases.

Bathurst et al. (1979) obtainable the field data for calculating the bed shear stress in a curved river and it is obtained that the bed shear stress distribution is affected by both the location of core of the main velocity and the structure of secondary flows.

Rajaratnam and Ahmadi (1981) demonstrated that the boundary shear stress reduces from the centre of the meandering channel toward the edge of the meandering channel. At that point it sharply increases at the interface with the edges, afterwards it decreases and levels off for most of the width and finally decreases near the wall. They also concluded that the impact of the meandering channel is to reduce the boundary shear stress. This is a direct effect of the reduction of velocity in the meandering channel resulting from the slow moving flow towards wall.

Knight and Demetriou (1983) completed arrangement of investigations in straight symmetrical compound channels to discover the characteristics of discharge, boundary shear stress and boundary shear force distributions. Equations to calculate the percentage of shear force carried by the floodplain were being proposed. The apparent shear force was seen to be higher at the lower flow depth. For high floodplain widths for vertical interface between main channel and floodplain the apparent shear force was also found to be higher.

Knight and Mohammed (1984) expressed that in straight channels, the longitudinal velocity in the channel is the most part quicker. This causes a shear layer at the interface of straight channel. Due to the vicinity of this shear layer, the flow in the straight channel decreases due to the impacts of the quicker. This result gives that the flows diminishes the entire release of the cross section,

Knight and Patel (1985) take the laboratory experiments results which concerning the boundary shears distribution in smooth rectangular cross section for diverse angle proportions

somewhere around 1 and 10. The boundary shear distributions were indicated to be subjective by the number and shape of the secondary flow cells, which, was depended mainly on the aspect ratio. Equations were given for the maximum, centreline and mean boundary shear stresses on the channel walls regarding the aspect ratio.

Tominaga et. al. (1989) and *Knight and Demetriou (1983)*, it increases where the auxiliary currents flow toward the wall and reduced when they flow away from the wall. Numerous different perspectives influence the boundary shear stress distribution across the channel.

Knight, Yuan and Fares (1992) gives the experimental data of SERC-FCF about the boundary shear stress distributions in meandering channels through the path of one complete wave length. They additionally reported the experimental data on surface topography, velocity vectors, and turbulence for meandering channels. They studied the effects of channel sinuosity, secondary currents, and cross section geometry on the value of boundary shear in meandering channels and exhibited an energy power offset for the flow.

Rhodes and Knight (1994) expressed that the bank slope had critical consequences for the boundary shear stress distribution at the interface between the main channel and floodplain. Adopting a model that predicts precisely the boundary shear stress distribution across the channel is crucial for river engineers since it represents sediment transport, bank erosion and morphology.

Shiono, Muto, Knight and Hyde (1999) exhibited the secondary flow and turbulence data utilizing two components Laser- Doppler anemometer. They built up the turbulence models, and studied the behaviour of secondary flow for both in bank and over bank flow conditions. They investigated the energy losses for compound meandering channels resulting from boundary friction, secondary flow, turbulence, expansion and contraction. They categorized the channel into three sub areas, namely (i) the main channel below the horizontal interface (ii) the meander belt above the interfaces and (iii) the area outside the meander belt of the

flood plain. They reported that the energy loss at the horizontal interface due to shear layer, the energy loss due to bed friction and energy loss due to secondary flow in lower main channel have the real commitment to the shallow over-bank flow and concluded that the energy loss due to expansion and contraction in meander belt have the huge part to the high over-bank flow.

Knight and Sterling (2000) broke down the boundary shear distribution in a circular channels flowing partially full with and without a smooth level bed using Preston-tube method. The outcomes have been investigated that the variety of local shear stress with perimeter distance and the percentage of total shear force acting on wall or bed of the channel. The %SFW results have been accepting with Knight's (1981) empirical formula for prismatic channels.

Patra and Kar (2000) reported the test outcomes concerning the boundary shear stress, shear force, and discharge characteristics of compound meandering river areas made out of a rectangular main channel and maybe a couple floodplains disposed of to its sides. Five dimensionless channel parameters were utilized to frame equations representing the total shear force percentage carried by floodplains. An arrangement of smooth and rough sections was studied with aspect ratio altering from 2 to 5. They proposed a variable- slanted interface for which apparent shear force was calculated as zero. Observational comparisons were introduced by foreseeing proportion of release conveyed by the main channel and floodplain.

Jin et. al. (2004) proposed a semi investigative model for forecast of boundary shear distribution in straight open channels. Secondary Reynolds stress terms were involved to add the simplified stream-wise vorticity equation. An observational model was produced for figuring the impact of the channel boundary on shear stresses.

Duan (2004) found that a 2D model could be better because of being computationally cost-effective for parametric examinations required by policy and administration planning and also preparatory outline applications. They compared due to the flow analysis in gently and

sharply curved or meandering channels through the use of depth averaged 2-D model and full 3-D model and established that the last one is more skilled than the previous in taking the flow fields in meandering channels. At last the author concluded that the 1D, 2D and 3D numerical models ought to be incorporated and cost effectiveness.

Patra and Kar (2004) reported the test outcomes concerning the flow and velocity distribution in meandering river sections. By using power law, they displayed equations about the three-dimensional variety of longitudinal, transverse, and vertical velocity in the principle channel and floodplain of meandering compound sections regarding the channel parameters. The consequences of definitions contrasted well with their respective experimental channel data obtained from a series of symmetrical and unsymmetrical test channels with smooth and unpleasant surfaces. They additionally confirmed formulations against the natural river and other meandering compound channel data.

Khatua (2008) amplified the work of **Patra and Kar (2000)** to meandering compound channels. By utilizing five parameters (sinuosity, amplitude, relative depth, width ratio and aspect ratio) general mathematical equations indicating the total shear force percentage conveyed by floodplain was presented. The proposed equations are simple, quite reliable and gave good quality results with the experimental data for straight compound channel of *Knight and Demetriou (1983)* and also for the meandering compound channel.

Khatua (2010) reported the circulation of boundary shear force for highly meandering channels having particularly different sinuosity and geometry. Taking into account the experimental results, the interrelationship between the boundary shear, sinuosity and geometry parameters has been indicated. The models are also accepted by utilizing the all around distributed information of different investigators.

Patnaik (2013) examined boundary shear stress at the bend apex of a meandering channel for both in bank and overbank flow conditions. Under different discharge and relative depths the

experimental data were gathered by keeping up the geometry, slope and sinuosity of the channel. Impact of aspect ratio and sinuosity on wall (inner and outer) and bed shear forces were evaluated and equation was developed to determine the percentage of wall and bed shear forces in smooth trapezoidal channel for in bank flows only. The proposed comparisons were contrasted and past studies and the model was stretched out to wide channel.

Pradhan (2014) analysed the flow along the meander path of a highly sinuous rigid channel. Variations in the depth of the channel and boundary shear distributions along the width were investigated.

2.4 PREVIOUS RESEARCH ON NUMERICAL MODELLING ON OPEN CHANNEL FLOW

2.4.1 ANSYS

Salvetti et al. (1997) has conducted LES simulation at a relatively large Reynolds number for producing results of bed shear, secondary motion and vorticity well comparable to experimental results.

Rameshwaran P, Naden PS.(2003) analyzed three dimensional nature of flow in compound channels.

Sugiyama et al. (2006) utilized turbulence model consists of transport equations for turbulent energy and dissipation, in conjunction with an algebraic stress model based on the Reynolds stress transport equations. They have exposed that the fluctuating vertical velocity approaches zero near the free surface. In addition, the compound meandering open channel is clarified somewhat based on the calculated results. As a consequence of the analysis, the present algebraic Reynolds stress model is shown to be able to reasonably predict the turbulent flow in a compound meandering open channel.

Cater and Williams (2008) exhibited exhaustive Large Eddy Simulation of turbulent flow in a long compound open channel with one floodplain. The Reynolds number is about 42,000 and the free surface was treated as fully deformable. The results are in concurrence with experimental measurements and support the use of high spatial resolution and a large box length in contrast with a previous simulation of the same geometry.

Jing, Guo and Zhang (2009) simulated a three-dimensional (3D) Reynolds stress model (RSM) for compound meandering channel flows. The velocity fields, wall shear stresses, and Reynolds stresses are ascertained for a scope of information conditions. Great similarity between the simulated results and measurements demonstrates that RSM can successfully predict the complicated flow occurrence.

B. K. Gandhi, H.K. Verma and Bobby Abraham (2010) observed the velocity profiles in both the directions under different real flow conditions, as ideal flow conditions rarely exist in the field. 'Fluent', a commercial computational fluid dynamics (CFD) code, has been used to numerically model various situations. He investigated the effects of bed slope, upstream bend and a convergence / divergence of channel width of velocity profile.

Esteve et.al., (2010) simulated the turbulent flow structures in a compound meandering channel by Large Eddy Simulations (LES) using the experimental configuration of Muto and Shiono (1998). The Large Eddy Simulation is performed with the in-house code LESOCC2. The predicted flow wise velocities and secondary current vectors as well as turbulent intensity are in good agreement with the LDA measurements.

Ansari et.al., (2011) determined the distribution of the bed and side wall shear stresses in trapezoidal channels and analyzed the contact of the variation of the slope angles of the side walls, aspect ratio and composite roughness on the shear stress distribution. The grades explained a significant contribution on secondary currents and overall shear stress at the boundaries.

RasoolGhobadian and Kamran Mohammadi (2011) replicated the subcritical flow pattern in 180° uniform and convergent open-channel bends using SSIIM 3-D model with maximum bed shear stress. He found at the end of the convergent bend, bed shear stress show higher values than those in the same region in the channel with a uniform bend.

Khazae& M. Mohammadiun (2012) investigated three-dimensional and two phase CFD model for flow distribution in an open channel. He approved the finite volume method (FVM) with a dynamic Sub grid-scale for seven cases of different aspect ratios, different inclination angles or slopes and convergence divergence condition.

OmidSeyedashraf, Ali Akbar Akhtari&MiladKhatibShahidi (2012) done that the standard k- ϵ model has the capability of capturing specific flow features in open channel bends more precisely. Comparing the area of the minimum velocity occurrences in an ordinary sharp open channel bend, the minimum velocity occurs near the inner bank and inside the separation zone along the meandering.

Larocque, Imran, Chaudhry (2013) existing 3D numerical simulation of a dam-break flow using LES and k- ϵ turbulence model with tracking of free surface by volume-of-fluid model. Outcomes are compared with published experimental data on dam-break flow through a partial breach as well as with results obtained by others using a shallow water model. The results explained that both the LES and the k - ϵ modelling satisfactorily reproduce the temporal variation of the measured bottom pressure. However, the LES model captures better the free surface and velocity variation with time.

Ramamurthy et al. (2013) simulated three-dimensional flow outline in a sharp bend by using two numerical codes along with different turbulent models, and by comparing the numerical results with experimental results validated the models, and claimed that RSM turbulence model has a better agreement with experimental results.

Mohanta(2014) simulated the Flow Modelling of a Non Prismatic compound channel By Using CFD. Large eddy simulation model is used to accurately predict the flow features for both in-bank and over-bank flows at different width ratios in symmetrically converging flood plain compound sections.

2.4.2 CES

Wark&James(1994) developed a procedure to calculate conveyance in meandering channels with flood plains based on horizontal division of the cross section. It represented a significant change to the current practice of using vertical division of separating the flood plain was roughened.

McGahey& Samuels (2003) examined the estimating conveyance in a range of channel types and flow conditions, including straight, skewed and meandering arrangement form shape; simple, two-stage and multi-string channels; and an assortment of vegetation .

2.4.3 CCHE2D

CCHE2D (National Centre for Computational Hydro science and Engineering's Two-Dimensional (2D) Model) is a depth-averaged 2D model for flow, sediment transport, water quality, and ecology in aquatic systems (Wu, 2004).

Scott and Jia (2006) established CCHD2D model capability for addressing sediment transport was utilized to simulate long-term analysis. Estimation of sedimentation in the point bar dike for a ten-year period of record flow was conducted in the Catfish point reach (L=25 miles) and the effect of a series of dikes were constructed to reduce dredging in the Redeye Crossing reach (L=5.5 miles).

He et al. (2009) used CCHE2D model to examine how much large wood structures affected the flow, sediment transport, riverbed change, and fish surroundings in the Little Topashaw Creek (L=2 km), North Central Mississippi.

Tena et al. (2012) assessed impacts of a flushing flow from dams in the lower Ebro River (L=12 km) on the riverbed using CCHE2D. Results showed erosion happened by 30 mm, 4 km downstream of the dam and the flushing flow did not cause severe riverbed change.

From literature survey, it was found that very limited work on velocity distribution, boundary shear stress have been reported for meandering channel. Although adequate literature is available on numerical studies that make use of different turbulence models for modelling meandering channels but the literature lacks substantial experimental works for meandering channels.

3.1 OVERVIEW

Evaluation of discharge capacity in meandering channel is a critical process due to the variation in shape of geometry, surface roughness, types of channel alignments and flow conditions. The evaluation of discharge capacity is directly dependent on proper forecasting of velocity distribution in the meandering channel. The velocity distribution is never uniform across a cross sectional area of meandering channel. It is higher in the deeper main channel than the shallower floodplain, as in compound channel and the adjoining shallow floodplains.

To study the flow patterns and characteristics of meandering rivers, a meandering channel is constructed and the different velocity and shear changes are measured for the entire meander path. The study helps to analysis the movement of rivers in natural meanders.

3.2 DESIGN AND CONSTRUCTION OF CHANNEL

Experimental channel was built in a large tilting flume of 1.67m wide and 9.67m long. The flume has an arrangement of hydraulic jacks to produce different bed slopes on tilting. The present research work executes the flume facility available in the Fluid Mechanics and Hydraulic Engineering Laboratory of the Civil Engineering Department at the National Institute of Technology, Rourkela, India. The primary objective behind these experiments is to assume a better understanding of the variation of velocity distribution. The following cross section provides a brief overview of details of hydraulic and geometric parameters of the present meandering channel, experimental arrangements, measuring equipment's and procedure used in the experimentation process.

The meandering channel is constructed having a bank full depth of 0.12m with a bottom width of 0.28m. Fig. 3.1 illustrates the schematic view of the channel setup. The main channel is a sinuous channel, similar to a sine curve of one and half wave length. The total

wavelength being $\lambda = 2.04m$ which is preceded and followed by a bell mouth section for proper flow field development at the experimental which is from the second bend apex to the next bend apex of the central curve.

Water is supplied through a Centrifugal pump (15 HP) discharging into an RCC overhead tank. (Figure 3.4). There is a measuring tank at the downstream end (Figure 3.9) which followed by a sump and feeds back water to the overhead tank through pumping for completing the recirculation path. Water is supplied to the flume from an underground sump via an overhead tank by centrifugal pump and returns back to the sump after flowing through the meandering channel and a downstream volumetric tank fitted with closure valves or calibration purpose. Water enters the channel by flow straighteners (Figure 3.5) via an upstream rectangular notch specifically built to measure discharge and it is also provided in the upstream section sufficiently ahead of rectangular notch to reduce turbulence and velocity of approach in the flow near the notch section. At the downstream end another adjustable tail gate (Figure 3.7) is provided for controlling the flow depth and maintain a uniform flow in the channel. A movable bridge (Figure 3.6) is provided across the flume for both spans wise and stream wise movements over the channel area so that each location on the plan of meandering channel which could be operated for taking measurements.

The parameters of the channel are aspect ratio of the main channel (δ), width ratio (α). Experimentation has taken place in the meandering channel by taking two different aspect ratio (α) value, i.e. $\alpha=2.54$, $\alpha=9.33$ in different position and depth. All the measurements are observed from the second bend apex to the next corresponding bend apex of the experimental channel from the upstream end. Observations are recorded under steady and uniform conditions. Experimentations are taking place at various depths and position longitudinally in a bend apex and also in crossover. The measuring instruments such as point gauges and Pitot tube

are arranged on the bridge such that each section along the meander path is accessible for measurements.

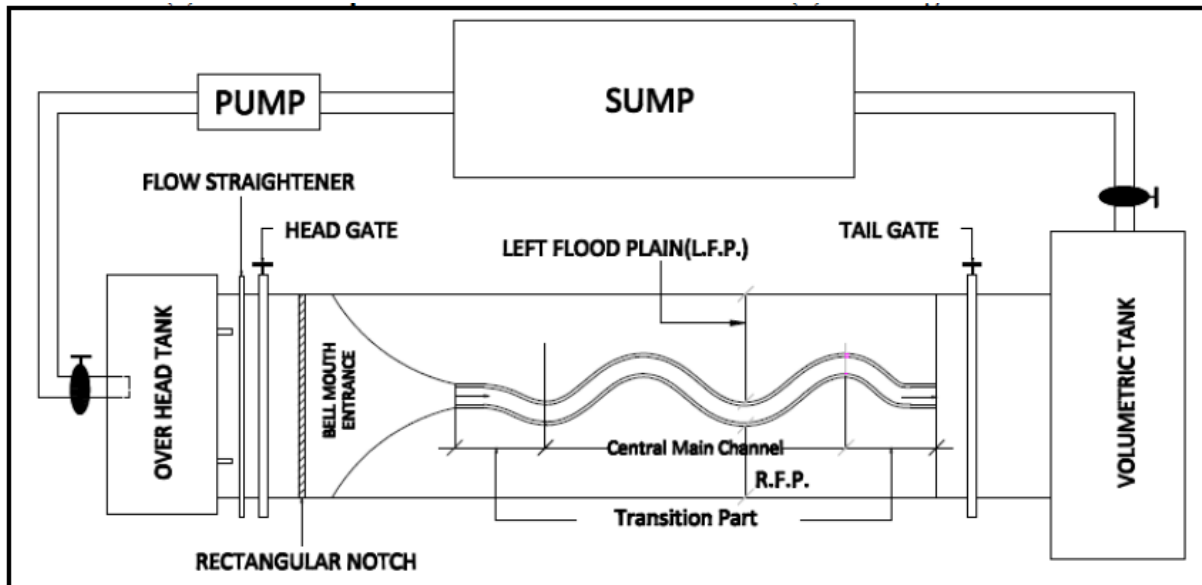


Figure. 3.1. Plan view of the experimental setup of the channel

3.3 APPARATUS AND EQUIPMENTS, USED:-

The moving bridge arrangement is fitted with one Pitot tube which is properly set with an external diameter of 4.7mm along with a pointer gauge of least count 0.1mm. The moving bridge crosses over the meander path to every section and respective readings are taken. The pointer gauge is used to figure out the water surface profile over the channel width at every section. The Pitot tube, measures the pressure difference at every predefined area across every section. Velocity at those points is then calculated from the pressure difference. The Pitot tube is connected to one manometer which is arranged on an inclined board having a spirit level. The spirit level helps to maintain the inclinity of the manometers. A rectangular notch arrangement is provided in the upstream area to keep up and calculate the discharge of water into the meandering channel. The following photographs show the measuring devices used for data collection.



Figure 3.2-Pitot tube Arrangement

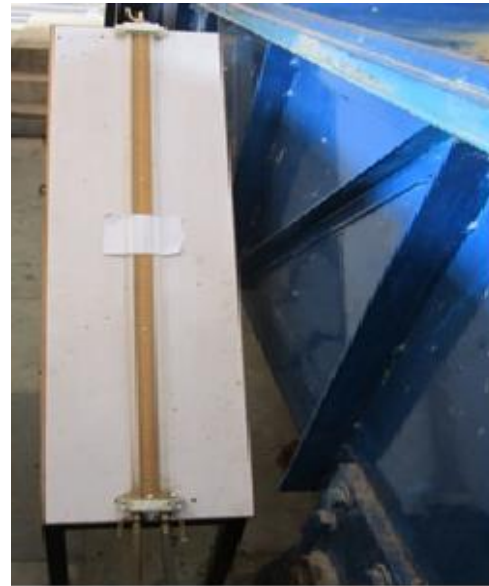


Figure 3.3-Inclined Manometer

3.4. EXPERIMENTAL PROCEDURE

3.4.1 Experimental channel

Experiments are conducted in a meandering channel having symmetric flood plains inside a concrete flume measuring in 14×1.5×0.3 the hydraulic engineering laboratory of the National Institute of Technology Rourkela, India. The channel has the width ratio(α) width ratio (α) as $1 \leq \alpha \leq 1.8$ and the aspect ratio (δ) of 5. The meandering angle of the channel is 60° . The channel is made up of cement concrete. Details of experimental parameters for meandering channel are shown in Table 3.1.

<i>Sl.no</i>	<i>Description</i>	<i>Types</i>
1.	<i>Type of Channel</i>	<i>Meandering channel</i>
2.	<i>Flume Size</i>	<i>(14*1.5*0.3)</i>
3.	<i>Meandering Channel Geometry</i>	<i>Rectangular</i>
4.	<i>Type of Bed Surface</i>	<i>Smooth</i>
5.	<i>Section of Channel</i>	<i>0.25m</i>
6.	<i>Bank Full Depth</i>	<i>0.12m</i>
7.	<i>Meandering Angle</i>	<i>60°</i>
8.	<i>Width Of Main Channel Section</i>	<i>0.28m</i>
9.	<i>Bed Slope Of Main Channel</i>	<i>0.0006</i>
10.	<i>Top Width Of Compound Channel</i>	<i>1.67m</i>
11.	<i>Type Of Flood Plain</i>	<i>Symmetric</i>
12.	<i>Wave Length (L)</i>	<i>2.230</i>
13.	<i>Amplitude (A)</i>	<i>1.130</i>
14.	<i>Sinuosity</i>	<i>2.04</i>
15.	<i>Aspect Ratio (δ)</i>	<i>2.434</i>

Table: 3.1Details of experimental parameters for meandering channel



Overhead Tank



Figure 3.4-Front view of RCC Overhead Tank Figure 3.5 - Flow straighteners



Figure 3.6 - Flooded Meandering Channel



Figure 3.7 - Flow at Bend Apex of the channel



Figure 3.8. - Tail Gate of Volumetric Tank Figure 3.9- Photo of Volumetric tank

3.4.2 LOCATION OF MEASUREMENT

The observations are recorded at the second bend apex and the next equivalent crossover of the meandering channel. An angle of 60° is formed for both the curves. This is the crossover angle or the arc angle. Channel sections along the width, i.e. perpendicular lines drawn to both the curves from these points. A steady discharge is maintained while taking the readings for the entire meandering path. A Pitot-tube with moving bridge arrangement is made to measure the velocity at different points of the flow axis of the channel. The measurements are taken at different reaches along the meander path for every section. Data are observed from left edge to the right edge of the main channel in the direction of flow. The lateral spacing of the grid points has been taken as 5cm on either side of the centerline. The Pitot tube is crossed upwards from the bed of the channel. The bed of the channel represented here is the position of the radius of the Pitot tube which is 0.2385cm from the bed. This is accomplished by setting the Pitot tube at the surface of the channel. Readings are taken on the bed and then moved up by $0.4H$, $0.6H$, $0.8H$ and $0.9H$ from the bed. H here is the average depth of water at

the each relating segment along the meander path. Fig.3.10 demonstrates the grid diagram used for the experiments.

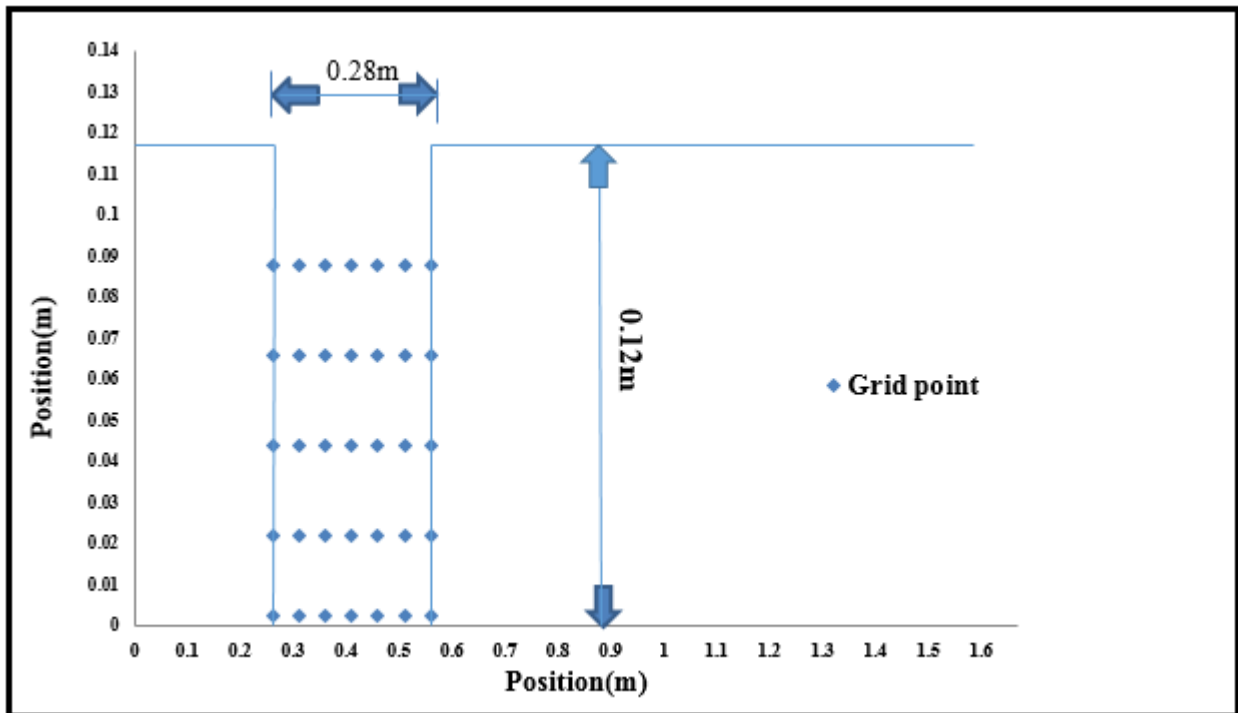


Fig.3.10 the grid diagram used for the experiments

3.4.3 MEASUREMENT OF BED SLOPE

For estimation of bed slope, the water level piezo metric tube is utilized. Water level with respect to the bed of the main channel at the upstream and then at the downstream of the flume is taken which are about 12m apart. The water level taken is from the bed of the flume without considering the thickness of the Perspex sheet. Distinction in the two corresponding points was measured. The slope is measured by dividing this level difference with the distance between the observed points. Five such readings are taken and averaged for accuracy. The slope calculated is 0.006 which is the slope of the flume or the valley slope. With a meandering channel sinuosity of 2.04.

3.4.4 MEASUREMENT OF LONGITUDINAL VELOCITY DISTRIBUTION

Pitot tube is used for the estimation of velocity. The Pitot tube arrangement is used for measurement of the pressure difference at every predefined point on the channel cross-section throughout the meander path. The Pitot tube has an external diameter of 4.7mm. The Pitot tube is attached to an inclined manometer placed on a vertical board. The inclined board has a spirit level to keep the manometers in vertical level. The connections between the Pitot tube and the manometer are made from a long transparent PVC tube of small diameter. Extra care is taken to drive out any air bubbles inside the tubes.

Pitot tube is put against the direction of flow perpendicular to it. The pressure difference at every pre-defined grid of the channel section along the meander path is accomplished. The point form velocity is measured by $v = \sqrt{2gh}$, where g is the acceleration due to gravity and h is the pressure difference. Here the tube coefficient is taken as a unit and the error because of turbulence considered insignificant while measuring velocity.

The velocity data are taken on the bed (0.002385 from bed) and then moved up by $0.2H, 0.4H, 0.6H, 0.8H$ and $0.9H$ from the bed. Here H is the average flow depth of water in the every corresponding section along the meander path. While the representation of the vertical velocity profile, the velocity value at the surface is assumed to be zero considering the no slip condition.

3.4.5 MEASUREMENT OF BOUNDARY SHEAR STRESS

Estimation of shear stress in open channel flow helps in comprehension shear bed load transport, momentum transfer, channel migration; etc. The shear forces at the bed are advantageous in the examination of bed load transfer whereas shear forces at the walls give a general survey of the channel migration pattern. Although there are a few systems methods to evaluate bed and wall shear, the Preston - tube method being an indirect estimate, is broadly utilized for experimental observations.

Preston (1954) added to a fundamental methodology for measuring local shear stress on smooth boundaries utilizing a Pitot tube in contact with the surface. His system was based on the assumption of an inner law relating the boundary shear stress to the velocity distribution near the wall. Preston showed a non-dimensional relationship between the Preston tube differential pressure ΔP , and the limit shear stress (τ) of the form:

$$\left(\frac{\tau d^2}{4\rho v^2}\right) = F\left(\frac{\Delta P d^2}{4\rho v^2}\right) \quad (1)$$

Where d is the external diameter of the Preston tube, ρ is the density of the flow, ν is the kinematic viscosity of the fluid and F is an empirical function. Patel (1965) further extended the research and his adjustment is given about of two non-dimensional parameters x^* and y^* which are utilized to change over pressure readings to boundary shear stress, where

$$x^* = \log_{10}\left(\frac{\Delta P d^2}{4\rho v^2}\right) \text{ and } y^* = \log_{10}\left(\frac{\tau d^2}{4\rho v^2}\right) \quad (2)$$

In the form

$$\text{For } y^* < 1.5 \quad y^* = 0.5x^* + 0.037 \quad (3)$$

$$\text{For } 1.5 < y^* < 3.5 \quad y^* = 0.8287 - 0.1381x^* + 0.1437x^{*2} - 0.006x^{*3} \quad (4)$$

And

$$\text{For } 3.5 < y^* < 5.3 \quad x^* = y^* + 2 \log_{10}(1.95y^* + 4.10) \quad (5)$$

In the present case, all shear stress estimations are taken at all the thirteen sections through the meander path between the two bend apexes. The pressure readings were taken utilizing pitot tube along the predefined points over all the portions purposes of the channel along the bed and side slopes. The manometer is attached to the Pitot tube which gives the head distinction between the dynamic and static pressures. Then the differential pressure is calculated from the readings on the vertical manometer by,

$$\Delta P = \rho g \Delta h \quad (6)$$

Where Δh is the distinction between the two readings from the dynamic and static, g is the acceleration due to gravity and ρ is the density of water. Here the tube coefficient is taken as a unit and the error due to turbulence is considered negligible while measuring velocity.

Accordingly, out of the Eq. 3.2-3.5, the appropriate one was chosen for processing computing the wall shear stress based on the range of x^* values. After that the shear stress value was facilitated over the whole perimeter to calculate the aggregate shear force per unit length normal to flow cross-section carried by the meandering section. The total shear in this way computed was then contrasted with the resolved component of weight force of the liquid along the flow-wise direction to check the accuracy of the measurements.

4.1 DESCRIPTION OF NUMERICAL MODEL PARAMETERS

In this study, Fluent, a Computational Fluid Dynamics simulation tool is used for model verification, which is based on the three-dimensional form of the Navier-Stokes equations. Computational Fluid Dynamics (CFD), is the branch of fluid mechanics that uses numerical methods and algorithms to analyze and solve problems that involve fluid flows. The computers are used to perform calculations which required to simulate the interaction of liquids and gases with surfaces defined by boundary conditions. Ongoing research yields software which improves the accuracy and speed of complex simulation scenarios such as transgenic or turbulent flows. The CFD based simulation relies on the combined numerical accuracy, modeling precision and computational cost.

Generally CFD uses a finite volume method (FVM). Fluent can utilize both structured and unstructured networks. In free-surface modeling, e.g. VOF (Ferziger and Peric 2002) and height of liquid (HOL) or LES, the principal equations are discretized in both space and time which generally requires transient simulation. Here Large Eddy Simulation model is used for turbulence modeling. The LES equations are discretized in both space and time. In this study the algorithms adopted to solve the combination between pressure and velocity field is PISO, the pressure implicit splitting of operatoruses in Fluent (Issa 1986). A noniterative result method PISO is used to calculate the transient problem which helps to converge the difficulties faster. When the residuals of the discretized transport equation reach a value of 0.001 or when the result do not change with further iterations, then the numerical solution is converged. To promote the convergence of the result, the changing variables are controlled during the calculations. For the simulations with an unsteady solver, the difference in the mass flow rates at the velocity inlet and pressure outlet is monitored to be less than 0.01% in

the final solution. Hence, a number of extra time steps are added to verify the stability of the flow field in the final solution.

The essential source of almost all CFD complications is the Navier- Stokes equations, which express any single-phase fluid flow. These equations can be simplified by take away terms describing viscosity to yield the Euler equations. Moreover simplification, by taking away terms.

Describing vorticity yields the full potential equations. Finally, for small perturbations in subsonic and supersonic flows these equations can be linearized potential equations

$$\frac{\partial}{\partial t}(\rho u_i) + \frac{\partial(\rho u_i u_j)}{\partial z_i} = \frac{\partial}{\partial z_j} \left(\mu \frac{\partial \sigma_{ij}}{\partial z_j} \right) - \frac{\partial p}{\partial z_i} - \frac{\partial \tau_{ij}}{\partial z_j} \quad (7)$$

Where σ_{ij} and τ_{ij} are normal and shear stress component on any assumed plane normal to I along j direction. u_i, u_j are the time averaged instantaneous velocity component along i, j directions, p= pressure, ρ = density, μ =co-efficient of viscosity.

4.2 TURBULENCE MODELLING

“Turbulence is an asymmetrical movement which all in all shows up in liquid, fluids, or gaseous, when they flow past strong surfaces or even when neighboring streams of the same fluid flow past or more than each other.” GI Taylor and von Karman, 1937

“Turbulent fluid movement is an unpredictable state of flow in which the different amounts demonstrate a random variation with time and space coordinates, so that statistically distinct normal qualities can be observed.” Hinze, 1959

The flow in a channel is turbulent in nature. Turbulent flow is a flow administration portrayed by chaotic and stochastic property changes. This incorporates low momentum diffusion, high momentum convection, and quick variation of pressure and velocity in space and time.

Turbulence happens when the latency compels in the fluid get to be huge contrasted with viscous forces, and is portrayed by a high Reynolds Number. For the most part turbulence is irregular dimensional time-ward eddying movement with numerous substantial scale eddies. The three dimensional nature of turbulent flows are decayed into two different parts, i.e. mean part and fluctuation part, which is no doubt understood as Reynolds decay. The spatial character of turbulence reveals the eddies with wide range scales. In turbulence, isolated fluid particles are united close together by eddying movement which causes the successful trade of heat, mass and momentum. The turbulence in meandering channel is unpredictable and the flow structure included in it makes uncertainty in forecast of flow variables. Especially in meandering channels, turbulent structures are summed by large shear layers created by distinction of velocity between main channels. This large shear layer region creates vortices both longitudinal as well as vertical direction. The anisotropy and inhomogeneity of turbulent structure cause an auxiliary current, which makes the velocity dip and influences the flow variables. Hence, in this study an exertion is made to perceive the effect of the turbulence in meandering channel. Joining turbulence, CFD considers the prompt velocity segment and a fluctuating speed part given as

Instantaneous velocity = mean velocity + fluctuating velocity given like

$$u = \bar{u} + u' \quad (8)$$

The Navier-Stokes momentum equation is taken as:

$$\frac{\partial \rho u_i u_j}{\partial x_j} = -\frac{\partial p}{\partial x_i} + \frac{\partial}{\partial x_j} \left(\mu \frac{\partial u_j}{\partial x_j} \right) \quad (9)$$

By substituting $\bar{u} + u'$ for u in equation (4.2) and averaging the term we get:

$$\frac{\partial \bar{u}}{\partial x} = \frac{\partial (\overline{\bar{u} + u'})}{\partial x} = \frac{\partial \bar{u}}{\partial x} \quad (10)$$

For non-linear function the equation (1) becomes

$$\frac{\partial(uu)}{\partial x} = \frac{\partial \overline{uu}}{\partial x} + \frac{\partial \overline{u'u'}}{\partial x} \quad (11)$$

Now the Navier-Stokes equations become:

$$\frac{\partial \overline{u}}{\partial x_j} = 0$$

$$\frac{\partial \rho \overline{u_i u_j}}{\partial x_j} = -\frac{\partial \overline{p}}{\partial x_j} + \frac{\partial}{\partial x_j} \left(\mu \frac{\partial \overline{u_i}}{\partial x_j} \right) - \frac{\partial \rho (u'_i u'_j)}{\partial x_j} \quad (12)$$

The term $\frac{\partial \rho (u'_i u'_j)}{\partial x_j}$ is known as the ‘‘Reynolds stress’’. Due to closure problem of both the equations 4.5 and 4.6 we have to come up with ways of replacing the extra terms with other terms that were known or devising ways of calculating these terms. A first attempt at closing the equations is:

$$\frac{\partial}{\partial x_j} \left(\mu \frac{\partial \overline{u_i}}{\partial x_j} \right) = \frac{\partial \rho (u'_i u'_j)}{\partial x_j} \quad (13)$$

In equation (4.7) both terms represent a diffusion of energy. The term $\frac{\partial}{\partial x_j} \left(\mu \frac{\partial \overline{u_i}}{\partial x_j} \right)$ represent diffusion of energy through viscosity and the other term $\frac{\partial \rho (u'_i u'_j)}{\partial x_j}$ represent the diffusion through turbulence. By defining μ_t as turbulent viscosity, equation (4.6) becomes:

$$\frac{\partial \rho \overline{u_i u_j}}{\partial x_j} = -\frac{\partial \overline{p}}{\partial x_j} + \frac{\partial}{\partial x_j} \left((\mu + \mu_t) \frac{\partial \overline{u_i}}{\partial x_j} \right) \quad (14)$$

To enable the effects of turbulence to be predicted, a large amount of CFD research has concentrated on methods which make use of turbulence models. Turbulence models have been specifically developed to account for the effects of turbulence without recourse to a prohibitively fine mesh and direct numerical simulation. Most turbulence models are arithmetical turbulence models, as mentioned below.

4.2.1 Turbulence Models

- Algebraic (zero-equation) model.
- K- ϵ , RNG k- ϵ model.
- Shear stress transport model.
- K- ω model.
- Reynolds stress transport model (second moment closure).
- K- ω Reynolds stress.
- Detached eddy simulation (DES) turbulence model.
- SST scale adaptive simulation (SAS) turbulence model.
- Smagorinsky large eddy simulation model (LES).
- Scalable wall functions.
- Automatic near-wall treatment, including integration to the wall.
- User-defined turbulent wall functions and heat transfer.

4.3 GOVERNING EQUATION

Here the governing equation utilized is based on conservation of mass, momentum and energy. The C.F.D package, in particular Fluent was employed to solve the governing equations, which uses Finite Volume Method (FVM) to solve the equations. FVM includes discretization and integration of the governing equations over the control volume. The numerical method FVM was taking into account the essential protection, which is applied for solving the partial difference, i.e. Navier-Stokes equation then calculates the values of the variables, averaged across the volume. The integration of the equations over each control volume results in a balance equation. The conservation law is enforced on small control volumes which is defined by computational mesh. The set of balance equations, then discretized as for an arrangement of discretization schemes and is solved by using the initial and boundary conditions.

The governing Reynolds Averaged Navier-Stokes and continuity equations are stated:

$$\frac{\partial(\rho)}{\partial t} + \frac{\partial(\rho u_i)}{\partial x_i} = S_m \quad (15)$$

$$\frac{\partial(\rho u_i)}{\partial t} + \frac{\partial(\rho u_i u_j)}{\partial x_j} = -\frac{\partial p}{\partial x_j} + \frac{\partial}{\partial x_j} \mu \left[\frac{\partial u_i}{\partial x_j} + \frac{\partial u_j}{\partial x_i} \right] + \frac{\partial(-\rho \overline{u'_i u'_j})}{\partial x_j} \quad (16)$$

Where t =time, u_i = i -th component of the Reynolds-averaged velocity, x_i = i -th axis, ρ =water density, p = Reynolds averaged pressure, g =acceleration due to gravity, μ =viscosity (here it is equal to zero), S_m =mass exchange between two phases (water and air).

Here for unsteady solves the time-averaged values of velocities and other solution variables are taken instead of instantaneous values. The term $(-\rho \overline{u'_i u'_j})$ is called as Reynolds Stress. To link the mean rate of deformation with Reynolds stresses, Boussinesq hypothesis is used:

$$(-\rho \overline{u'_i u'_j}) = \mu_t \left(\frac{\partial u_i}{\partial x_j} + \frac{\partial u_j}{\partial x_i} \right) \quad (17)$$

Where μ_t =the turbulent viscosity

4.3.1 VOLUME OF FLUID (VOF) MODEL

The VOF formulation in ANSYS FLUENT is generally used to compute a time dependent Solution. In VOF model, while solving a momentum equation for each phase the interface must be tracked as an Eulerian variation in which the secondary phase is not dispersed within the primary phase but rather there is an interface between the phases. The volume of fluid (VOF) method is a computational tool for the analysis of free surface flows (Hirt and Nichols 1981). For the volume fraction of one (or more) of the phases, the interface between the phases is accomplished by the solution of a continuity equation. For the q^{th} phase, this equation has the subsequent form (Rahimzadeh et al. 2012):

$$\frac{\partial \alpha_q}{\partial t} + \nabla \cdot (\vartheta \cdot \alpha_q) = 0 \quad (18)$$

Where α_q is volume fraction of the q^{th} phase.

In each control volume, the volume fractions of all phases sum up to unity. The following three conditions are possible for each cell:

If $\alpha_q = 0$, the cell is empty.

If $\alpha_q = 1$, the cell is full.

If $0 < \alpha_q < 1$, the cell contains the interface between the q^{th} phase and one or more other phases. In each cell the average properties are computed according to the volume fraction of each phase. VOF method was developed to trace the moving free surface of the incompressible viscous flow.

4.3.1.1 VOLUME FRACTION EQUATION

For the volume fraction of one (or more) of the phases the tracking of the interface(s) between the phases is accomplished by the solution of a continuity equation. For the q^{th} phase the volume fraction equation is defined as:

$$\frac{1}{\rho_q} \left[\frac{\partial}{\partial t} (\alpha_q \rho_q) + \nabla \cdot (\alpha_q \rho_q \vec{v}_q) \right] = S_{\alpha_q} + \sum_{p=1}^n (m_{pq} - m_{qp}) \quad (19)$$

Where m_{qp} indicates the mass transfer from phase q to phase p.

m_{pq} indicates the mass transfer from phase p to phase q.

Here S_{α_q} , the source term is equal to zero. But sometimes a constant or a user defined mass source is specified for each phase.

The volume fraction equation will not be solved for the primary phase. The primary phase volume fraction will be computed based on:

$$\sum_{p=1}^n \alpha_q = 1 \quad (20)$$

4.3.1.2 MATERIAL PROPERTIES

By the presence of the component phases, the properties appearing in the transport equations are determined in each control volume. In a two-phase modelling, if the phases are represented by the subscripts 1 and 2, and the mixture density in each cell is given by:

$$\rho = \alpha_2 \rho_2 + (1 - \alpha_2) \rho_1 \quad (21)$$

In general, for n phase system, the volume-fraction-averaged density takes on the following form:

$$\rho = \sum \alpha_q \rho_q \quad (22)$$

All other properties (e.g., viscosity) are also computed in this way.

4.3.1.3 MOMENTUM EQUATION

A single momentum equation is solved throughout the domain and the resulting velocity field is shared among the phases. The momentum equation is dependent on the volume fractions of all phases through the properties ρ and μ and the equation is given as.

$$\frac{\partial}{\partial t} (\rho \vec{v}) + \nabla \cdot (\rho \vec{v} \vec{v}) = -\nabla p + \nabla \cdot [\mu (\nabla \vec{v} + \nabla \vec{v}^T)] + \rho \vec{g} + \vec{F} \quad (23)$$

In shared-field approximation when large velocity differences exist between the phases, the accuracy of the velocities computed near the interface is undesirably affected.

4.3.2 MIXTURE MODEL

The mixture model is a simplified multiphase model. The mixture model allows to select granular phases and calculates all properties of the granular phases. Generally it is applied for in liquid-solid flows.

4.3.2.1 CONTINUITY EQUATION

$$\frac{\partial}{\partial t} (\rho_m) + \nabla \cdot (\rho_m \vec{v}_m) = 0 \quad (24)$$

Where \vec{v}_m is the mass average velocity.

$$\vec{v}_m = \frac{\sum_{k=1}^n \alpha_k \rho_k \vec{v}_k}{\rho_m} \quad (25)$$

And ρ_m is the mixture density.

$$\rho_m = \sum_{k=1}^n \alpha_k \rho_k \quad (26)$$

α_k is the volume fraction of phase k.

4.3.2.2 MOMENTUM EQUATION

The momentum equation for the mixture can be obtained by summing the individual momentum equations for all phases. It can be expressed as:

$$\frac{\partial}{\partial t} (\rho_m \vec{v}_m) + \nabla \cdot (\rho_m \vec{v}_m \vec{v}_m) = -\nabla p + \nabla \cdot [\mu_m (\nabla \vec{v}_m + \nabla \vec{v}_m^T)] + \rho_m \vec{g} + \vec{F} + \nabla \cdot (\sum_{k=1}^n \alpha_k \rho_k \vec{v}_{dr,k} \vec{v}_{dr,k}) \quad (6.1)$$

Where n is the number of phase, \vec{F} is the body force and μ_m is the viscosity of the mixture and defined as

$$\mu_m = \sum \alpha_k \mu_k \quad (27)$$

$\vec{v}_{dr,k}$ is the drift velocity for secondary phase k.

Where

$$\vec{v}_{dr,k} = \vec{v}_k - \vec{v}_m \quad (28)$$

4.3.2.3 VOLUME FRACTION EQUATION FOR SECONDARY PHASE:

FROM THE CONTINUITY EQUATION FOR SECONDARY PHASE P, THE VOLUME FRACTION EQUATION P CAN BE OBTAINED AS:

$$\frac{\partial}{\partial t} (\alpha_p \rho_p) + \nabla \cdot (\alpha_p \rho_p \vec{v}_m) = -\nabla \cdot (\alpha_p \rho_p \vec{v}_{dr,p}) + \sum_{q=1}^n m_{qp} - m_{pq} \quad (29)$$

4.3.2.4 Smagorinsky Model

In this study Smagorinsky model is used to carry out the simulation. LES is modelled most simply by an eddy viscosity model and the SGS stress tensor, τ_{ij} , aids in providing model closure for the LES. In these models the SGS stress tensor is related to the determined strain rate tensor $\overline{S_{ij}}$ throughout a scalar eddy viscosity coefficient. The SGS stress tensor is written as:

$$\tau_{ij}^R = 2\rho v_R \overline{S_{ij}} + \frac{1}{3} \delta_{ij} \tau_{kk}^R \quad (6.5)$$

Where $\overline{S_{ij}}$ is defined as:

$$\overline{S_{ij}} = \left(\frac{\partial \overline{U_i}}{\partial x_j} \right) + \frac{\partial \overline{U_j}}{\partial x_i} \quad (6.6)$$

Where the eddy viscosity of the residual motion, $v_R = C_s^2 l^2 (2\overline{S_{ij}S_{ij}})^{1/2}$ (30)

Where C_s is the Smagorinsky constant.

5. METHODOLOGY OF ANSYS

The process of the numerical simulation of fluid flow using the above equation generally involves the four altered steps and the details are given below.

(a) *Problem identification*

1. Defining the modelling goals
2. Identifying the domain to model

(b) *Pre-Processing*

1. Creating a solid model to characterize the domain (Geometry Setup)
2. Create and design the mesh (grid)

(c) *Solver*

1. Set up the physics
 - Defining the condition of flow (e.g. turbulent, laminar etc.)
 - Specification of appropriate boundary condition and temporal condition.
2. Using different numerical schemes to discretize the governing equations.
3. Controlling the convergence by iterating the equation till accuracy is achieved
4. Compute Solution by Solver Setting.
 - Initialization
 - Solution Control
 - Monitoring Solution

(d) *Post processing*

1. Visualizing and examining the results
2. X-Y Plots
3. Contour Draw

5.1.1 PREPROCESSING

In this initial step all the important data which characterizes the issue is allotted by the user. This comprises of geometry, the properties of the computational grid, different models to be utilized, and the quantity of Eulerian stages, the time step and the numerical plans.

5.1.1.1 Creation Geometry

The initial phase in CFD analysis is the clarification and production of computational geometry of the fluid flow district. A predictable edge of reference for coordinate axis was reference for creation of geometry. Here in coordinate system, x axis related the stream wise direction of fluid flow. Y axis aligned with the lateral direction which shows the width of channel bed and Z axis represented the vertical component or aligned with depth of water in the channel. The origin was placed at the upstream boundary and corresponded with the base of the centre line of the channel. The water flowed along the positive direction of the x-axis. The simulation was done on a meandering channel. The setup of the meandering channel is shown in Figure 5.1 and the cross-section of channel geometry is shown in Figure 5.2.

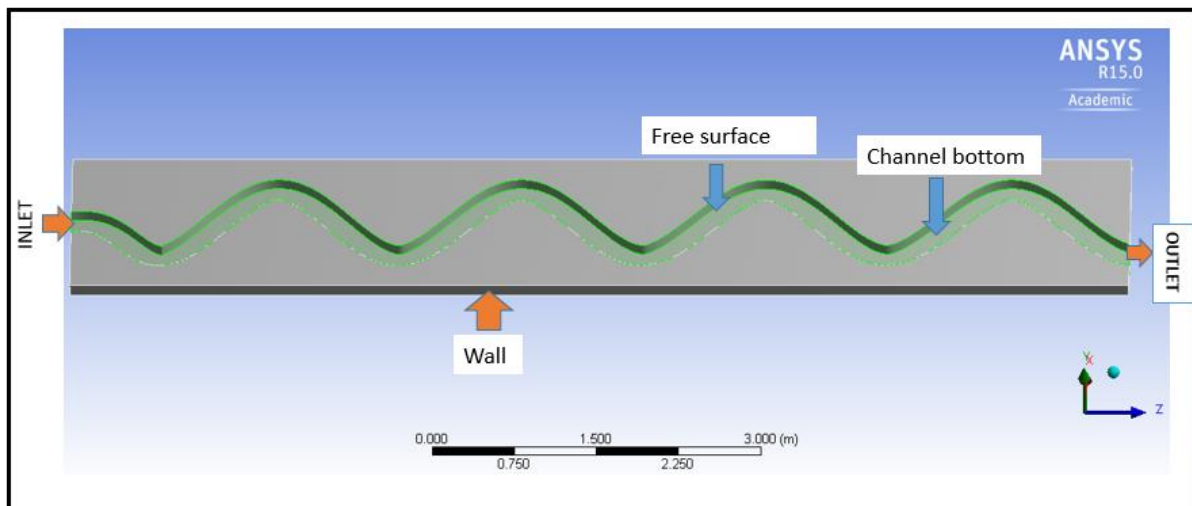


Figure 5.1. Geometry Setup of a meandering Channel

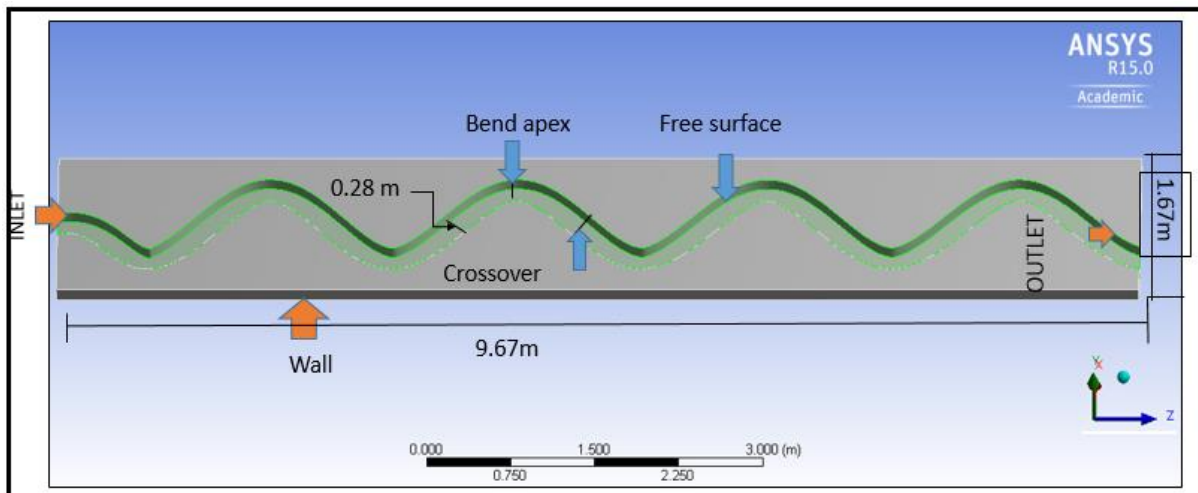


Figure 5.2. Cross sectional geometry of the meandering channel

As can be seen from the Figure 5.2, the channel geometries were 0.30 m height, 1.67 m width and 2m length. In the meandering channel, the width of main channel was 0.28m and main channel height was 0.12m. In addition the fact that the channel is rectangular.

During the model construction, an additional consideration is to classify any entity of the geometry which need to be identified for future location as to recognize a particular domain for conduct some analysis and for applying boundary condition upon a particular domain.

Figure 5.3 shows the geometrical entities used in a meandering channel.

For identify the domain six different surfaces are generated.

- Inlet
- Outlet
- Free Surface
- Side Wall
- Channel Bottom
- Centre line

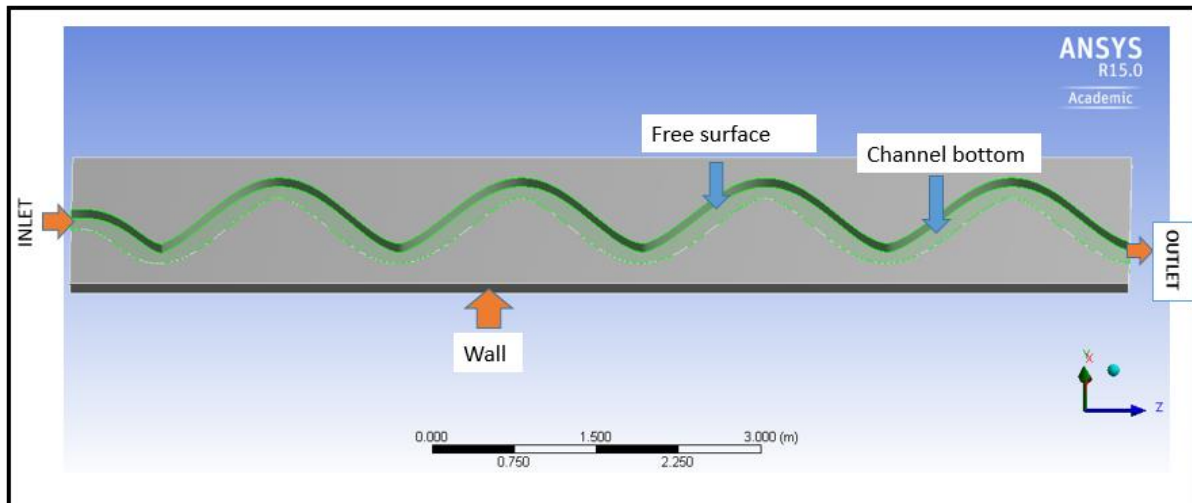


Figure 5.3 Different Geometrical entities used in a meandering channel

5.1.2 MESH GENERATION

Second and very most important step in numerical analysis is setting up the grid related with the construction of geometry. The Navier-Stokes Equations are non-linear partial differential equations, which consider the whole fluid domain as a continuum. In order to simplify the problem the equations are simplified as simple flows have been directly solved at very low Reynolds numbers. The simplification can be made using what is called discretization. The construction of mesh involves discretizing or subdividing the geometry into the cells or elements at which the variables will be computed numerically. By using the Cartesian coordinate system, the fluid flow governing equations i.e. momentum equation, continuity equation are solved based on the discretization of domain. The CFD analysis needs a spatial discretization scheme and time marching scheme. Meshing divides the continuum into finite number of nodes. Usually the domains are discretized by three different ways i.e. Finite element, Finite Volume and Finite Difference Method. Finite element method is based on dividing the domain into elements. In finite element method the numerical solutions are obtained by integrating the shape function and weighted factor in an appropriate domain. This method is suitable for both structured and unstructured mesh. But the Finite Volume method

divides the domain into finite number of volumes. Finite volume method solves the discretization equation in the centre of the cell and calculates some specified variables. The values of quantities, such as pressure, density and velocity that are present in the equations to be solved are stored at the centre of each volume. The flux into a region is calculated as the sum of the fluxes at the boundaries of that region. As the values of quantities are stored at nodes but not at boundaries this method requires some interpolation at nodes. Generally finite Volume method is suitable for unstructured domain. Whereas finite Difference method is based on approximation of Taylor's series. This method is more suitable for regular domain.

Domain	Nodes	Elements	Tetrahedra	Hexahedra
Fluid	10112	6615	0	6615
Solid	61793	171118	111657	0
All Domains	71905	177733	111657	6615

Table: 5.1. Mesh information for FLU

Domain	Minimum Face Angle	Maximum Face Angle	Maximum Edge Length Ratio	Maximum Element Volume Ratio
Fluid	46.1583[degree]	134.273[degree]	1.44154	1.25798
Solid	3.54265[degree]	170.58[degree]	7.61865	118.397
All Domains	3.54265[degree]	170.58[degree]	7.61865	118.397

Table: 5.2. Mesh statistics for FLU

For transient problems an appropriate time step needs to be specified. To capture the required features of fluid flow within a domain, the time step should be sufficiently small but not too much small which may cause waste of computational power and time. Spatial and time discretization are linked, as evident in the Courant number.

5.1.2.1 Courant Number

A criterion frequently used to determine time step size is known as Courant number. The Courant number stops the time step from being large enough for information to travel entirely through one cell during one iteration. For explicit time stepping schemes Courant number should not be greater than 1. For implicit time stepping schemes this number may be higher than 1. The Courant number is defined as:

$$C_r = \frac{\bar{U}\Delta t}{\Delta l} \quad (31)$$

Where C_r is the Courant number, \bar{U} is the average velocity, Δt is the maximum time step size and Δl is the largest grid cell size along the direction of flow.

A mesh consists of too few nodes cause quick solution of simulation but not a very accurate one. However a very dense mesh of nodes causes excess computational time and memory. For analysis of CFD, more nodes are required in some areas of interest, for example near wall and wake regions, in express to capture the large variation of fluid properties. Thus, structure of grid lines causes additional wastage of computer storage due to further refinement of mesh. Here the flow domain is discretized using structured grid and body-fitted coordinates.

It must be illustrious that the running time is low and it is obtained by grid-independent results. The grid arrangement must be fine sufficient, especially near the wall boundaries (in order to consider the viscous flow), nearer to converge (the rapid changes area) and at free surface. In this numerical simulation, various computational trials are conducted with different number of grid cells. It is done that the results are almost independent from the grid size and running time is most favourable. The detailed meshing of the flow domain with viewis shown in Figure 5.4.

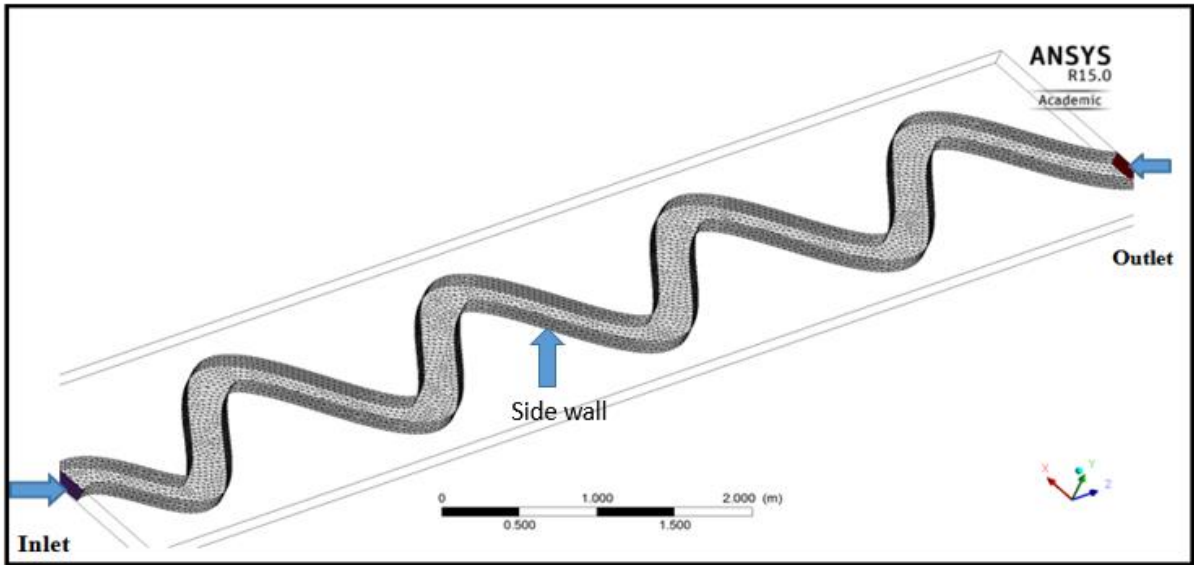


Figure 5.4. Meshing of Inlet, Outlet and free surface of a meandering channel

5.1.2.2 SETUP PHYSICS

For a given computational domain, boundary conditions are compulsory which can occasionally over specify or under-specify the problem. Usually, after imposing boundary conditions in non-physical domain may lead to failure of the solution to converge. It is therefore important, to understand the meaning of well-posed boundary conditions. The boundary conditions implemented for this study are shown in Figure 5.5. Subsequently these conditions are discussed in the follows:

Domain	Boundaries	
fluid	Boundary - contact region trg	
	Type	INTERFACE
	Boundary - free_surface_symmetry	
	Type	SYMMETRY
	Boundary - inlet	
	Type	VELOCITY-INLET
solid	Boundary - outlet	
	Type	PRESSURE-OUTLET
	Boundary - channel_bottom	
	Type	WALL
	Boundary - contact region src	
	Type	INTERFACE
solid	Boundary - wall	
	Type	WALL

Table.5.3: Boundary information for FLU

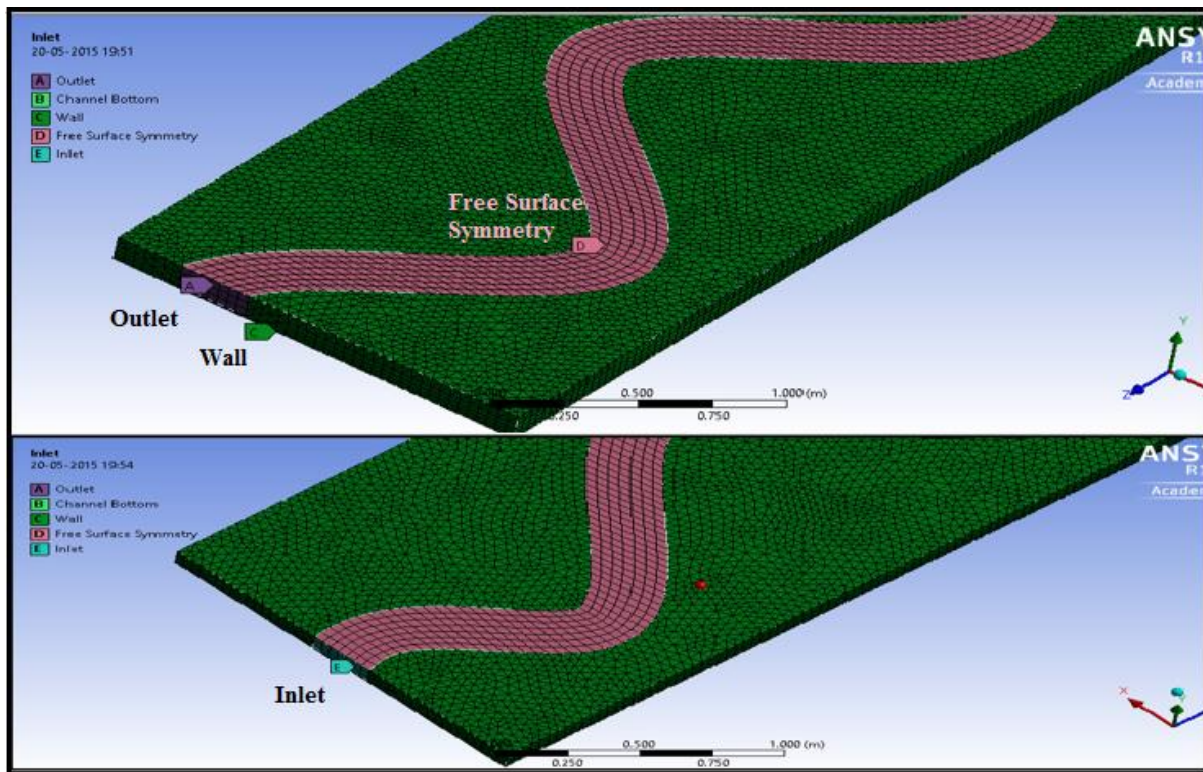


Figure 5.5. A Schematic Diagram of meandering channel with boundary conditions

5.1.2.3 Inlet and Outlet Boundary Condition

All of the channels reported were performed with translational periodic boundaries in the stream wise direction of the flow which allow the values on the inlet and outlet boundaries to coincide. Further the pressure gradient was specified across the domain to drive the flow. To initialize the flow, a mean velocity is specified over the whole inlet plane upon which velocity fluctuations are imposed. The inlet mean velocities are derived from the experimental average values. The mean velocity was specified over the whole inlet plane and is computed by $U_{in} = Q/A$, where Q is the flow discharge of the channel and A is the cross sectional area of the inlet. In order to simplify slope changes and specify the pressure gradient the channel geometries were all created flat. The effects of gravity and channel slope implemented via a resolved gravity vector. Here the angle θ represents the angle between the bed of the channel and the horizontal, the gravity vector is resolved in x, y and z components as :

$$(\rho g \sin \theta, 0, -\rho g \cos \theta) \quad (32)$$

Where θ = angle between bed surface to horizontal axis and $\tan \theta$ =slope of the channel. Here, the x component causes the direction responsible for flow of water along the channel and the z component is responsible for creating the hydrostatic pressure upon the channel bed. From the simulation, “z” component of the gravity vector ($-\rho g \cos \theta$) is found to be responsible for the convergence problem of the solver.

5.1.2.4 Wall

The channel walls i.e. side walls and bottom are represented as non-slip walls. A no-slip boundary condition is the most common boundary condition implemented at the wall and prescribes that the fluid next to the wall assumes the velocity at the wall, which is zero i.e.

$$U = V = W = 0 \quad (33)$$

5.1.2.5 Free-Surface

For top free surface generally symmetry boundary condition is used. This specifies that the shear stress at the wall is zero and the stream wise and lateral velocities of the fluid near the wall are not retarded by wall friction effects as with a no-slip boundary condition. This condition follows that, no flow of scalar flux occurs across the boundary. Thus, there is neither convective flux nor diffusive flux across the top surface. In implementing this condition normal velocities are set to zero and values of all other properties outside the domain are equated to their values at the nearest node just inside the domain. Here the experimental bulk velocity of the flow is initially approximated as:

$$U = 0.569 \text{ m/s}, V = 0, W = 0 \text{ and } \frac{\partial u}{\partial x} = 0, \text{ for } \alpha = 2.54 \text{ and}$$

$$U = 0.51 \text{ m/s}, V = 0, W = 0 \text{ and } \frac{\partial u}{\partial x} = 0, \text{ for } \alpha = 9.33$$

5.1.3 NEAR WALL MODELLING

Nearer to a no-slip wall, there are strong gradients in the dependent variables. Generally at boundary layer regions, rapid variation of flow variables occurs i.e. in viscous layer. Also in boundary layer viscous effects on the transport processes are large. Further transition from viscous to buffer layer produces large variation within the flow features. Therefore, it is essential to imitate these changes in the discretization process to carry out simulation process successfully. Hence, near wall modelling is done to include these changes in flow features for this study. The representation of these processes within a numerical simulation raises the problems about the viscous effects at the wall and how to resolve the rapid variation of flow variables, which occurs within the boundary layer region. Experimental and numerical analysis have shown that the near-wall region can be subdivided into two layers. The flow will be stationary at the wall itself and therefore there will be a narrow boundary layer of laminar flow which is call as “viscous sublayer”. At viscous sublayer, molecular viscosity plays a dominant role in momentum and energy transfer problem. Further away from the wall there is mixing process takes place and produces turbulence, is known as the “logarithmic layer”. Finally, there exists a region between the viscous sublayer and the logarithmic layer which is called as the “buffer layer”. At buffer layer the effects of molecular viscosity and turbulence are of equally significance. The Figure 5.10 exemplifies these subdivisions of velocity profile as the near-wall region, buffer and outer region of the flow.

Wall functions are the most popular technique to account wall effects. The mesh node next to the wall is placed in the turbulent boundary layer and a model of flow in that region is used for defining wall function. At that point the sets values of velocity, pressure and turbulent quantities are replaced the solution with the Navier-Stokes Equation. In CFX the wall-function approach is an extension of the method derived by Launder and Spalding

(1974). The logarithmic nature of the velocity profile in open channels is well known as “log-law of the wall”. Assuming that the logarithmic profile practically approximates the velocity distribution near the wall and numerically computes the fluid shear stress as a function of the velocity at a given distance from the wall. This is known as “wall function”. The Figure 5.11 illustrates wall functions. In the log-law region, the near wall tangential velocity is related to the wall shear stress τ_w by means of a logarithmic relation.

$$u^+ = \frac{U_t}{u_*} = \frac{1}{k} \ln(y^+) + C \quad (34)$$

$$\text{Where } y^+ = \frac{\rho \Delta y u_*}{\mu} \quad (35)$$

$$u_* = \left(\frac{\tau_w}{\rho} \right)^{1/2} \quad (36)$$

Here u^+ is the near wall velocity, u_* is the friction velocity, U_t is the known velocity tangent to the wall at a distance of Δy from the wall, y^+ is the dimensionless distance from the wall, τ_w is the wall shear stress, k is the von Kármán constant and c is a log-layer constant dependent on wall roughness. The execution of a wall function eliminates the need for very fine meshes at the time of discretization process nearer to the wall, which resolve the flow down to the wall.

However, when performing LES method, an extremely fine grids are required to resolve the viscous sub-layer down to a wall at normal distance y^+ , where, $y^+ = (u_* y)/\nu$, y = depth at a point. Therefore LES directly computes the variables down to the wall without the application of a wall function. Even though LES does not replace the N-S equations with a wall function near the wall, it uses a wall-function approximation to make an estimate of u_* at the wall. This is accurate for numerically simulated open channel flows and involves fitting a log-law to the mean velocity profile and calculating a shear velocity from it. Thomas and Williams (1995a) adopt this method and draw comparison between u^+ and y^+ for experiment, LES and Equation 5.27, for which all are comparable. Nezu and Rodi (1986) show a wall-

function approximation to be satisfactory for wide channels, and Gavrilakis (1992) suggest that the logarithmic profile (based on local shear velocity) found for turbulent flow in a square duct exhibits a logarithmic region similar to Equation 5.27. The profile for the channel simulated in Thomas and Williams (1995a) was considered intermediate between square duct and open channel.

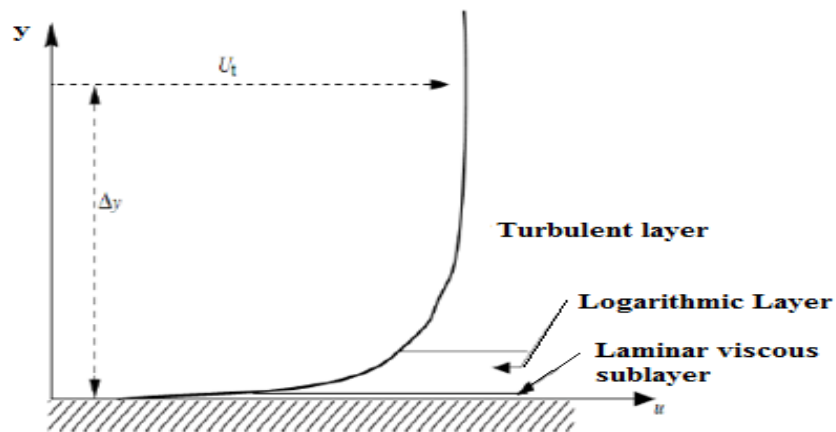


Figure 5.6. The subdivisions of the near-wall region

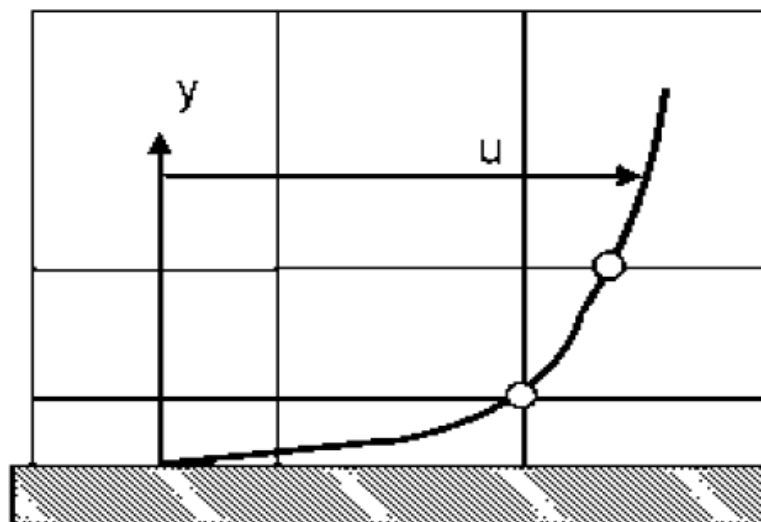


Figure 5.7 Wall functions used to resolve boundary layer

5.2 METHODOLOGY OF CONVEYANCE ESTIMATION SYSTEM (CES)

The Environment Agency for England and Wales identified the need to reduce the uncertainty associated with flood level prediction through incorporating the recent research

advances in estimating river and floodplain conveyance in response to the cry for a simpler, user friendly yet physics based approach instead of prevalent empirical based approaches as used to be done by applying Manning's or Chezy's formula. The new conveyance system has been developed taking into account the advances made in research in channel conveyance, the vast diversity in roughness of river and associated floodplains and finally understanding and quantifying the uncertainty due to methodology adopted and model inputs (Project Record W5A, 2001-04). To improve the conveyance prediction for solution of the St Venant Equations. Also, it can serve as a tool for further educational/academic research across the universities and institutes Conveyance Estimation System was conceived and developed after certain shortcomings were pointed out in the existing ID models such as ISIS, HECRAS, and MIKE11 in their methodology of estimating conveyance.

The CES includes a component termed the 'Roughness Advisor', which provides advice on the surface friction or 'roughness', and another component termed the 'Conveyance Generator', which determines the channel capacity based on both this roughness and the channel morphology. In addition, the CES includes a third component, the 'Uncertainty Estimator', which provides some indication of the uncertainty associated with the conveyance calculation.

The primary outputs from the CES components are:

- Roughness Advisor: roughness values
- Conveyance Generator: stage-conveyance relationship
- Uncertainty Estimator: upper and lower bands for the stage-conveyance relationship.

5.2.1. Development of the model for CES

Two important approaches e.g. The Energy loss approach (Ervine & Ellis, 1987; Shiono et al, 1999) and The Reynolds Averaged Navier-Stokes (RANS) Approach (Shiono&Knight, 1990; James &Wark, 1992; Ervine et al, 2000) were selected for further testing and subsequent adoption in the CES package. Both the approaches were then reviewed in terms of:

- The theoretical and physical basis of the method.
 - Consideration of all energy losses.
 - Representation of energy loss hierarchy with variation in water level/sinuosity e.g. changes in secondary current direction and structure.
 - Previous testing of the method against physical model and real river data.
 - Reliable and readily available calibration/empirical parameters.
 - The ease of the method implementation for a range of channel types.
 - The outputs i.e. discharge for a given water level (high priority), lateral velocity/bed shear stress distributions.

where:

ρ = fluid density (kg/m³)

g = gravitational acceleration (m/s²)

H = local water depth normal to the bed (m)

h = water level (m)

x = streamwise direction parallel to the bed (m)

y = lateral distance across section (m)

Ud = depth-averaged streamwise velocity (m/s)

Vd = depth-averaged lateral velocity (m/s)

τ_b = bed shear stress (N/m²)

τ_{yx} = Reynolds stress (N/m²)

β' = coefficient for the influence of lateral bed slope on the bed shear stress

And the terms represent the:

(I) variation in hydrostatic pressure along the reach

$$\underbrace{\rho g H \frac{dh}{dx}}_{(I)} - \underbrace{\beta' \tau_b}_{(II)} + \underbrace{\frac{\partial}{\partial y} (H \bar{\tau}_{yx})}_{(III)} = \underbrace{\frac{\partial}{\partial y} [H (\rho \overline{UV})_d]}_{(IV)} \quad (37)$$

5.2.1.2. Outline of Steps for Modelling through CES

The user has to use the steps as outlined below to run the software tool to obtain the results of simulation through CES. First the roughness file named *.RAD File has to be created for the physical domain where the flow has to be simulated. For this the user needs to choose various roughness components comprising of vegetation, ground material and irregularity for all the three zones of the channel namely ;bed, bank and floodplain by selecting from the catalogue available for various morphotypes of vegetation, substrates for ground material and irregularity types inside the component ‘_Roughness Advisor’ of CES.

- At this stage if there is some doubt about the actual value of roughness of the real vegetation , irregularity & substrates etc. the user can assign the lower and upper values for the assigned value so that CES accordingly computes the uncertainty band for the result outputs.

- After saving the RAD file, the Conveyance generator component needs to be activated for creating *.GEN file for where all general data for the physical domain such as name of reach, sinuosity, cross section details measurement (through lateral offsets and heights of various points on the cross section from bed to top of water surface) etc. are to be entered.

- Then all zones of the reach e.g. bed, bank & floodplains need to be assigned the roughness values as assigned previously through RAD file.

- By exercising the options available in advanced options tab in Conveyance Generator for various parameters e.g. no. of depth intervals, minimum depth . used in calculation, value of lateral eddy viscosity in the main channel, no. of vertical segments used in computation, relaxation parameter for convergence criteria, maximum no. of iterations and wall height multiplier etc. the user can vary the results of simulation so as to get the best possible outcome. Also, there is a separate option of adopting Colebrook-White solver for experimental flumes where the temperature during the experiment has to be mentioned. Finally the Conveyance Generator provides outputs for the whole cross-section, which are given at every depth, as below: which are given at every depth, as below

- Total flow rate Q (m³/s)
- Area A (m²)
- Average velocity U_{av} (m/s)
- Conveyance K (m³/s)
- Froude Number $Fr(R = \text{hydraulic mean depth or ratio of area to surface width})$
- Reynolds Number $Re[(uRh)/\nu$ and Rh is the hydraulic radius]
- Coriolis' (energy) coefficient α
- Boussinesq's (momentum) coefficient β
- Surface water width B (m).

For each depth, the lateral variation of the following variables is also available.

- Zco-ordinate (i.e. Channel bed profile)
- Unit flow q (m²/s)
- Depth-averaged velocity Ud (m/s)
- Unit conveyance k ($= K/m$) (m²/s)
- Shear velocity U^* (m/s)
- Bed shear stress τ (N/m²)
- Bed friction(f)
- Dimensionless eddy viscosity (λ)

5.3CCHE2D MODEL

The CCHE modelling, analysis system is an integrated system which is composed of a Graphical Users Interface (CCHE-GUI), a separate hydrodynamic numerical model (CCHE2D model) and a structured mesh generator (CCHE2D Mesh Generator).

- CCHE-GUI provides file management, run management, results visualization, and data reporting etc.
- CCHE2D Model is the numerical engine for hydrodynamic simulations. Presently the CCHE2D_EEM (Efficient-Element-Method-based) model is available.
- The CCHE2D Mesh Generator is a necessary and useful tool for structured mesh generation in geometrically complex domains.

5.3.1. General Procedure

The numerical modelling based on solving the depth averaged Navier-Stokes equations is an initial-boundary value problem. It is necessary to provide initial conditions and the boundary conditions. The general procedure of a numerical simulation can be simply listed as follows:

- Mesh generation
- Specification of boundary condition

- Parameters setting
- Simulation
- Results visualization and interpretation

5.3.1.1. Mesh Generation

The mesh represents the computational domain. It should be prepared with utmost care and sufficient background knowledge in order to obtain a good simulation. A good quality mesh meeting certain criteria is a prerequisite to any successful simulation. As per the CCHE2D v.4.0.user's manual (Zhang, 2009) the mesh must be built so as to meet the criteria as listed below:

- The interested zones have sufficient resolution;
- Transition between areas of different densities is smooth;
- Inlet(s) and outlet(s) should be sufficiently far away from the zones of interest;
- The mesh should be smooth and orthogonal as much as it allows.

For meeting the above and creating the mesh for the different physical domains the module 'CCHE-MESH' available in the package can be used by following a step by step procedure. Usually CCHE-MESH creates a structured mesh which consists of families of mesh lines with the property that members of a single family do not cross each other and cross each member of the other families only once. The mesh generation takes place in CCHE-MESH in two major steps. An algebraic mesh is generated first where a quick but crude initial mesh is created for further refinement and generation of a numerical mesh. Smoothness and orthogonality; the major two qualities are intermittently checked to evaluate the quality of mesh. For this purpose a mesh-evaluation table showing various parameters pertaining to mesh quality is available in the mesh module.

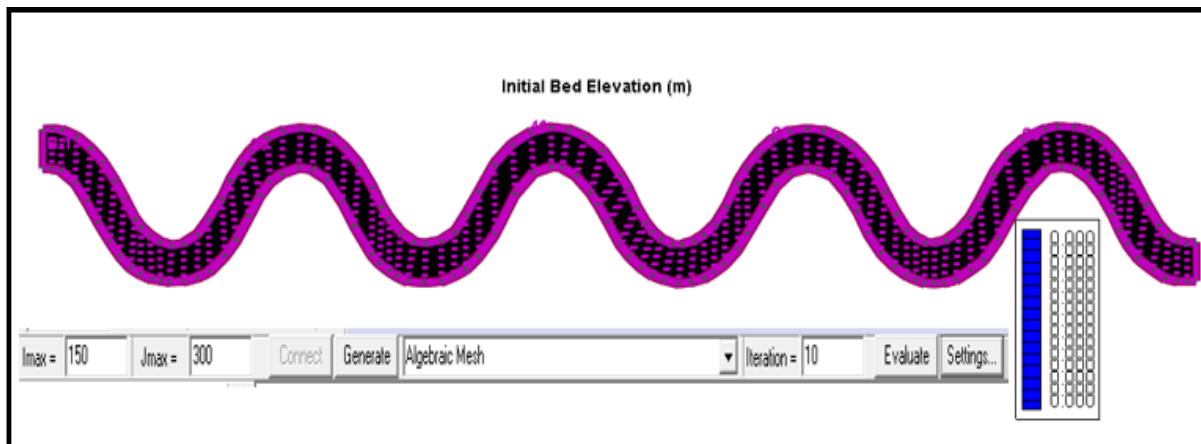


(Fig.5.8 Meshing of meandering channel)

5.3.1.2. Specification of boundary condition

Boundary conditions are the user set values which govern or guide the flow in the simulated zone. It must be carefully selected to represent the true physical behavior of the flow taking place. Mainly the inlet and outlet flow conditions of the domain are to be set. Often the discharge entering the domain can set an inlet flow boundary condition while the water surface level at the outlet of the domain is entered as the outlet boundary conditions.

5.3.1.3. Parameters setting

There are a number of groups of parameters which must be then set after setting the initial and boundary conditions. They are termed as flow parameters and three groups of parameters are to be set viz. Simulation parameters, bed roughness parameters and advanced parameters. Under the group of simulation parameter one has to choose the time step for each iteration and total simulation time thus fixing the time step, then one of the four turbulence closure options available and some other numerical parameters like wall slipness coefficient, method of iteration etc. Similarly in the bed roughness group there are a number of options to choose or specify the bed and wall roughness values such as Manning's n value or out of individuals from Wu & Wang (1999) or van Rajin (1989) formula as applicable to the case at hand. In the advanced group Coriolis force coefficient, gravitational acceleration, von Karman constant,

and kinematic viscosity of fluid, with default values that suffice for most cases, are available. However the user can change them if found necessary.

5.3.1.4. Simulation

After specifying all initial conditions and boundary conditions, setting the flow parameters the model simulation can be started. For this 'run simulation' tab with a number of options such as steady flow, unsteady flows, etc. are available and may be exercised depending on the user's need. Also, multiple runs may be necessary with some changes in flow parameters to get the desired results as numerical simulation is often a trial and error process.

5.3.3.5. Results visualization and interpretation

After the simulation is run for the desired no. of time steps the console window inside the GUI of CCHE2D indicates that the simulation is successful and the flow final results are ready for use. There are a number of output variables such as water surface; water depth; U & V velocity components (x & y components); U & V components of specific discharges; total specific discharge; X , Y components of shear stress; total shear stress; eddy viscosity (ϵ) and Froude no. (Fr) etc. Also if the user provides time interval to extract history results of simulation before setting up the simulation then CCHE2D can give history results at predetermined time intervals of 100 or 1000 time steps to analyse the progress of simulation in case an unsuccessful simulation. Then the results for different variables are to be interpreted with proper care and sufficient expertise for practical use.

6.1 NUMERICAL ANALYSIS RESULTS

Generally, experimental and theoretical analysis are the main tools for finding out the solution of open channel flow difficulties to meet the desires of field requirements. In recent times CFD techniques are being used extensively to solve the flow problems. In this study, a few simulations were carried out by using the viable code namely ANSYS to simulate the present experimental investigation. Simulation was carried out to predict the velocity distribution, streamlines along the channel and boundary shear stress distribution along the channel bed. Here Large Eddy Simulation model is used for turbulence modeling. The LES equations are discretized in both space and time. In this study the algorithms adopted to solve the coupling between pressure and velocity field is PISO which is the pressure implicit splitting operators use in Fluent (Issa 1986). A non-iterative solution method PISO is used to calculate the transient problem as it helps to converge the problems faster. Here the advection property is discretized with bounded central difference scheme and transient terms are discretized with Second order scheme. Courant number (Cr) is controlled between 0 - 0.5 and the transient time step size is taken as 0.0001 s. After that, the equation is iterated over and over till desirable level of accuracy of 10^{-3} of residual value is achieved. When the residuals of the discretized transport equation reach a value of 0.001 or when the solution do not change with further iterations, the numerical solution is converged. To promote the convergence of the solution the changing variables are controlled during the calculations. For the simulations with an unsteady solver, the difference in the mass flow rates at the velocity inlet and pressure outlet is monitored to be less than 0.01% in the final solution. Furthermore, a number of extra time steps are added to verify the steadiness of the flow field in the final solution.

The numerically simulated results are compared with the experimental results. Here mean bulk velocity is calculated using the formula:

$$U_b = \frac{\int u dA}{A} \quad (38)$$

Where, U_b = Bulk Velocity along Stream-line of flow. U = streamline velocity at any point, A = Cross-section area of the channel. The composite Manning's friction factor is calculated from the Manning's equation.

In this study, various flow variables are studied in a meandering channel with both bend apex and crossover sections for two different flow depths, which are discussed separately below. CFD simulation was carried out for two water flow depth such as 0.11cm and 0.03 cm. The positions of sections where the simulation results were studied are clearly shown in Figure 6.1. Positions of sections are decided to analyze the flow distribution in a meandering channel.

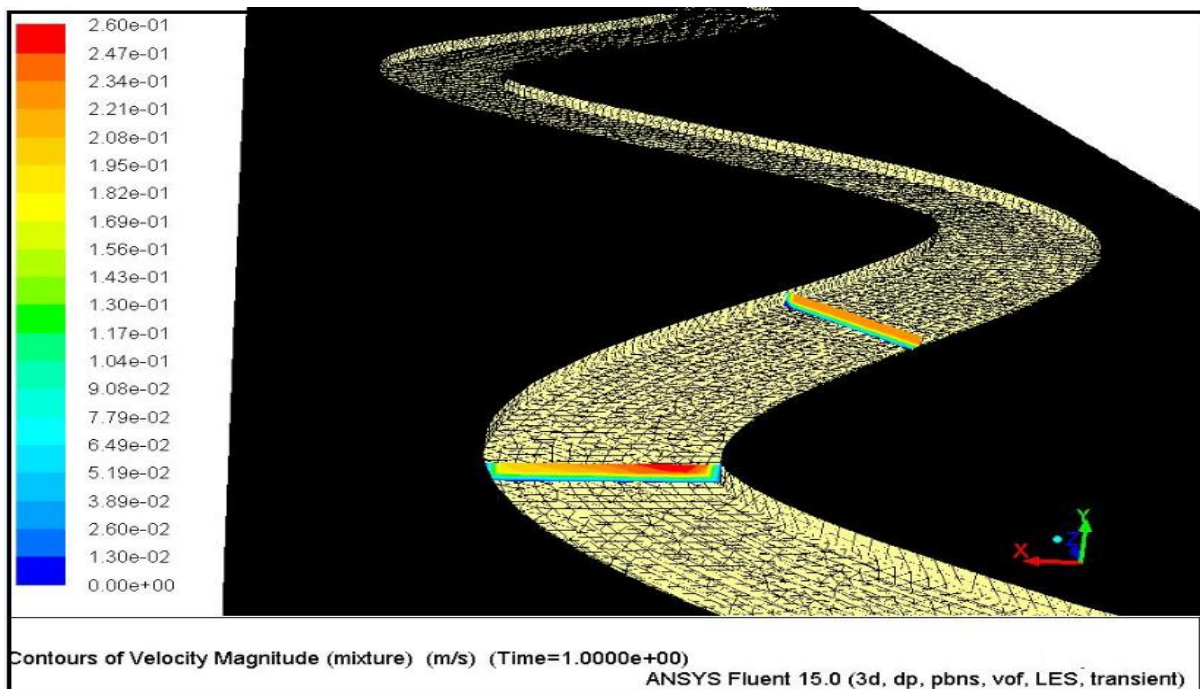


Figure 6.1. Velocity contours of different experimental sections

6.1.1 LONGITUDINAL VELOCITY DISTRIBUTION IN CHANNEL DEPTH

To compare the effect of the junction and to analyze the secondary flow structure in between the channel, velocity is measured at both bend apex and crossover experimentally by using Pitot tube, a velocity measuring instrument. The local velocities are measured in the experimental nodes located at different depths and aspect ratio in each section. In all of the bend apex and crossover, the vertical velocity distributions obey the logarithmic distribution law, except near the interface zone. Towards a longitudinal direction in a meandering channel, at interface zone the velocity gradient decreases gradually by taking $\alpha=2.54$ and $\alpha=9.33$.

Here the local velocities were also measured across the entire cross section, laterally every 50 mm and vertically at 0.2h, 0.4h, 0.6h, 0.8h and 0.9h level where “h” is the height of water for a particular bend apex and crossover section of the channel. The velocity distributions were then integrated over the flow depth to calculate the discharge and the depth-averaged velocity.

6.2.1. Validation of Numerical results with Experimentation for various water depths

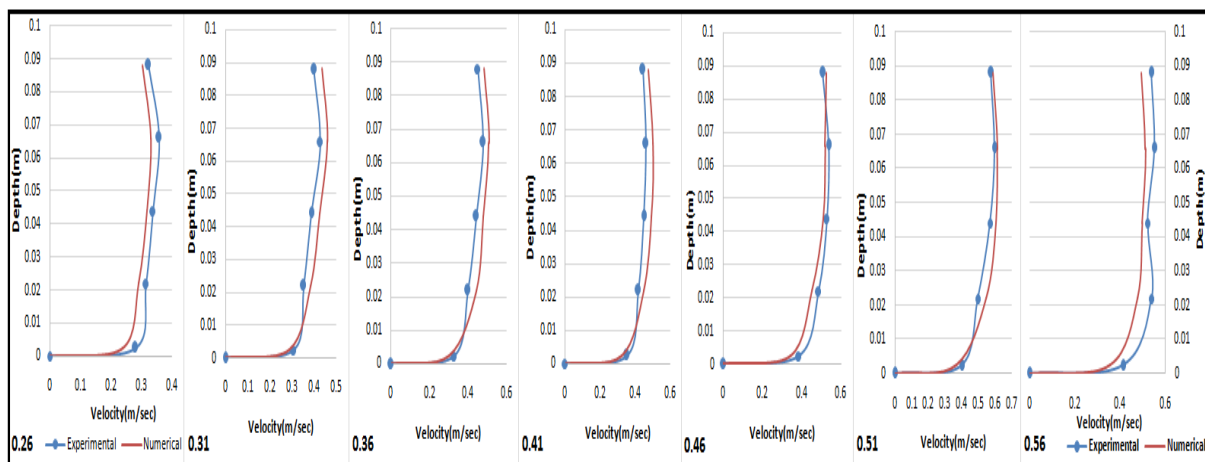


Figure 6.2. Longitudinal Velocity Profile of a bend apex section for $\alpha=2.54$

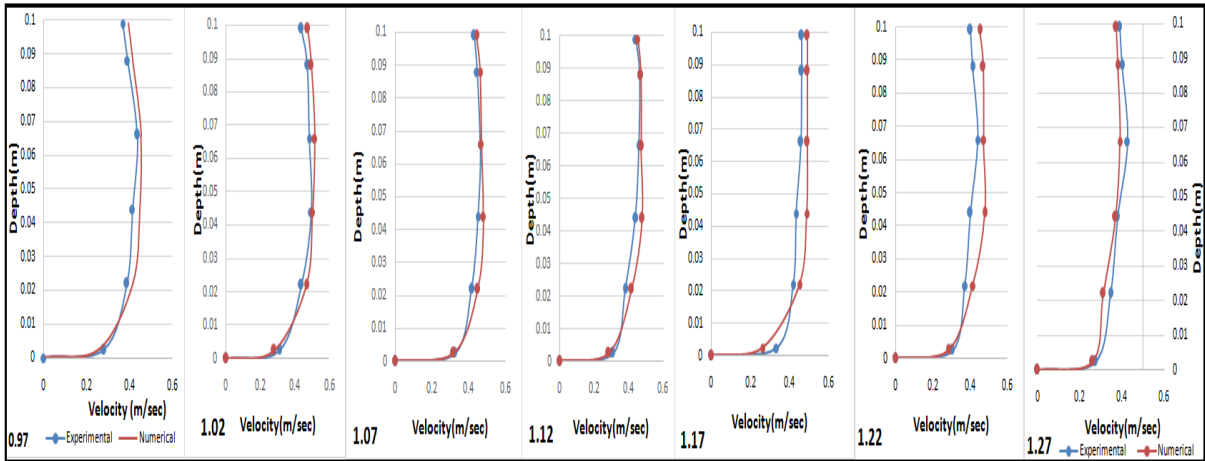


Figure 6.3. Longitudinal Velocity Profile of a crossover section for $\alpha=2.54$

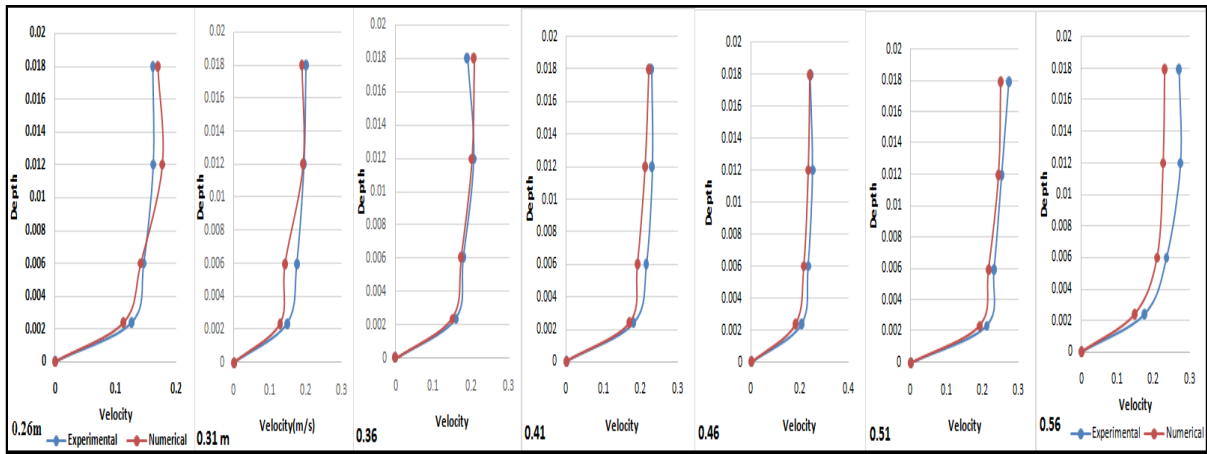


Figure 6.4. Longitudinal Velocity Profile of a bend apex section for $\alpha=9.33$

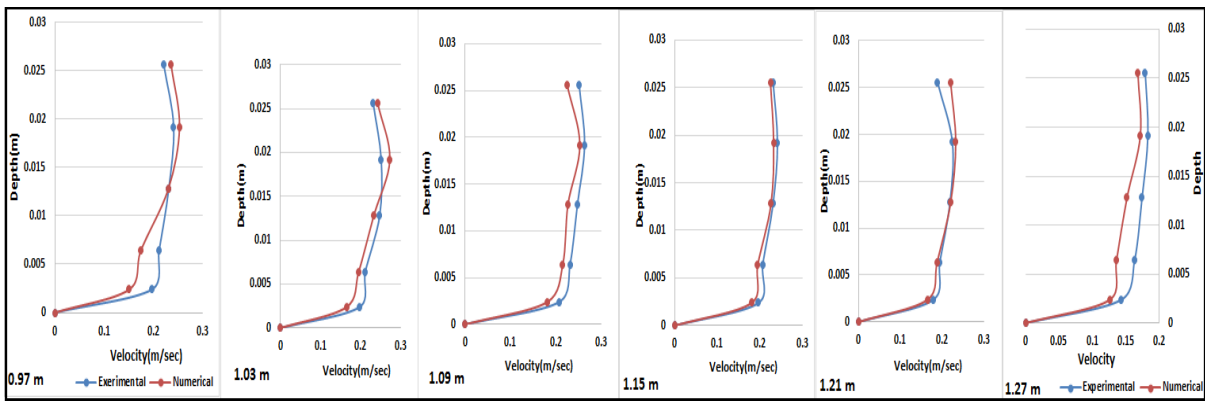


Figure 6.5. Longitudinal Velocity Profile of a crossover section for $\alpha=9.33$

6.2 DEPTH AVERAGE VELOCITY DISTRIBUTION FOR DIFFERENT CHANNEL DEPTH

6.2.1 Experimental Results

The depth-averaged velocity distribution in a cross section was measured at different experimental sections along the flume (Figure 6.1). Point depth-averaged velocity measurements were made laterally each 50 mm at a depth of $0.4H$ from the bed in the main channel at both bend apex and crossover with two different aspect ratios such that $\alpha=2.54$ and $\alpha=9.33$ are shown in Figure 6.6. Here Figure 6.6 shows the comparison of depth average velocity of $\alpha=2.54$ and $\alpha=9.33$ according to bend apex and crossover in a meandering channel flume.

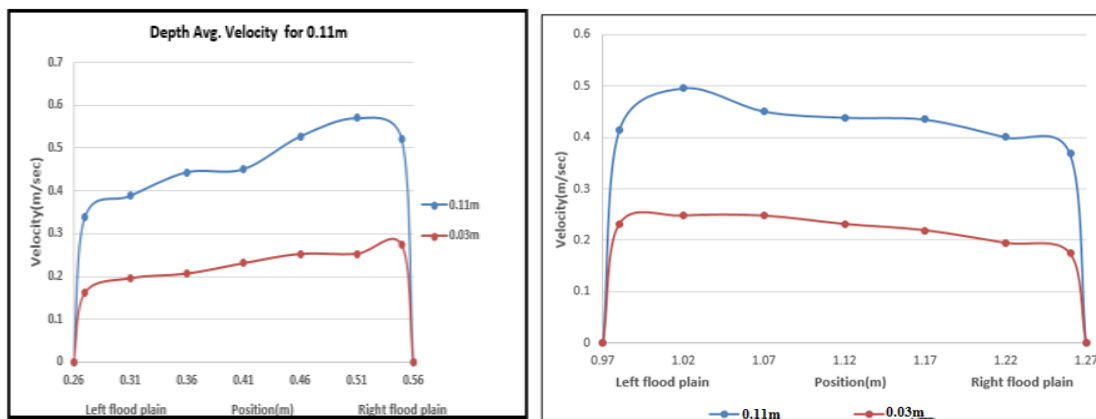


Figure 6.6. Comparison of Depth Average Velocity Profile with various depths

6.3. STAGE- DISCHARGE RELATIONSHIP

Making a flood prediction while using a hydraulic model which incorporates various flow features, is not an easy task. Researches have shown that the structures of the flow are even more difficult to analyze for meandering channel, due to an increase in the 3-Dimensional nature of flow (Shiono, Al-Romaih, and Knight 1999). In the present experimentation involving flow in a meandering channel, steady and uniform flow has been trying to achieve. Flow depths in the experimental channel runs are maintained that the water surface slope becomes parallel to the valley slope to minimize the energy losses. Under such conditions, the depths of flow at the channel centreline along one wave reach must be the same. This depth of

flow is considered as normal depth, which can carry a particular flow only steady and uniform condition. Figure 6.7 represent the graph of a stage discharge relationship in a main channel of a meandering channel.

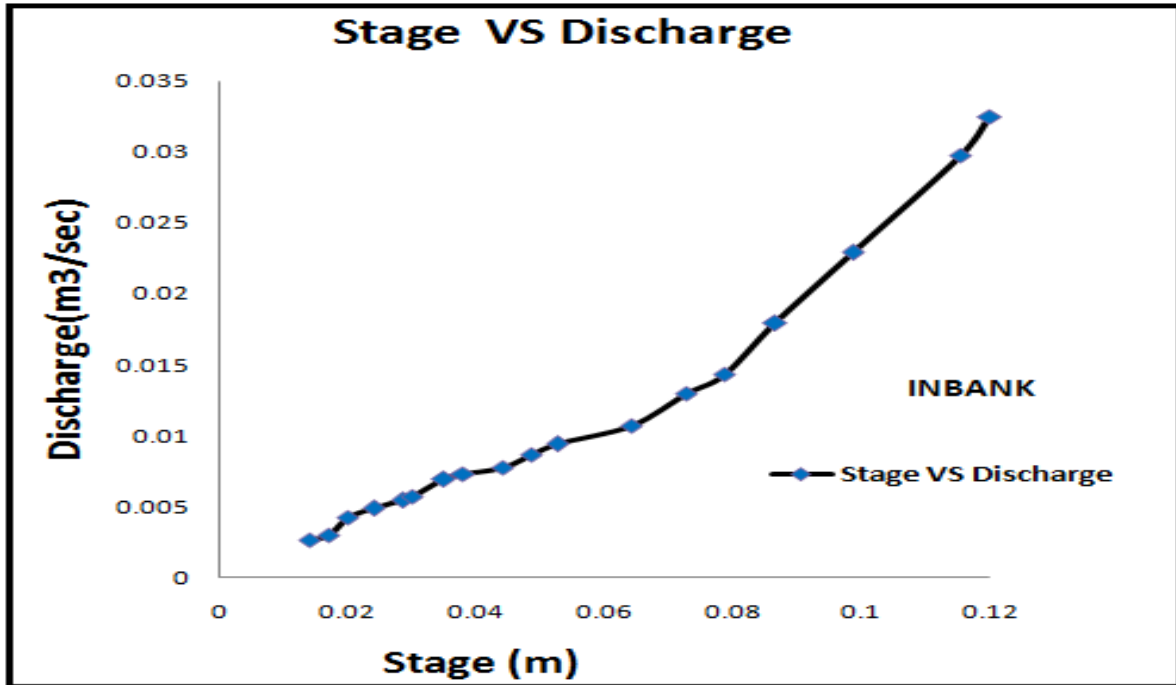


Figure 6.7. A graph of Stage- Discharge Relationship

6.4 DISTRIBUTION OF BOUNDARY SHEAR STRESS RESULTS

Shear stress distribution along the cross section of the channel is required to find out to know the variation of shear stress along the bed and it is also helpful in finding out the apparent shear stress in the channel section. In general Patel's equation is used to find out the shear stress develop at the bed and wall of the channel. Boundary shear stress at the bed and wall of the main channel at both bend apex and crossover are presented in the figure 6.8 and figure 6.9 respectively.

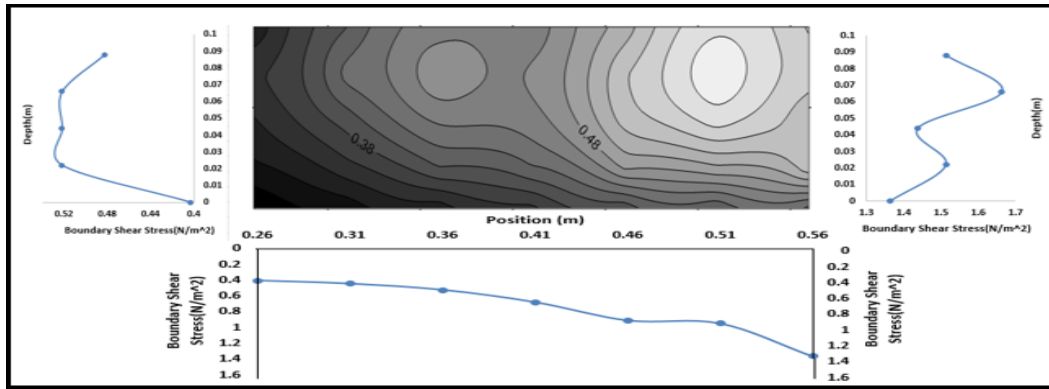


Figure 6.8. Boundary shear stress at bend apex

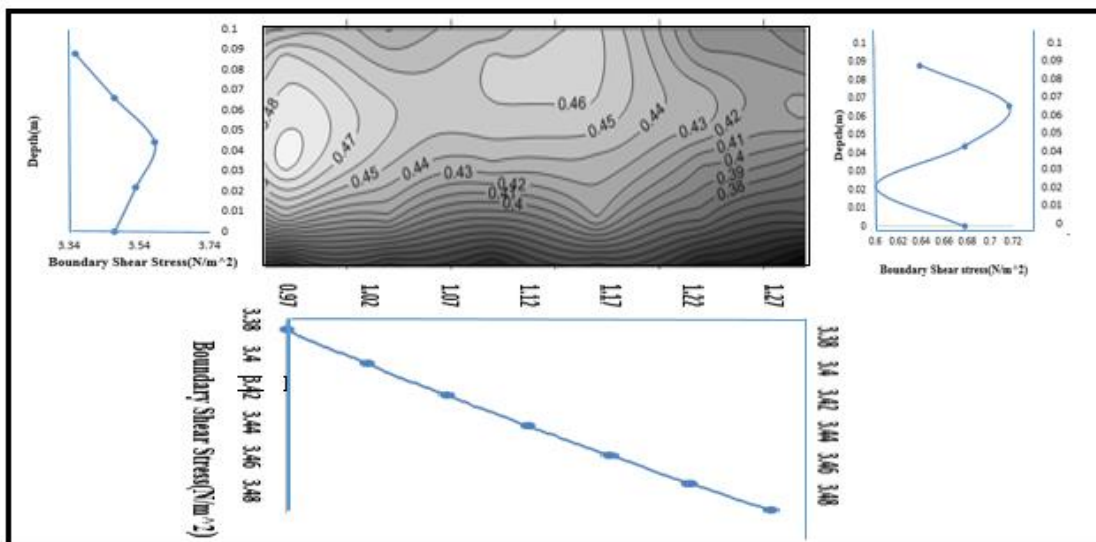


Figure 6.9. Boundary shear stress at crossover

6.5 NUMERICAL VALIDATION

6.5.1 Validation of Depth Average Velocity results with a 1-D CES tool

The **Conveyance Estimation System (CES)** is used to quantify the uncertainty in water level for a given flow rate, and present it in a manner which can be readily interpreted by the user and enable better, more informed decisions. CES considers all the physical flow processes that are present in a flow situation and where necessary, includes empirical or calibration coefficients based on previous research and expert advice.

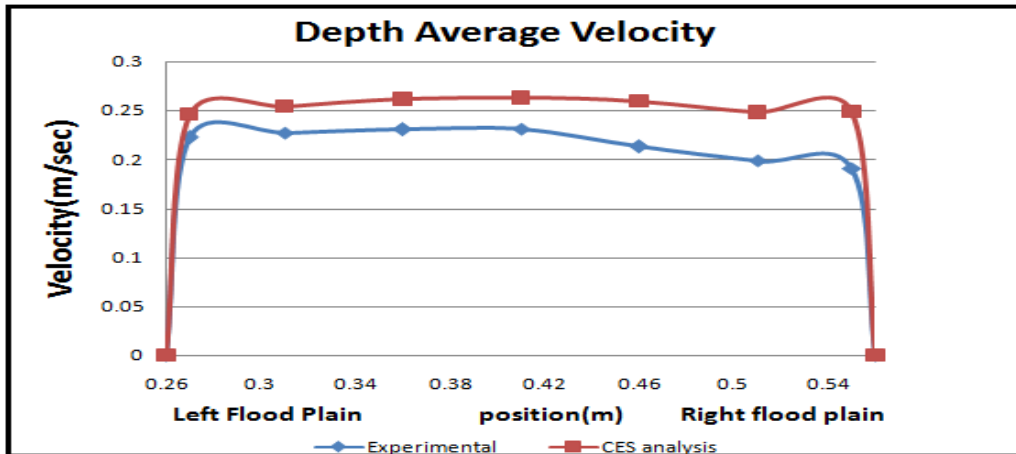


Figure. 6.10. Comparison of Depth Average Velocity Profile at bend apex

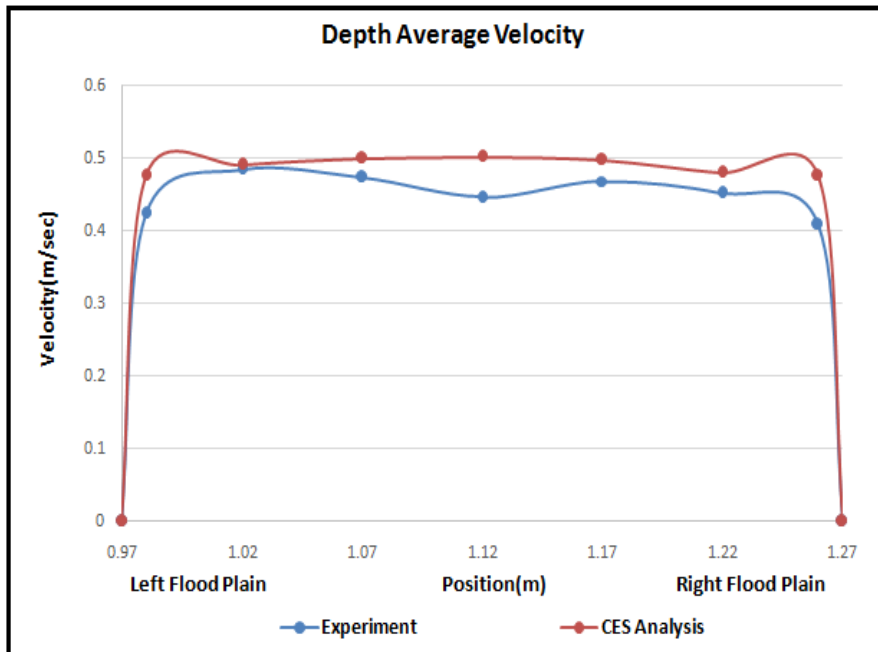


Figure. 6.11. Comparison of Depth Average Velocity Profile at crossover

Lateral depth-averaged velocity distributions are calculated and compared with the CFD results for two different $\alpha=2.54$ and $\alpha=9.33$. Figure 6.10 and 6.11 shows the validation of depth average velocity profile for accordingly by using experimental method and CES and figure 6.12 and 6.13 shows the validation of depth average velocity profile for accordingly by using experimental method and CFD simulation. As shown in these Figures, in the meandering channel the difference between the mean velocities in the main channel. From

the outer bank to inner bank, the velocity profile is gradually increase at bend apex but in the crossover the velocity gradually varied with different positions towards the outer bank.

6.5.2 Validation of Numerical Results for 0.11m

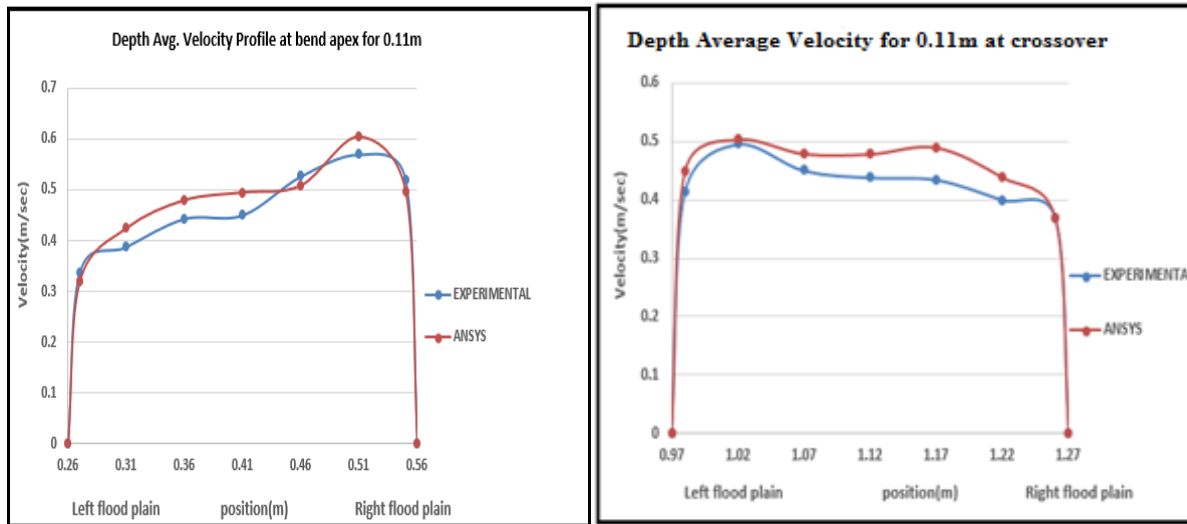


Figure 6.12. Comparison of Depth Average Velocity Profile for 0.11m

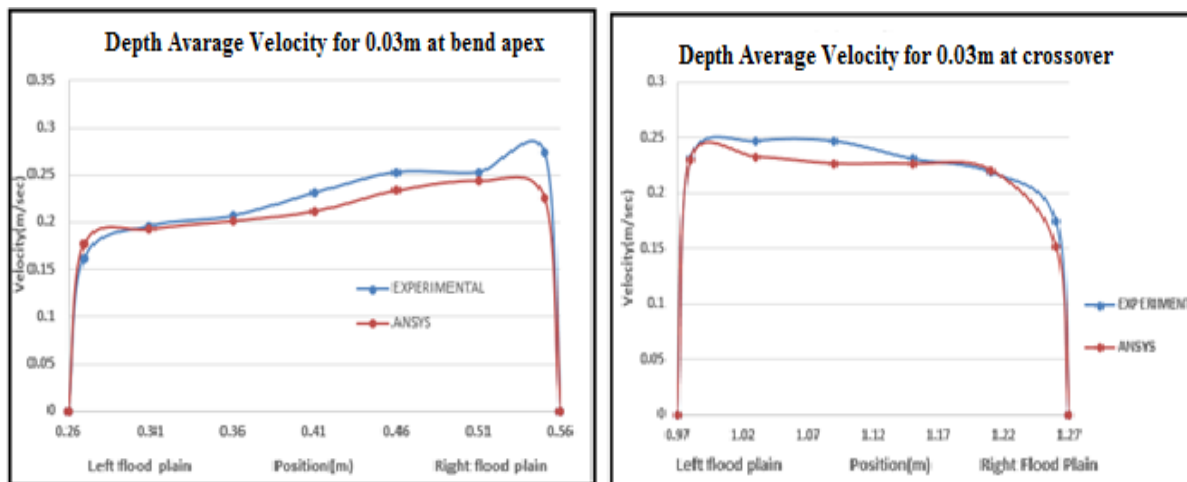


Figure 6.13. Comparison of Depth Average Velocity Profile for 0.03m

It obvious that the depth-averaged velocity distributions show good symmetrical patterns in different measurement sections. The Figures show the following effects of the contractions on the velocity distributions, (a) the numerical simulation gives good agreement with the experimentation, (b) the depth average velocity increases along the converging part of the

flume, (c) the velocity in the second half of the converging reach increases significantly, (d) for high relative depth, the effects of the lateral flow that comes into the main channel causes the velocity to increase locally near the main channel walls, especially in the second half of the convergence reach.

6.6 CONTOURS OF LONGITUDINAL VELOCITY

Figures 6.14 through 6.15 shows the longitudinal velocity contours at bend apex and crossover along the section for $\alpha=2.54$ of flow and Figures 6.16 through 6.17 show the longitudinal velocity contours for $\alpha=9.33$ different experimental sections. In figure 6.14, here numerical model will give approximate same value to be inclined towards the inner wall of bend apex, but the experimental contour shows highest value in inner side. In Figure 6.15, it shows maximum contour in inner side of the crossover in numerical model but the high-velocity zone tends to the center of the channel at crossover in experimental flume. Comparison of velocity contour between experimental data and numerical analysis of different sections are shown in Figures 6.14 through 6.15 respectively for $\alpha=2.54$. Similarly Figures 6.16 through 6.17 shows comparison of both results for $\alpha=9.33$.

6.6.1 Comparison of Velocity Contours having Depth of flow for $\alpha=2.54$

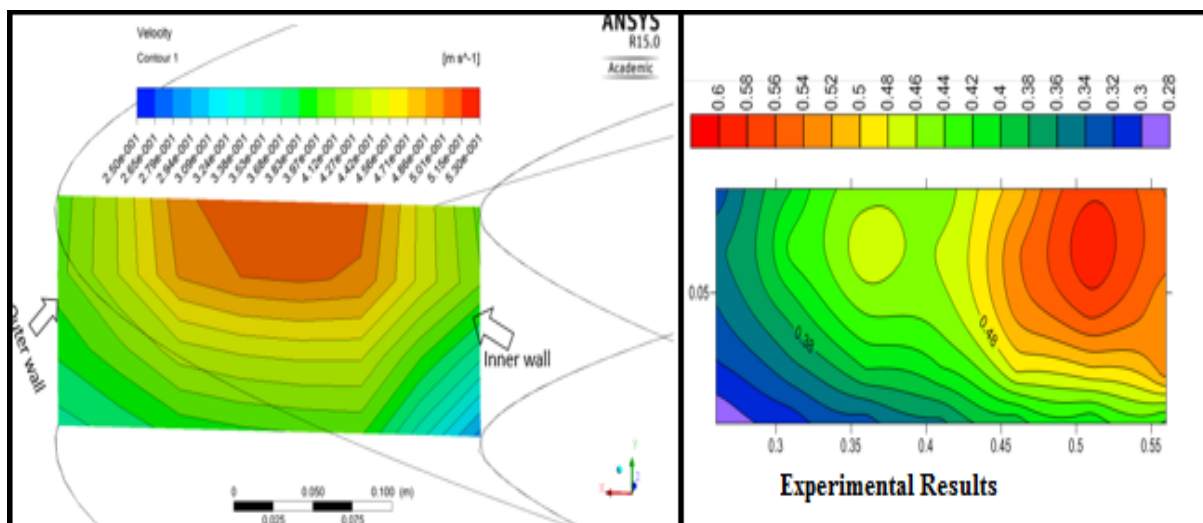


Figure.6.14. Comparison of Velocity contour for $\alpha=2.54$ at bend apex

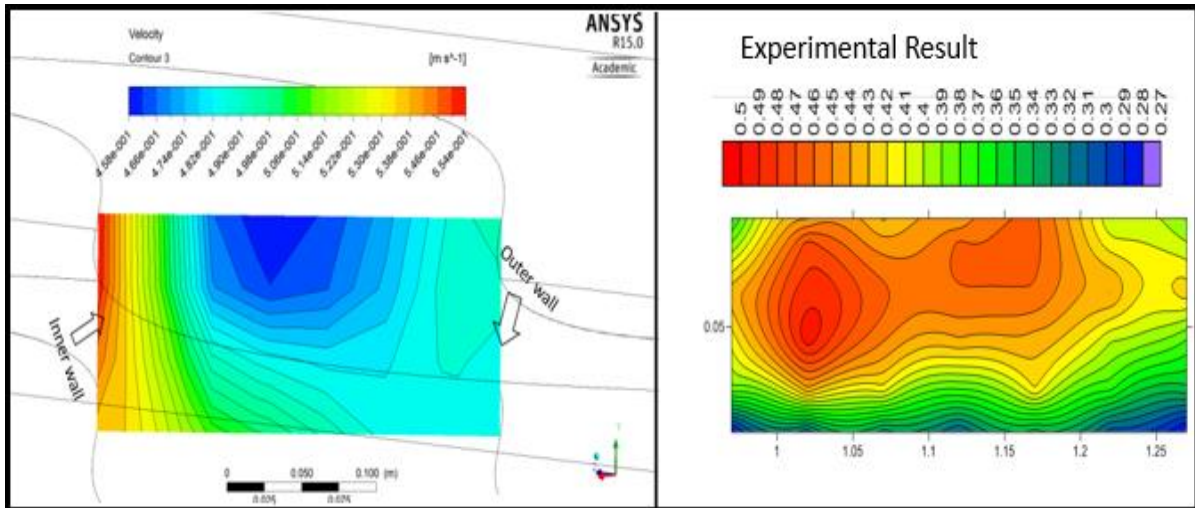


Figure.6.15. Comparison of Velocity contour for $\alpha=2.54$ at crossover

6.6.2 Comparison of Velocity Contours having Depth of flow

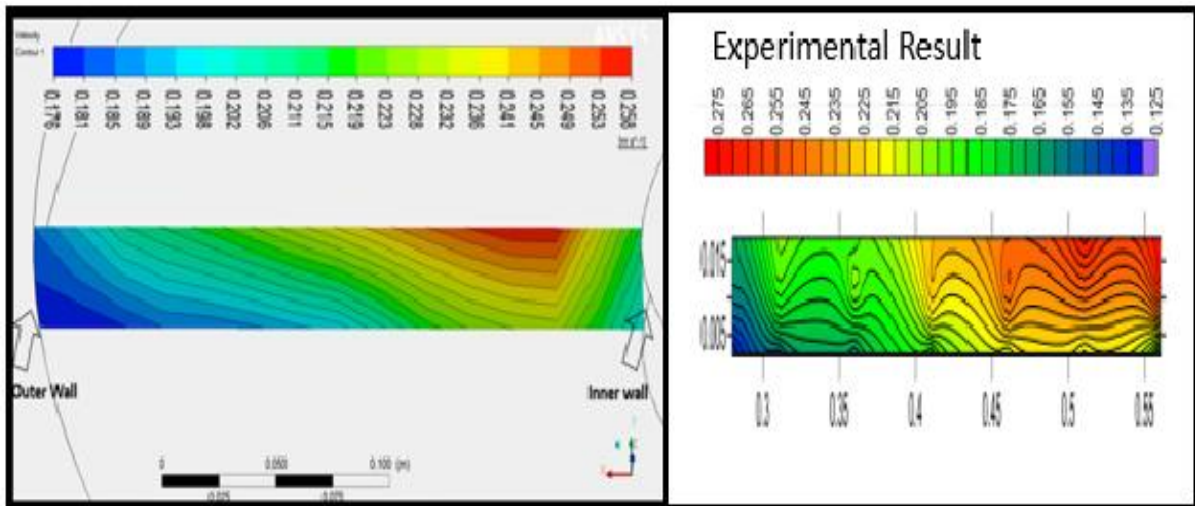


Figure.6.16. Comparison of Velocity contour for $\alpha=9.33$ at bend apex

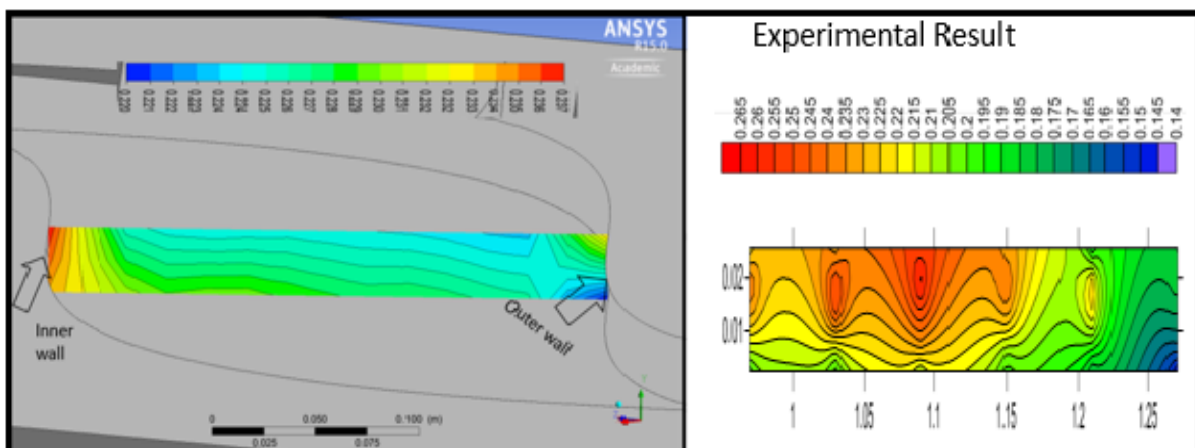


Figure.6.17. Comparison of Velocity contour for $\alpha=9.33$ at crossover

6.7. STREAMLINES ALONG THE BEND

In Figure 6.18, the streamline of a meandering channel is shown by taking the 0.11 m water level and it shows the streamlines of the meandering channel for $\alpha=2.54$. As seen in Figure 6.18, the streamlines get close to each other on the water surface, due to the major and minor secondary flows at the water surface. The flow direction on the main channel is obviously forced by the meandering angle. This direction is also observed in the downstream cross-section, for the velocities at the limit of the main channel. The slight outwards component of the bottom velocity in the downstream section confirms this secondary flow. In this state, the direction of both secondary flows (major and minor ones) is towards the middle of the channel. In the middle of the channel the flow maintains streamlines almost follow the channel curvature.

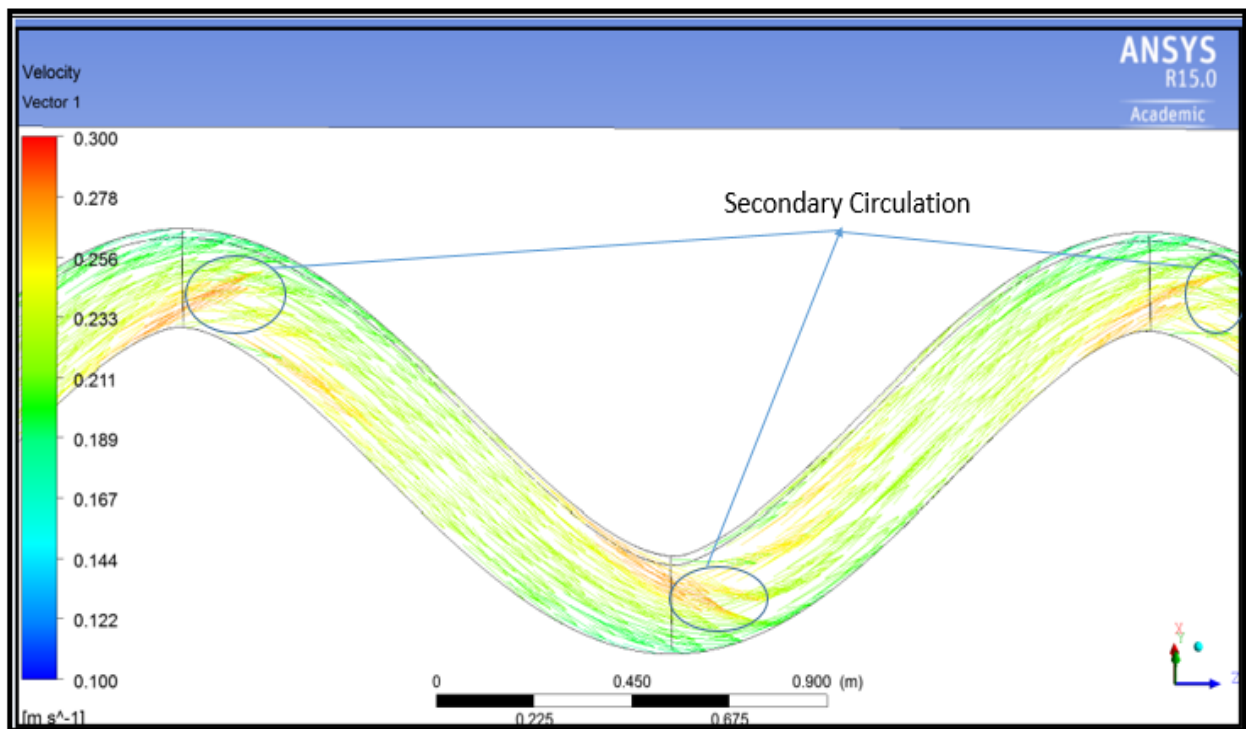


Figure.6.18. Simulation Result for streamlines vector

6.8 NUMERICAL 2D SIMULATION BY CCHE 2D

For flow, the initial conditions include the initial mesh, the initial bed elevation, the initial water surface and the bed roughness; and, for sediment, they include the initial bed erodibility, the initial bed layers, and the initial bed samples. In this project the flow simulation is done. At the first stage, define inlets and outlets, hydraulic structures, and set the boundary conditions associated with them. For flow simulation, only the flow parameters need to be set, while for sediment transport simulation, we need to set both flow parameters and sediment parameters. For extra simulations, such as water quality, chemical spill, cohesive sediment transport, and coastal courses, we need to set the corresponding parameters, respectively. After identifying all initial conditions and boundary conditions, setting the flow parameters the Model Simulation can be started. Also, multiple runs may be essential with some changes in flow parameters to get the desired results as numerical simulation is often a trial and error process. After the simulation is run for the desired no. of time steps the support window inside the GUI of CCHE2D indicates that the simulation is successful and the flow final results are ready for use. There are a number of output variables such as water surface; water depth; U & V velocity components (x & y components); U & V components of specific discharges; total specific discharge; X , Y components of shear stress; total shear stress; eddy viscosity (ε) and Froude no. (Fr) etc. Also if the user provides time interval to extract history results of simulation before setting up the simulation then CCHE2D can give history results at predetermined time intervals of 100 or 1000 time steps to analyze the progress of simulation in case an unsuccessful simulation. The results for different variables are then to be interpreted with proper care and sufficient expertise to practical use.

6.8.1 Visualization of Results By CCHE 2D

After the simulation is run for the desired no. of time steps the console window inside the GUI of CCHE2D indicates that the simulation is successful and the flow final results are ready for use. In visualization of result , figure 6.19 represent water surface level or water depth of a corresponding channel, figure 6.20.explain U velocity components or longitudinal velocity. In figure 6.21 shows the velocity magnitude contour and figure 6.22 shows the contour of boundary shear stress of a channel where it is higher in inner side of each bend apex. In velocity magnitude contour, it has higher value in outlet side .In figure 6.23 represent the contour of flow field along the channel. Due to boundary wall law, the velocity of flow water is maximum at inner side of bend apex for secondary circulation. In the figure 6.24 shows the counter of flow field along a particular bend apex of a main channel in meandering channel. In figure 6.25 represent the contour of specific discharge throughout the channel. In figure 6.26 shows the contour of flow depth throughout the channel. When flow of water moves towards the inlet to outlet side across the bend apex to crossover that time water flow creates secondary circulation or turbulence. For that reason when water turns its movements that time it has maximum depth in outer side than inner side. Also if the user provides time interval to extract history results of simulation before setting up the simulation then CCHE2D can give history results at predetermined time intervals of 100 or 1000 time steps to analyse the progress of simulation in case an unsuccessful simulation. Then the results for different variables are to be interpreted with proper care and sufficient expertise for practical use.

6.8.1.2 Water Surface Level

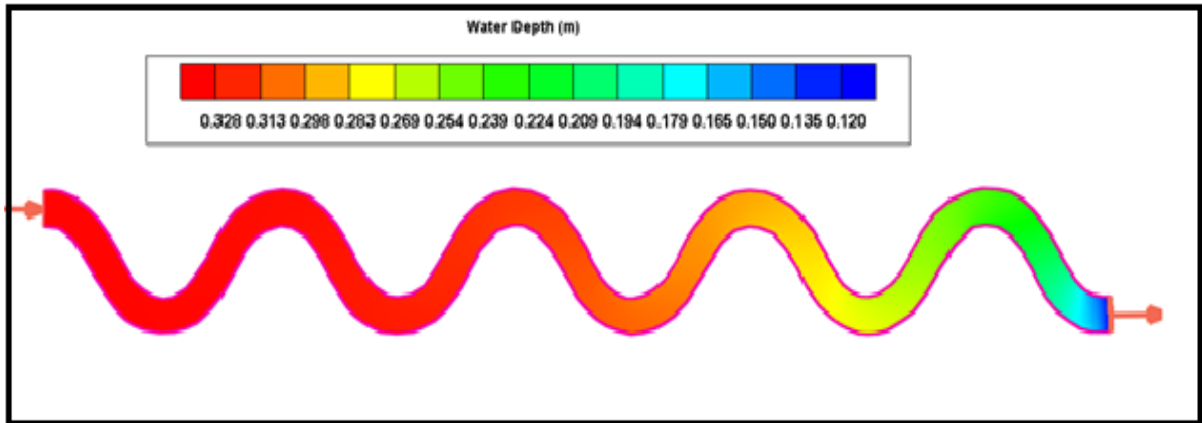


Figure 6.19. Contour of Water surface level

6.8.1.3 Longitudinal Velocity

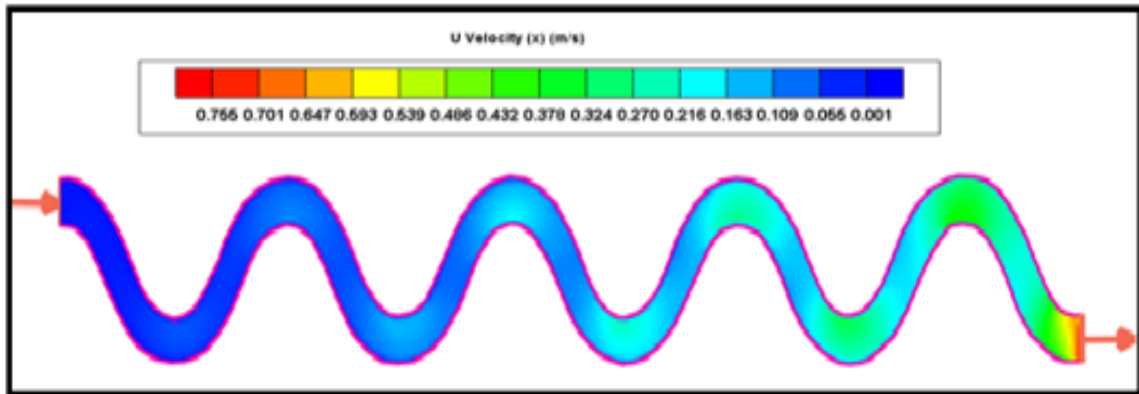


Figure 6.20. Contour of Longitudinal Velocity(m/sec)

6.8.1.4 Velocity magnitude

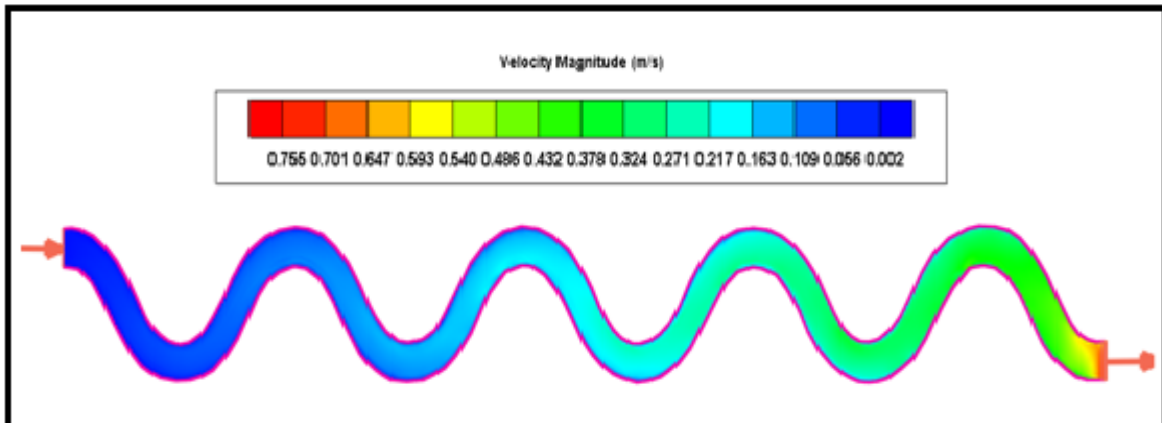


Figure 6.21. Contour of Velocity Magnitude(m/sec)

6.8.1.5 Boundary Shear Stress distribution

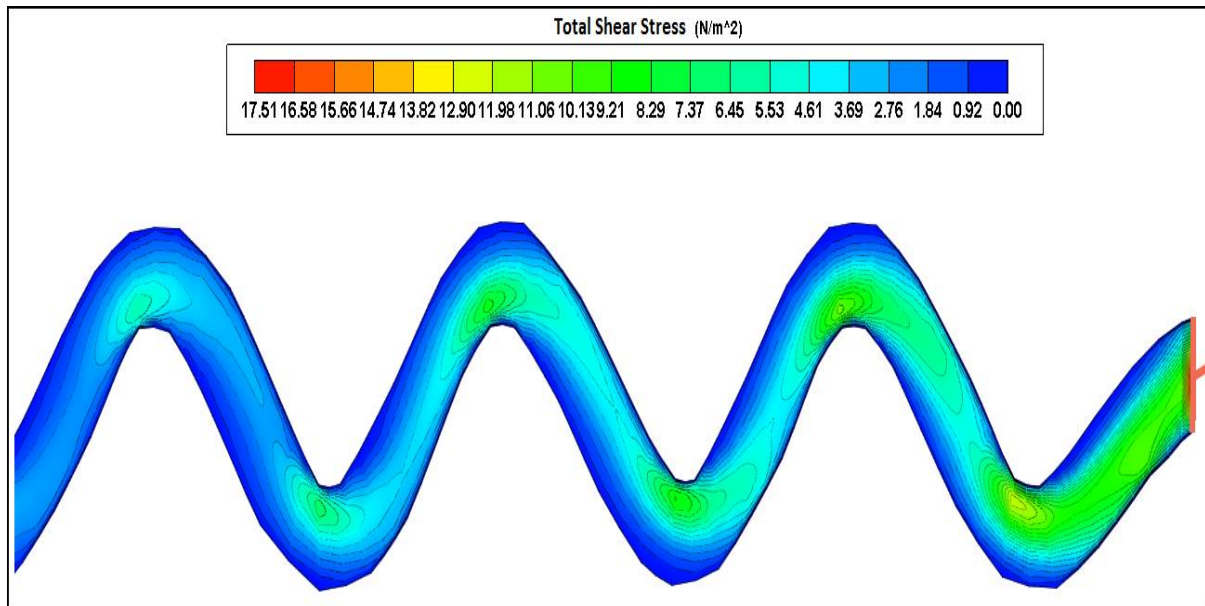


Figure 6.22. Contour of Boundary Shear stress distribution

6.8.1.6 Flow field, along the channel

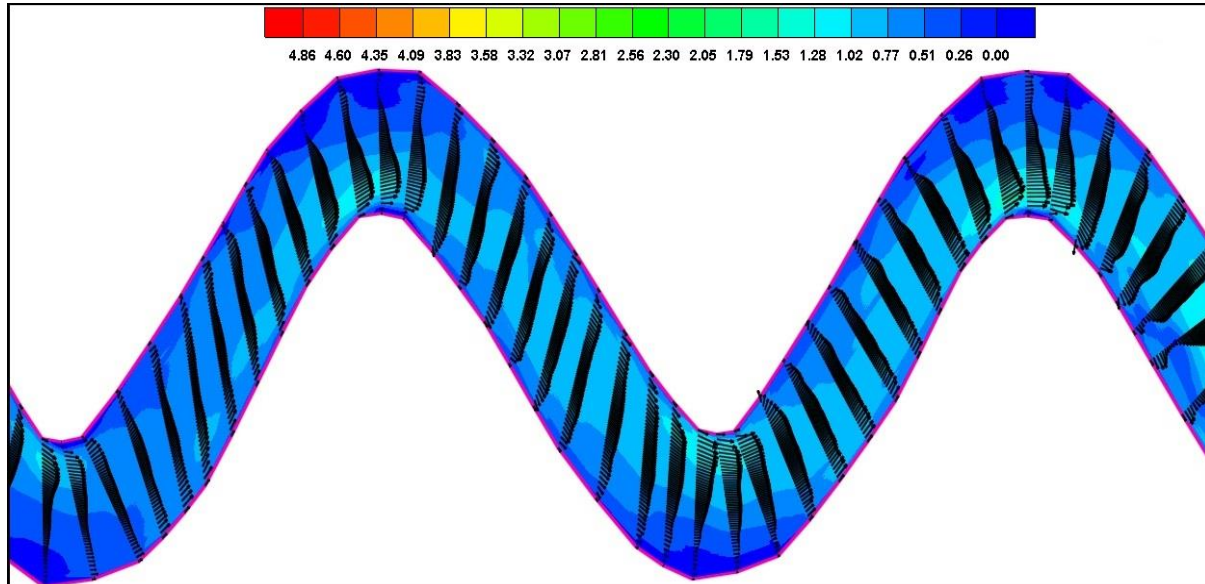


Figure 6.23. Contour of flow field along the channel

6.8.1.7 Flow field at bend apex

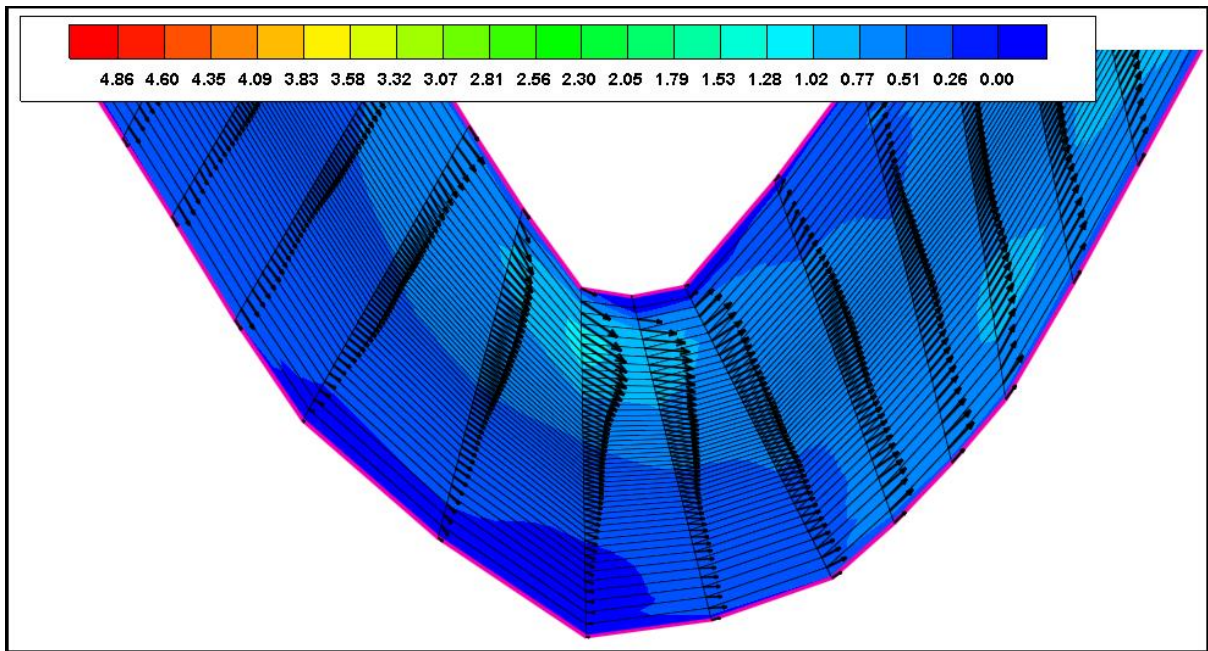


Figure 6.24. Contour of flow field at bend apex

6.8.1.8 Specific discharge throughout the channel

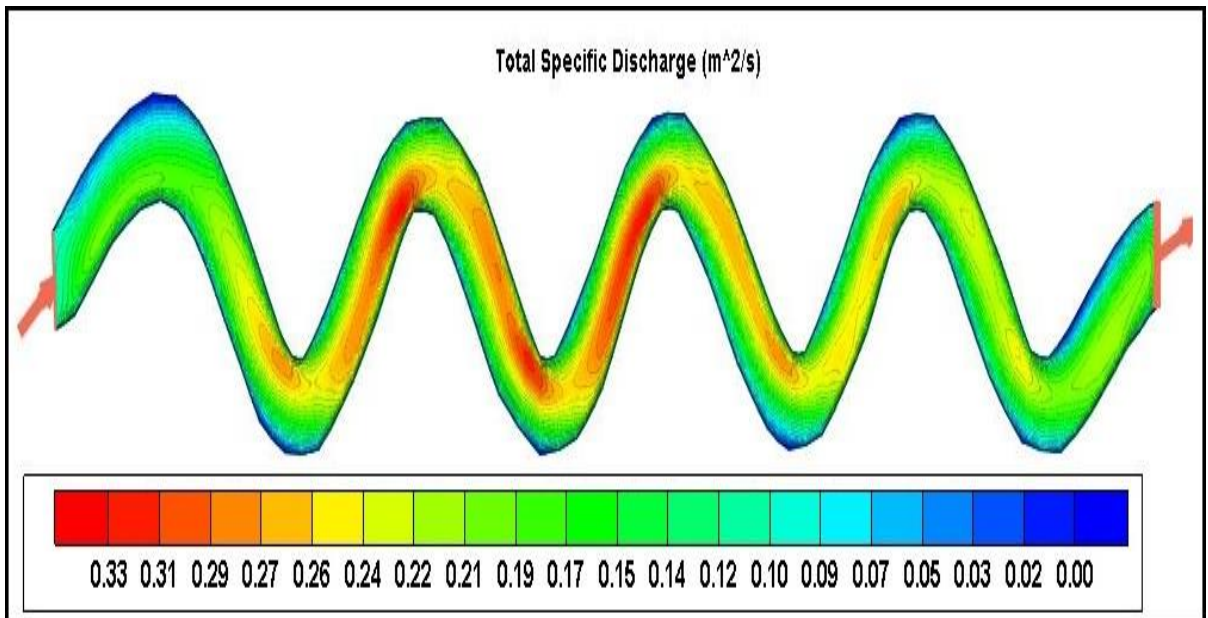


Figure 6.25. Contour of Specific discharge throughout the channel

6.8.1.9 Flow depth analysis throughout the channel

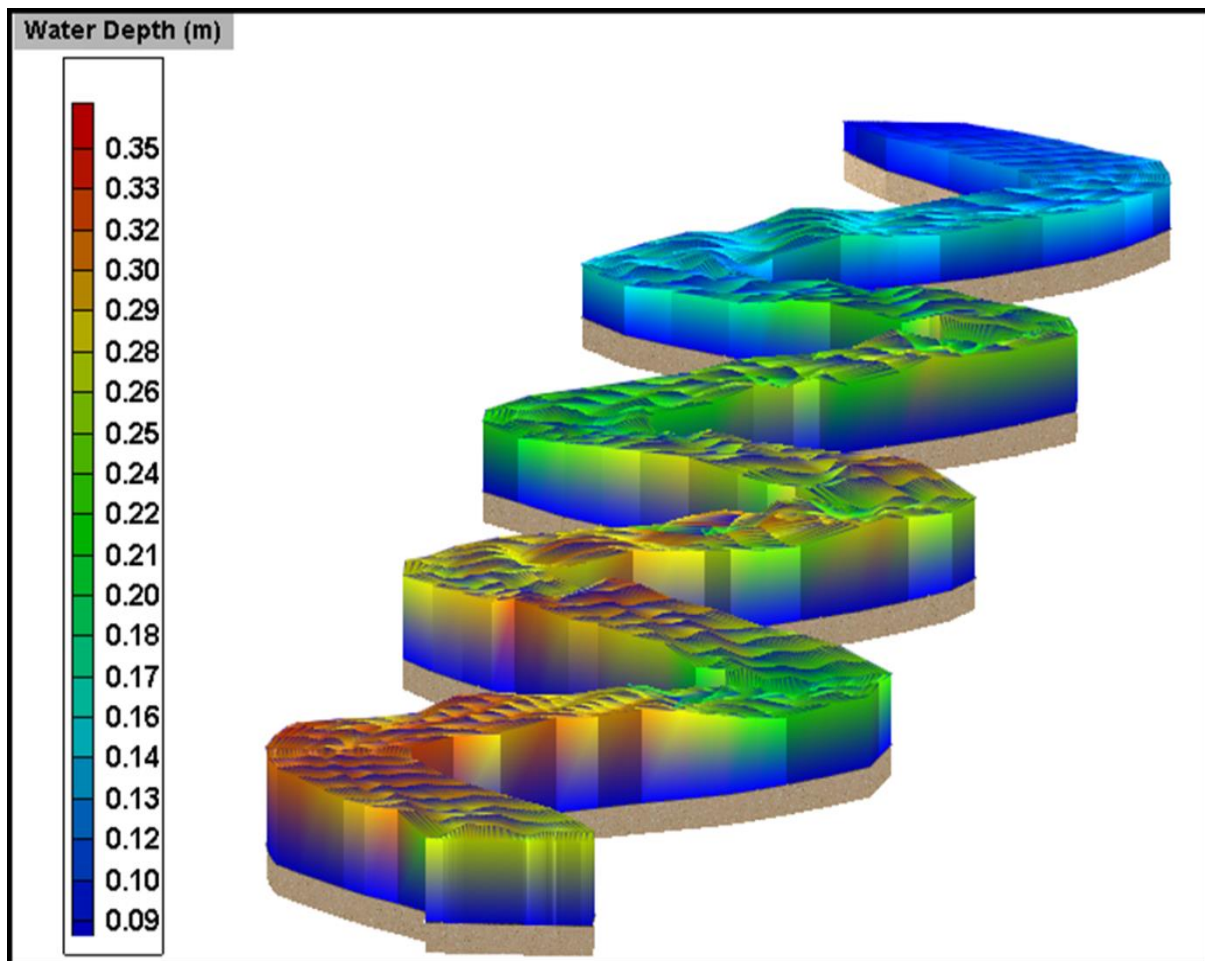


Figure 6.26. contour of flow depth analysis throughout the channel

CONCLUSIONS AND FURTHER WORK

7.1 CONCLUSIONS

In the present study, the experimental and numerical modelling of the flow pattern at a meandering channel has been carried out. On the basis of the investigations concerning flow, velocity distribution and depth average velocity distribution along the channel bed for two different aspect ratios of $\alpha=2.54$ and $\alpha=9.33$ in a meandering channel having 60° meandering angle, the point to point observations are drawn for different experimental sections. Findings of the work are as follows:

- The model for the depth-averaged velocity distribution proposed by Wilkerson (2005) does not fit to meandering channels. The modeled equations (3, 4) which include the influencing dimensionless channel parameters are found to be adequate for the present set of simple meander channel data and can be used to compute the depth average velocity across the channel cross sections.
- From outer bank to inner bank the velocity profile has gradually increase at bend apex but in the crossover the velocity gradually varied with different positions towards the outer bank.
- The simulation of streamlines vectors shows the streamlines get close to each other at the water surface, due to the major and minor secondary flows at the water surface. The direction of both secondary flows (major and minor ones) is towards the middle of the channel. In the middle of the channel the flow maintain streamlines almost follow the channel curvature in a meandering channel.
- The aspect ratio of 2.54 numerical model will gives approximate same value to be inclined towards the inner wall of bend apex but the experimental contour shows highest value in inner side for longitudinal velocity contour. The figure for aspect ratio 9.33, shows maximum contour in inner side of crossover in numerical model but

the high-velocity zone tends to the centre of the channel at crossover in experimental flume.

- Full three dimensional modelling of the free surface flow in the meandering channel as relatively complex geometry have been successfully verified with a mesh refinement studies and validated with experiments.
- Here experimental results related to longitudinal velocities are compared with the corresponding values obtained from Numerical analysis for with both bend apex and crossover sections in the meandering channel for two different aspect ratio of flow and concluded that the variation of longitudinal velocity in main channel region is found to be less as compared to that in the flood plain region.
- Using LES, the computed secondary flow pattern in the meandering channel hardly deviates from the measured flow pattern and the turbulence is reproduced correctly.
- CCHE2D predictions are in very good agreement with their experimental values.
- CCHE2D is quite capable of producing results in agreement with their physical values and also it partly agrees with results of CES.
- It can be fairly concluded that CES can be used to estimate stage-discharge relationship whereas CCHE2D can be used to predict the span wise velocity and boundary shear in wide smooth compound meandering channel.
- CES is quite satisfactory although a small variation is found at some depths .This is due to the calculation being performed in a meandering channel where there is considerable variation in flow depths at inner bank and outer banks owing to curvilinearity in flow path.

7.2 SCOPE FOR FUTURE WORK

The present work leaves a wide scope for future investigators to explore many other aspects of a meandering channel analysis. The future scope of the present work may be summarized as:

- Distributions of boundary shear stress components in lateral and vertical directions can be evaluated which has implications for the sediment transport studies.
- LES modeling for other hydraulic and geometrical conditions can be carried out. LES and other turbulence closure models like $k-\epsilon$, $k-\omega$, RSM etc. can be used to simulate various channel geometry with different hydraulic conditions.
- Further investigation is required to study the flow properties and develop models for channels with roughness in the sub-sections.
- Further investigations can be done to study depth-averaged velocity in vertical and lateral directions and develop models using analytical and numerical approaches which are more convenient than conventional methods.
- Proceedings on lateral velocity distribution can be done on mobile bed to represent real situation prevailing in natural rivers; so that sediment load transport and boundary shear distribution can be determined to its accuracy.
- By the help of dimensional analysis the given model can be further verified.
- The current data can be used to validate with data of other investigators.

REFERENCES

1. Absi, R. (2011). "An ordinary differential equation for velocity distribution and dip-phenomenon in open channel flows" *Journal of Hydraulic Research*, IAHR, Taylor and Francis, Vol. 49, N° 1, pp. 82-89
2. Ansari, K., Morvan, H. P. and Hargreaves, D. M. (2011), "Numerical Investigation into Secondary Currents and Wall Shear in Trapezoidal channels." *Journal of Hydraulic Engineering (ASCE) 2011*; Vol.137 (4):432-440.
3. Baghalian, S., Bonakdari, H., Nazari, F., Fazli, M.(2012), "Closed-Form Solution for Flow Field in Curved Channels in Comparison with Experimental and Numerical Analyses and Artificial Neural Network". *Engineering Applications of Computational Fluid Mechanics* Vo.6, No.4, pp. 514-526.
4. Bathurst, J. C., Hey, R. D., & Thorne, C. R. (1979). "Secondary flow and shear stress at river bends.", *Journal of the Hydraulics Division*, 105(10), 1277-1295.
5. Bhowmik, N. G., and Demissie, M. (1982), "Carrying capacity of flood plains". *Journal of the Hydraulics Division*, 108(3), 443-452.
6. Bonakdari, H., Baghalian, S., Nazari, F., Fazli, M.(2011), "Numerical Analysis and Prediction of the Velocity Field in Curved Open Channel using Artificial Neural Network and Genetic Algorithm". *Engineering Applications of Computational Fluid Mechanics* Vo.5, No.3, pp. 384-396.
7. Boussinesq, J.(1868). Mémoires sur l'"influence des frottements dans les mouvement reguliers des fluids. *J. Math. Pures Appl.* (2me sér.), 13, 377-424.
8. Chang, H. H. (1984), "Variation of flow resistance through curved channels", *Journal of Hydr. Engrg.*, ASCE, 110(12), 1772-1782.
9. Chow, V. T. (1959), "Open Channel Hydraulics", McGraw-Hill Book Co, New York.
10. Coles, D. (1956). "The law of the wake in the turbulent boundary layer". *Journal of Fluid Mechanics*, 1(02), 191-226.
11. Cruff R.W. (1965), "Cross Channel Transfer of Linear Momentum in Smooth Rectangular Channels", *U. S. G. S Water Supply*, Paper 1592-B.
12. Dash, S. S. (2013), "Stage-Discharge Modelling of Meandering Channel". Thesis Presented to the National Institute of Technology, Rourkela, in partial fulfilment of the requirements for the Degree of Doctor of philosophy.
13. Ervine D. A., Koopaei K.B., and Sellin R. H. J. (2000). "Two-Dimensional Solution for Straight and Meandering Over-bank Flows." *Journal of Hydraulic Engineering*, ASCE, Vol. 126, No. 9, September, paper No.22144, 653-669.
14. Ghosh, S. N., Jena, S. B.(1971), "Boundary Shear Distribution in open Channel Compound", *Proc. I. C. E*, Vol. 49, August .

15. "Guide for selecting roughness coefficient "n" values for channels". (1963). Soil Conservation Service, *U.S. Dept. of Agric.*, Washington
16. Guo, J., and Julien, P. Y. (2005). "Boundary shear stress in smooth rectangular openchannels." Proc., 13th Int. Association of Hydraulic Research, APD Congress, Singapore, Vol. 1, 76–86.
17. "Hydraulic capacity of meandering channels in straight floodway" (1956), Tech.Memorandum No. 2-429, U.S. Army Corps of Engineers, Waterways Experiment Station, Vicksburg, Miss.
18. Inglis, C.C.(1947), "Meander and Their Bering on River Training.", *Proceedings of the Institution of Civil Engineers, Maritime and Waterways Engineering Div., Meeting, 1947.*
19. James, M., and Brown, R. J.(1977), "Geometric parameters that influence flood plain flow", U. S. Army Engineer Waterways Experimental Station, Vicksburg, Miss., June, Research report H-77.
20. Jarrett, R. D. (1984). "Hydraulics of high gradient streams", *Journal of Hydr. Engg.*,ASCE, 110, 1519–1539.
21. Javid,S., and Mohammadi,M.(2012). "Boundary Shear Stress in a Trapezoidal Channel." IJE TRANSACTIONS A: Basics Vol. 25, No. 4, (October 2012) 365-373.
22. Jin,Y.C.,Zarrati, A. R. andZheng,Y. (2004). "Boundary Shear Distribution in Straight Ducts and Open Channels" *J. Hydraul. Eng.*, ASCE, 130(9), 924-928.
23. Johannesson, H., & Parker, G. (1989). "Linear theory of river meanders.",*Water Resources Monograph, 12*, 181-213.
24. Khatua, K. K. (2008), "Interaction of flow and estimation of discharge in two stage meandering compound channels". Thesis Presented to the National Institute of Technology, Rourkela, in partial fulfilment of the requirements for the Degree of Doctor of philosophy.
25. Khatua, K.K and Patra, K.C,(2010). Evaluation of boundary shear distribution in a meandering channel.Proceedings of ninth International Conference on Hydro-Scienceand Engineering, IIT Madras, Chennai, India, ICHE 2010, 74.
26. Khatua K.K., Patra K.C., (2013) "stage–discharge prediction for meandering channels", *Int. J. Comp. Meth. and Exp. Meas.*, Vol. 1, No. 1 80–92
27. Khatua K.K., Patra K.C., Nayak P. (2012), "Meandering effect for evaluation of roughness coefficients in open channel flow" *Sixth international conf. on river basin management, WIT Transactions on Ecology and the Environment (ISSN 1743-3541), CMEM, WIT Press.*, 146(6):213-227.
28. Knight, D. W. (1981). "Boundary shear in smooth and rough channels." *J. Hydraul. Div., Am. Soc. Civ. Eng.*, 107(7), 839–851.
29. Knight D. W. and Demetriou J.D. (1983). "Floodplain and main channel flow interaction." *J. Hydraul. Eng.*, ASCE, 109(8), 1073–92.

30. Knight, D. W., and MacDonald, J. A. (1979). "Open-channel flow with varying bed roughness." *J. Hydraul. Div., Am. Soc. Civ. Eng.*, 105(9), 1167–1183.
31. Knight, D. W., and Sterling, M. (2000), "Boundary shear in circular pipes running partially full." *Journal of Hyd. Engg., ASCE* Vol.126, No.4.
32. Knight, D.W., Yuan, Y. M., and Fares, Y. R. (1992). "Boundary shear in meandering channels." *Proceedings of the Institution Symposium on Hydraulic research in nature and laboratory*, Wuhan, China (1992) Paper No.11017, Vol. 118, Sept., pp. 151-159.
33. Langbein, W. B., & Leopold, L. B. (1966). "River meanders--Theory of minimum variance" (pp. 1-15). US Government Printing Office.
34. Leighly, J. B. (1932). "Toward a theory of the morphologic significance of turbulence in the flow of water in streams." *Univ. of Calif. Publ. Geography*,6(1), 1–22.
35. Mellor GL, Herring HJ. "A survey of mean turbulent field closure." *AIAA Journal* 1973; 11:590 – 599.
36. Mohanty, L. (2013), "Velocity Distribution in Trapezoidal Meandering Channel". Thesis Presented to the National Institute of Technology, Rourkela, in partial fulfilment of the requirements for the Degree of Doctor of philosophy.
37. Mohanty, P.K., Dash, S. S. and Khatua, K. K. (2012). "Flow Investigations in a Wide Meandering Compound Channel." *International Journal of Hydraulic Engineering* 2012, 1(6) : 83-94
38. Myers, W. R. C. (1978). "Momentum transfer in a compound channel." *J. Hydraul. Res.*,16(2), 139–150.
39. Patel, V. C. (1965). "Calibration of the Preston tube and limitations on its use in pressure gradients." *Journal of Fluid Mechanics*, 23(01), 185-208.
40. Patnaik, M. (2013), "Boundary Shear Stress Distribution in Meandering Channels". Thesis Presented to the National Institute of Technology, Rourkela, in partial fulfilment of the requirements for the Degree of Doctor of philosophy.
41. Patra, K.C, and Kar, S. K. (2000), "Flow Interaction of Meandering River with Floodplains". *Journal of Hydr. Engrg., ASCE*, 126(8), 593–604.
42. Patra, K. C., and Kar, S. K., Bhattacharya, A. K. (2004). "Flow and Velocity Distribution in Meandering Compound Channels." *Journal of Hydraulic Engineering, ASCE*, Vol. 130, No. 5. 398-411.
43. Preston, J. (1954). "The determination of turbulent skin friction by means of Pitot tubes." *Journal of the Royal Aeronautical Society*, 58(518), 109-121.
44. Rajaratnam, N., and Ahmadi, R.M. (1979). "Interaction between Main Channel and Flood Plain Flows." *Journal of Hydraulic Division, ASCE*, Vol..105, No. HY5, pp. 573-588.

45. Rhodes, D. G., and Knight, D. W. (1994). "Distribution of Shear Force on Boundary of Smooth Rectangular Duct.", *Journal of Hydralic Engg.*, 120-7, 787– 807.
46. Saine S. Dash, K. K. Khatua, P. K Mohanty (2013), "Energy loss for a highly Meandering open Channel Flow", *Res. J. Engineering Sci.*, Vol. 2(4), 22-27, April (2013).
47. Saine S. Dash, K. K. Khatua, P. K. Mohanty (2013), "Factors influencing the prediction of resistance in a meandering channel", *International Journal of Scientific & Engineering Research* , Volume 4, Issue 5, May-2013.
48. Sellin R. H. J. (1961.), "A Study of the Interaction between Flow in the Channel of a River and that over its Floodplain", Ph. D Thesis, University of Bristol, Bristol, England
49. Sellin, R. H. J. (1964), "A Laboratory Investigation into the Interaction between the Flow in the Channel of a River and that over its Floodplain", *La. Houille Blanche*.
50. Shiono K., Al-Romaih I. S., and Knight D. W., (1999), "Stage-discharge assessment in compound meandering channels", *Journal of Hydraulic Engineering*, ASCE, 125 (1), 66-77, Mar., 45-54, and discussion in 1993, 101, Dec., 251-252.
51. Shiono, K., Muto, Y., Knight, D.W. & Hyde, A.F.L.(1999), "Energy Losses due to Secondary Flow and Turbulence in Meandering Channels with Overbank Flow.", *Journal of Hydraulic Research*, IAHR, Vol. 37, No. 5, pp. 641-664.
52. Shukry A. (1950), "Flow around Bends in an Open Flume", *Transactions ASCE*, Vol. 115, pp 75L788.
53. Song CG, Seo IW, Kim YD." Analysis of secondary current effect in the modeling of shallow flow in open channels", *Advances in water resources*, 41 (2012): pp. 29-48.
54. Sugiyama H, Hitomi D, Saito T. "Numerical analysis of turbulent structure in compound meandering open channel by algebraic Reynolds stress model", *International journal for numerical methods in fluids*, 51 (2006): pp. 791-818
55. Thomson J. (1876), "On the origins of windings of rivers in alluvial plains, with remarks on the flow of water round bends in pipes", *Proc. Royal Society of London*, Vol. 25, 5-8.
56. Thomas TG. and Williams J.(1995a). "Large eddy simulation of a symmetric trapezoidal channel at Reynolds number of 430,000." *J. Hydraul. Res.*..33(6), pp. 825-842.
57. Thomas TG. and Williams J.(1999). "Large eddy simulation of flow in a rectangular open channel". *J. Hydraul Res.* 37(3), pp. 345-361.
58. Toebe, G.H., and Sooky, A.A. (1967), "Hydraulics of Meandering Rivers with Floodplains." *Journal of the waterways and Harbor Division, Proceedings of ASCE*, Vol.93, No.WW2, May, pp. 213-236.
59. Willetts B.B. and Hard Wick R.I. (1993), "Stage dependency for overbank flow in meandering channels", *Proc. Instn Civ. Engrs, Wat., Marit. & Energy*, 101.

60. Wormleaton, P.R., Allen, J., and Hadjipanous, P. (1982). "Discharge Assessment in Compound Channel Flow." *Journal of Hydraulic Engineering, ASCE*, Vol.108, No.HY9, pp. 975-994.
61. Yang, S. Q. and McCorquodale, John A. (2004) "Determination of Boundary Shear Stress and Reynolds Shear Stress in Smooth Rectangular Channel Flows." *Journal of Hydr. Engrg.*, Volume 130, Issue 5, pp. 458-462.
62. Zarrati, A. R., Tamai, N. and Jin, Y. C. (2005). "Mathematical Modelling of Meandering Channels with a Generalized Depth Averaged Model". *J. Hydraul. Eng.*, ASCE, 131(6), 467-475.
63. Zhang, Y. (2009). "CCHE-GUI" Graphical Users Interface for NCCH Model User's Manual. *NCHE, University of Mississippi, US.*
<http://www.ncche.olemiss.edu/download>.

APPENDIX-I

Publications from the present work

1. Palai P. D, Mohanta A., Patra K. C,(2014), "Variation of Roughness in a Non-Prismatic Converging Compound Channel 1" in *International Journal on Recent and Innovation Trends in Computing and Communication*. ISSN 2321-Vol (2), issue 10,October (2014), pp. 3311 – 3316
2. Palai P. D, Mohapatra M., Patra K. C,(2015), "Numerical Analysis of Velocity Distribution in A Meandering Compound Channel" in *IOSR Journal of Mechanical and Civil Engineering (IOSR-JMCE)*. e-ISSN: 2278-1684, p-ISSN: 2320-334X. PP 26-31.
3. Mohapatra M, Mohanta A., Patra K. C, Khatua K.K, Palai P. D,(2015), "CFD Simulation And Two Phase Modeling Of a Compound Meandering Channel" in *IOSR Journal of Mechanical and Civil Engineering (IOSR-JMCE)*. e-ISSN: 2278-1684, p-ISSN: 2320-334X. PP 07-12.